Computing Upper and Lower Bounds on Linear Functional Outputs from Linear Coercive Partial Differential Equations

by

Alexander M. Sauer-Budge

S.M., Massachusetts Institute of Technology, 1998
B.S., University of California, Davis, 1996

Submitted to the Department of Aeronautics and Astronautics
in partial fulfillment of the requirements for the degreeof
Doctor of Philosophy in Aeronautics and Astronautics
at the
Massachusetts Institute of Technology
2003 September

Author .....
Department of Aeronautics and Astronautics
August 1, 2003

Certified by .....
Jaime Peraire
Professor of Aeronautics and Astronautics
Thesis Supervisor

Certified by .....
Anthony T. Patera
Professor of Mechanical Engineering

Certified by .....
David L. Darmofal
Associate Professor of Aeronautics and Astronautics

Accepted by .....
Edward M. Greitzer
H.N. Slater Professor of Aeronautics and Astronautics
Chair, Committee on Graduate Students

Computing Upper and Lower Bounds on Linear Functional Outputs from Linear Coercive Partial Differential Equations

by

Alexander M. Sauer-Budge

Submitted to the Department of Aeronautics and Astronautics
on August 1, 2003, in partial fulfillment of the
requirements for the degree of
Doctor of Philosophy in Aeronautics and Astronautics

Abstract

Uncertainty about the reliability of numerical approximations frequently undermines the utility of field simulations in the engineering design process: simulations are often not trusted because they lack reliable feedback on accuracy, or are more costly than needed because they are performed with greater fidelity than necessary in an attempt to bolster trust. In addition to devitalized confidence, numerical uncertainty often causes ambiguity about the source of any discrepancies when using simulation results in concert with experimental measurements. Can the discretization error account for the discrepancies, or is the underlying continuum model inadequate?

This thesis presents a cost effective method for computing guaranteed upper and lower bounds on the values of linear functional outputs of the exact weak solutions to linear coercive partial differential equations with piecewise polynomial forcing posed on polygonal domains. The method results from exploiting the Lagrangian saddle point property engendered by recasting the output problem as a constrained minimization problem. Localization is achieved by Lagrangian relaxation and the bounds are computed by appeal to a local dual problem. The proposed method computes approximate Lagrange multipliers using traditional finite element discretizations to calculate a primal and an adjoint solution along with well known hybridization techniques to calculate interelement continuity multipliers. At the heart of the method lies a local dual problem by which we transform an infinite-dimensional minimization problem into a finite-dimensional feasibility problem.

The computed bounds hold uniformly for any level of refinement, and in the asymptotic convergence regime of the finite element method, the bound gap decreases at twice the rate of the $\mathcal{H}^1$-norm measure of the error in the finite element solution. Given a finite element solution and its output adjoint solution, the method can be used to provide a certificate of precision for the output with an asymptotic complexity that is linear in the

number of elements in the finite element discretization. The complete procedure computes approximate outputs to a given precision in polynomial time. Local information generated by the procedure can be used as an adaptive meshing indicator. We apply the method to Poisson's equation and the steady-state advection-diffusion-reaction equation.

Thesis Supervisor: Jaime Peraire
Title: Professor of Aeronautics and Astronautics

Acknowledgments

First and foremost, I would like to thank my advisor, Professor Jaime Peraire, for his constant vision and continual supply of ideas, as well as for his encouragement and patience during the course of this research. Second, I would like to heartily thank Professor Anthony Patera for taking me under his wing during my advisor's sabbatical and for introducing me to functional analysis in the context of the finite element method. I would like to thank everyone who participated in the "bounds sessions" organized by Professor Patera. In particular, I would like to thank Luc Machiels, Dimitrios Rovas, Ivan Oliveira, Karen Veroy, and Christophe Prud'homme for everything that they taught me as well as for their camaraderie. I would like to thank Professor Gilbert Strang for opening my mind to the underlying beauty of mathematics, and then Professor Dimitris Bertsimas to the underlying mathematical beauty of decision making. I would like to thank my committee as a whole, Professors Jaime Peraire, Anthony Patera, David Darmofal, and Dimitris Bertsimas for their helpful comments and insight. Further, I would like to thank Javier Bonet, Antonio Huerta, and Robert Freund for helpful discussions of various aspects of the method proposed in this thesis. As this work could not have been completed without financial support, I would also like to thank Thomas A. Zang for the support provided through NAG-1-1978 and the Singapore-MIT Alliance. I could not have overcome the many frustrations and disappointments experienced during the course of my studies without the unwavering support of my family and friends. I would especially like to thank my wife, Alexis, and my parents, Roger and Leslee Budge, whose constant love and encouragement renewed my strength when I thought that I could not continue. Finally, I would like to thank my Lord and Savior, Jesus Christ, for setting me free from a life of vanity and for teaching my heart, mind, body, and spirit not only about the wonders of grace, peace, faith, and hope, but about the very thing for which we were created— to love and be loved.

Contents

List of Figures

List of Tables

Chapter 1

Introduction

Uncertainty about the reliability of numerical approximations frequently undermines the utility of field simulations in the engineering design process: simulations are often not trusted because they lack reliable feedback on accuracy, or are more costly than necessary because they are performed with greater fidelity than necessary in an attempt to bolster trust. In addition to devitalized confidence, numerical uncertainty often causes ambiguity about the source of any discrepancies when using simulation results in concert with experimental measurements. Can the discretization error account for the discrepancies, or is the underlying continuum model inadequate?

To disambiguate, we define *precision* to be the conformity of a simulation result to the exact solution of the continuum model, and we define *accuracy* to be the conformity of a simulation result to the physical fact. Three essential questions must be answered before a simulation result can be trusted and effectively used in the making important decisions. Do the mathematical equations model the relevant phenomena? Does the software actually solve the discretized mathematical

model? Does the simulation result contain sufficient precision to be considered a solution of the mathematical model?

The verification and validation process has emerged to help answer these questions [AIA98, OT02, SWCP01]. Verification ensures that the simulation reproduces known analytical results and trusted benchmarks, while validation ensures that the simulation results agree with trusted experimental data. The former confirming that the simulation software solves the discretized mathematical model with sufficient precision for the verification test cases, and the latter substantiating the capacity of the mathematical model to represent the relevant phenomena for the validation test cases. Verification and validation are necessary steps in assessing the reliability of simulation results, but these steps alone do not certify the accuracy of results for cases outside the test suite.

The reliability of every simulation result used in decision making should be taken into account, but it is often prohibitively expensive to do so. *A priori* error estimates inform us of the asymptotic rates of convergence, but cannot answer the ever present engineering question, "can I trust the current approximation?" Such questions often revolve around concerns of mesh fidelity and feature resolution – issues of numerical uncertainty which erode confidence in the simulation. As confidence erodes, so does the utility of the simulation in the engineering design process: either the simulation is not trusted, or it is more costly than necessary.

While confidence in the precision of a field simulation can be buoyed by performing convergence studies, such studies are computationally very expensive and in practice are often not performed at more than a few conditions, if at all, due to cost and time constraints. For this reason, researchers and practitioners employ

adaptive methods to converge the solution in a manner that costs less in time and resources than uniform refinement. Adaptive methods powered by current error estimation technology [Ver94, BKR00, BR78a, BSUG95b, BR96a, BBRW98, HR99, RS97, RS99, SBD+00, VD03, VD02], however, provide only asymptotic guarantees of precision, at best, and no guarantees of precision, at worse, since the convergence of adaptive methods remains an open question [MNS02, BV84, Dor96].

Our observations of engineering practice inform us that integrated quantities such as forces, total fluxes, average temperatures and displacements are frequently queried quantitative outputs from field simulations and that design and analysis does not always require the full precision available. In particular, we will restrict our attention to integrated outputs defined by linear functionals, which depend linearly on the solution field. The primary objective of our method, therefore, is to certify the precision of integrated outputs for low fidelity simulations as well as high fidelity simulations.

We call our bounds *uniform* to differentiate our goal of obtaining quantitative bounds for all levels of refinement from the lesser goal of obtaining quantitative bounds only asymptotically in the limit of refinement. In this regard, the complete procedure can be viewed as a polynomial time algorithm in the number of mesh elements that provides a certificate of precision for a predicted output. The certificate guarantees a minimum level of precision in the output from a particular *finite-dimensional* approximation with respect to the output from the *infinite-dimensional* model that it is approximating. Furthermore, the procedure provides local information that can be used in conjunction with adaptive meshing to efficiently drive a solution to an arbitrary and guaranteed precision.

The method can answer the question "Does the simulation result contain sufficient precision to be considered a solution of the mathematical model?" by certifying the precision of integrated outputs from finite element simulations for any level of mesh refinement. The method can help answer the question "Does the software actually solve the discretized mathematical model?" because it has easily checkable preconditions to help verify correctness of the simulation software. The quantification of numerical error removes uncertainty about the fidelity of the discretization and aides the practitioner in distinguishing modeling error from numerical error when validating the simulation and thus can aid in answering the question "Do the mathematical equations model the relevant phenomena? ". In particular, the method can *invalidate* mathematical models when the error bounds returned by the method do not overlap with the experimental data. This can even be done with relatively low fidelity simulations in cases of gross deviation of the mathematical model from physical reality.

1.1 Techniques for Reliability Assessment

Verification and *a posteriori* error analysis have a long history in the development of the finite element method with a plethora of different approaches forwarded and investigated beginning with the pioneering work of Fraeijs de Veubeke in the mid-1960s and early 1970s [Fra64, Fra65, FH72]. Although powerful, his method was not practical because it required a *global computation.* In the late 1970s, Babuška and Rheinboldt initiated work on modern error estimation techniques by proposing the first inexpensive method requiring only *local computa-*

[BR78a, BR78b, BR81]. Ainsworth and Oden gi[illegible]ummary account of

the work on a posteriori error estimators in [AO97], while Babuška, Strouboulis, Updahyay and collaborators probe the quality and robustness of a number of contemporary error estimators in [BSUG97, BSUG94, BSUG95a, BSU+94, ZSB01] with numerical experiments. Additional comparisons and descriptions of the more popular methods can be found in [ODRW89, Zhu97, SH98, AC92, Ver94].

1.1.1 Recovery Based Error Estimators

Finite element a posteriori error estimators can be broadly classified as *recovery based methods* or *residual based methods*, although evidence exists that some methods which appear distinct under this categorization are equivalent [Zhu97, ZZ99] in special circumstances. Recovery based methods estimate the error in the energy norm by comparing the native finite element solution with one enhanced through a post-processing procedure. The post-processing procedure typically smoothes the finite element solution or exploits special superconvergent properties of the discretization to obtain a recovered solution which is assumed to be more accurate than the original. Zienkiewicz and Zhu first proposed recovery based methods in the late 1980s [ZZ87] and have subsequently improved them [ZZ92a, ZZ92b] by exploiting superconvergence. Recovery based methods have experienced popularity due to their simplicity as well as being very effective in practice [ZBS99, ZSB01].

Recovery based methods produce asymptotically exact error estimates when the post-processing produces a superconvergent recovered solution [CB02]. Asymptotically exact error estimates converge to the exact error in the asymptotic limit of mesh refinement, but do not provide any guarantees of one-sidedness required for bounding the error. Asymptotic exactness is a very useful property for an error

estimator, but without uniform one-sidedness an error estimator cannot provide confirmation of precision. Even if the error estimator produces reliable estimates for a number of validation cases, there is little to assure the practitioner that the estimate can be trusted for the case of interest. Such limitations relegate the error estimator to serving as an oracle for balancing error contributions (of uncertain magnitude) in mesh adaptivity, and undermine their effectiveness as methods for confirmation and building adaptive meshes with guaranteed error tolerances.

1.1.2 Residual Based Error Estimators

Residual based methods, like the first locally computed error estimators which were introduced by Babuška and Rheinboldt, estimate the error in the energy norm either from an explicit evaluation of the local residual or by solving an implicit relationship with the local residual as the data. The majority of the work on error estimation has focused on residual based methods and the method proposed by this thesis can be categorized as such a method. Consider the simple model problem for an unknown real scalar field variable u and some nonnegative scalar coefficient μ and data f posed on a two-dimensional domain

$$-\Delta u + \mu u = f \text{ in } \Omega \subset \mathbb{R}^2$$

subject only to homogeneous Dirichlet boundary conditions. The variational-weak statement follows as: find u in $\mathcal{H}_0^1(\Omega)$

$$a(u,v) = \ell(v), \quad \forall v \in \mathcal{H}_0^1(\Omega) \tag{1.1.1}$$

where

$$a(u,v) = \int_\Omega \nabla u \cdot \nabla v + \mu uv \, \mathrm{d}\Omega,$$

and

$$\ell(v) = \int_\Omega fv \, \mathrm{d}\Omega.$$

The operator $a : \mathcal{H}_0^1(\Omega) \times \mathcal{H}_0^1(\Omega)$ is symmetric, bilinear, continuous and coercive. We have introduced the usual Hilbert space

$$\mathcal{H}^1(\Omega) = \left\{ v \,|\, v \in \mathcal{L}^2(\Omega), \nabla v \in (\mathcal{L}^2(\Omega))^d \right\},$$

where d is the number of physical dimensions and

$$\mathcal{L}^2(\Omega) = \left\{ v \,\middle|\, \int_\Omega |v|^2 \, \mathrm{d}\Omega < +\infty \right\}$$

is the space of square integrable functions on Ω.

1.1.2.1 Explicit Estimators

Many of the first residual based a posteriori error estimators computed an error indicator explicitly from the approximate solution, without solving any additional problems [BR79, KGZB83, BM87]. Following Ainsworth and Oden [AO97], we can build an explicit error estimator for the above model problem by the so called *error equation* or *residual equation*

$$a(e,v) = a(u,v) - a(u_h,v) = \ell(v) - a(u_h,v), \quad \forall v \in \mathcal{H}_0^1(\Omega), \tag{1.1.2}$$

in which the error is defined as $e \equiv u - u_h$, where $u_h \in \mathcal{V}_h$ is a finite element approximation to the solution on some triangulation of the domain, $\mathcal{T}_h$. The error equation expands to

$$a(e, v) = \sum_{T \in \mathcal{T}_h} \int_T fv - \nabla u_h \nabla v - \mu u_h v \, \mathrm{d}\Omega, \quad \forall v \in \mathcal{H}_0^1(\Omega).$$

Assuming u_h to be in $\mathcal{H}^2(\Omega)$ and integrating by parts over the elements decomposes the error equation into local error contributions from each element

$$a(e, v) = \sum_{T \in \mathcal{T}_h} \left\{ \int_T rv \, \mathrm{d}\Omega - \int_{\partial T} \nabla u_h \cdot \boldsymbol{n} v \, \mathrm{d}\Gamma \right\}, \quad \forall v \in \mathcal{H}_0^1(\Omega),$$

where $r \equiv f + \Delta u_h - \mu u_h$ and $\boldsymbol{n}$ is the unit outward normal vector to ∂T_h. The trace of v is continuous along an edge, which allows the last term of the previous equation to be written as the jump discontinuity in the approximation to the flux.

$$a(e, v) = \sum_{T \in \mathcal{T}_h} \int_T rv \, \mathrm{d}\Omega - \sum_{\gamma \in \partial \mathcal{T}_h \setminus \partial\Omega} \int_\gamma [\nabla u_h \cdot \boldsymbol{n}] \, v \, \mathrm{d}\Gamma, \quad \forall v \in \mathcal{H}_0^1(\Omega),$$

where

$$[\nabla u_h \cdot \boldsymbol{n}] = \nabla u_h|_{T_h^+} \cdot \boldsymbol{n}^+ + \nabla u_h|_{T_h^-} \cdot \boldsymbol{n}^- = -R$$

is the jump discontinuity in the flux. We can now write

$$a(e, v) = \sum_{T \in \mathcal{T}_h} \int_T rv \, \mathrm{d}\Omega + \sum_{\gamma \in \partial \mathcal{T}_h \setminus \partial\Omega} \int_\gamma Rv \, \mathrm{d}\Gamma.$$

Galerkin orthogonality, $a(e, v_h) = 0, \forall v_h \in \mathcal{V}_h$, implies that

$$0 = \sum_{T \in \mathcal{T}_h} \int_T r \Pi_{\mathcal{V}_h} v \, \mathrm{d}\Omega + \sum_{\gamma \in \partial \mathcal{T}_h} \int_\gamma R \Pi_{\mathcal{V}_h} v \, \mathrm{d}\Gamma,$$

where $\Pi_{\mathcal{V}_h} : \mathcal{H}^1(T) \rightarrow \mathcal{V}_h(T)$ is the linear operator that projects the members of the infinite-dimensional continuous space, $\mathcal{H}^1(T)$, onto the finite-dimensional approximation subspace, $\mathcal{V}_h(T)$. We can subtract the previous two equations to obtain

$$a(e, v) = \sum_{T \in \mathcal{T}_h} \int_T r(v - \Pi_{\mathcal{V}_h} v) \, \mathrm{d}\Omega + \sum_{\gamma \in \partial \mathcal{T}_h} \int_\gamma R(v - \Pi_{\mathcal{V}_h} v) \, \mathrm{d}\Gamma, \quad \forall v \in \mathcal{H}_0^1(\Omega).$$

Applying the Cauchy-Schwartz Inequality gives

$$a(e, v) \leq \sum_{T \in \mathcal{T}_h} ||r||_{\mathcal{L}^2(T)} \, ||v - \Pi_{\mathcal{V}_h} v||_{\mathcal{L}^2(T)} + \sum_{\gamma \in \partial \mathcal{T}_h} ||R||_{\mathcal{L}^2(\gamma)} \, ||v - \Pi_{\mathcal{V}_h} v||_{\mathcal{L}^2(\gamma)}, \quad \forall v \in \mathcal{H}_0^1(\Omega),$$

Interpolation theory [Cia78, QV97] informs us that there exists a constant C which is independent of v and h, the diameter of the element, such that

$$||v - \Pi_{\mathcal{V}_h} v||_{\mathcal{L}^2(T)} \leq Ch|v|_{\mathcal{H}^1(T^\star)},$$
$$||v - \Pi_{\mathcal{V}_h} v||_{L_2(\gamma)} \leq Ch^{\frac{1}{2}}|v|_{\mathcal{H}^1(T^\star)},$$

where $T^\star$ denotes the subdomain consisting of all elements sharing a common edge with element T, and h is the diameter of T. Inserting these estimates into the

previous equation and absorbing the various constants, yields

$$a(e,v) \leq C|v|_{\mathcal{H}^1(\Omega)} \left\{ \sum_{T \in \mathcal{T}_h} h^2 ||r||^2_{\mathcal{L}^2(T)} + \sum_{\gamma \in \partial \mathcal{T}_h} h||R||^2_{\mathcal{L}^2(\gamma)} \right\}^{\frac{1}{2}}.$$

Finally, recalling that $|v|^2_{\mathcal{H}^1(\Omega)} \leq a(v,v)$, an *a posteriori* error estimate can be written

$$a(e,e) \leq C \left\{ \sum_{T \in \mathcal{T}_h} h^2 ||r||^2_{\mathcal{L}^2(T)} + \sum_{\gamma \in \partial \mathcal{T}_h} h||R||^2_{\mathcal{L}^2(\gamma)} \right\}.$$

Both interior and edge residual quantities comprise the estimate, but in many situations the edge contribution dominates the estimate [KV00, CV99].

Although simple, explicit error estimators of this sort have two obvious drawbacks. First and foremost, the estimate contains a generic unknown constant which renders the estimate useless for certifying the absolute precision of a numerical result. Second, the quantity on the right estimates the error in the energy norm measure which may or may not be relevant to particular decision for which the simulation was undertaken.

Linear Functional Output Error Measure An explicit estimator in a linear functional output can be bootstrapped from the above energy estimator and an output adjoint. These estimators, of course, still contain unknown constants which make them unsuitable for confirmation and validation, but by serving as indicators for mesh adaptivity they can be used to improve the efficiency with which engineering quantities of interest can be approximated with greater precision.

Defining a linear continuous output functional $\ell^{\mathcal{O}} : V \rightarrow \mathbb{R}$. First, find $\psi_h \in \mathcal{V}_h$

such that

$$a(\psi_h, v_h) = \ell^{\mathcal{O}}(v_h), \quad \forall v_h \in \mathcal{V}_h. \tag{1.1.3}$$

Galerkin orthogonality and the Cauchy-Schwarz Inequality allow us to write

$$\ell^{\mathcal{O}}(e) = a(e, \psi) = a(e, \psi - \psi_h) \leq C||e||_{\mathcal{V}_h} ||\psi - \psi_h||_{\mathcal{V}_h}, \tag{1.1.4}$$

where the solution error $||e||_{\mathcal{V}_h}$ was obtained above. A bound on the term $||\psi - \psi_h||_{\mathcal{V}_h}$, where $\psi \in \mathcal{H}_0^1(\Omega)$ is the exact adjoint defined as

$$a(\psi, v) = \ell^{\mathcal{O}}(v), \quad \forall v \in \mathcal{H}_0^1(\Omega),$$

can be obtained in an analogous manner to the solution error. This equation gives a lower bound, an upper bound can be found with the same process, but by solving for $-\ell^{\mathcal{O}}$.

1.1.2.2 Implicit Estimators

The simplicity and low computational cost of explicit estimators makes them attractive despite their lack of quantitative feedback, while the quantitative potential of implicit estimators makes them attractive despite their additional cost. That implicit estimators are typically formulated without explicit constants, however, belies the fact that the vast majority of such estimators tacitly depend on uncomputable quantities which must be approximated in a vitiating manner. As a result, existing implicit estimators cannot be used with confidence to validate the precision of a simulation result, despite the additional cost of such estimators.

An implicit estimator for the error in a linear functional output can be con-

structed from the error equation (1.1.2) using the approximate working solution u_h and the approximate adjoint ψ_h previously introduced. In order to reduce the computational cost of the resulting estimator, we introduce a domain decomposition by partitioning the domain with the finite element triangulation, $\mathcal{T}_h$. On the aggregate of elements, which we call the broken domain, we define a broken space $\hat{\mathcal{V}} = \prod_{T \in \mathcal{T}_h} \mathcal{H}^1(T)$ and a continuity bilinear form $b : \hat{\mathcal{V}} \times \Lambda$ constructed so that

$$\mathcal{V}(\Omega) = \left\{ \hat{v} \in \hat{\mathcal{V}}(\Omega) \,\middle|\, b(\hat{v}, \lambda) = 0, \quad \forall \lambda \in \Lambda \right\},$$

where Λ is the space of bounded linear edge functions (the dual of the trace space of $\mathcal{H}^1(T)$). Introducing the domain decomposition allows us to localize the error estimator computation to a single element.

After computing u_h and ψ_h with standard methods, we can compute equilibrating fluxes λ_h^u and λ_h^ψ by solving the equations

$$b(\hat{v}, \lambda_h^u) = \ell(\hat{v}) - a(u_h, \hat{v}), \quad \forall \hat{v} \in \hat{\mathcal{V}}_h,$$
$$b(\hat{v}, \lambda_h^\psi) = -\ell^{\mathcal{O}}(\hat{v}) - a(\hat{v}, \psi_h), \quad \forall \hat{v} \in \hat{\mathcal{V}}_h,$$

using well established and inexpensive equilibration techniques. *Equilibrating localization* techniques like this are an important ingredient to formulating robust and asymptotically exact implicit error estimators [AO93a, Ain96, ABF99, AO97, BW85].

By choosing a high fidelity *finite-dimensional* approximation space $\mathcal{V}_*(T)$ which we assume can safely be a surrogate for the *infinite-dimensional* space $\mathcal{H}^1(T)$, we

can solve a pair of high fidelity reconstructed error problems on each element

$$2a(e_T^u, v) = \ell(v) - a(u_h, v) - b(v, \lambda_h^u), \quad \forall v \in \mathcal{V}_*(T),$$
$$2a(e_T^\psi, v) = -\ell^{\mathcal{O}}(v) - a(v, \psi_h) - b(v, \lambda_h^\psi), \quad \forall v \in \mathcal{V}_*(T).$$

Upper and lower bounds on the output $s = \ell^{\mathcal{O}}(u)$ can then be computed from the expression

$$s_*^\pm = \ell^{\mathcal{O}}(u_h) - 2\sum_{T\in\mathcal{T}_h} a(e_T^u, e_T^\psi) \pm 2\left\{\left(\sum_{T\in\mathcal{T}_h} a(e_T^u, e_T^u)\right)\left(\sum_{T\in\mathcal{T}_h} a(e_T^\psi, e_T^\psi)\right)\right\}^{\frac{1}{2}}.$$

The quantities $s_*^\pm$ are quantitative bounds on the output from the hypothetical global high fidelity solution u_*: $s_*^- \leq \ell^{\mathcal{O}}(u_*) \leq s_*^+$.

The method we have outlined here follows that of Patera, Paraschivoiu, Peraire, et al. [PPP97, PP98, MPP99, PP00, BP02] in which the high fidelity approximation space $\mathcal{V}_*(T)$ is an h-refinement of the local element subdomain. As the method uses both a working mesh and "truth" mesh, it also falls under a category of two-level finite element methods studied by Brezzi and Marini [BM02]. Methods by other workers in the field have a similar character but use p-refinement for the local enriched approximation. Numerous implicit error estimation methods fall into this overarching scheme of computing high fidelity reconstructed errors from a localized working approximation. They differentiate themselves by the methods they choose for each step and how they measure the error. For instance, flux-free local problems may be computed on a patch of elements resulting from a partition of unity [MMP00, BPP01], or the error might be measured with respect to the constitutive law [Lad00, LR97, LL83].

What the methods all have in common is substitution of a computable finite-dimensional problem where an uncomputable infinite-dimensional problem is required to guarantee bounds [AK01, AO93b, BSG99, SBG00]. Error estimates that do not have the guarantee of one-sidedness, or that approach exactness but only in the asymptotic limit of either global or local problem resolution, cannot certify the precision of simulations posed on arbitrary meshes and require additional work to estimate the error in the error [SBG+99].

1.1.2.3 Summary of Residual Based Error Estimators

Residual based error estimators like the ones introduced above can be viewed broadly with the conceptual matrix of Table 1.1. Notice that the proposed method targets the lower-right quadrant, which yields both greater utility (output metric) and greater rigor (implicit methodology).

Metric	Methodology	
	Explicit	**Implicit**
Energy	Babuška, Miller, Rheinboldt,Verfürth, Kelly, Gago	Bank, Weiser, Ladevèze, Leguillon, Babuška, Rheinboldt, Verfürth, Ainsworth, Oden
Output	Becker, Rannacher	Patera, Peraire, et al.

Table 1.1: Error Estimator Methodology Conceptual Matrix

1.1.3 Relation to Other Methods

As the method presented in this thesis appeals to the dual of a minimization reformulation of the original problem, it can be conceptually viewed as an ex-

tension of complementary energy techniques for error estimation, first proposed by Fraeijs de Veubeke [Fra65] in the early 1970s and later pursued by Ladevèze and Leguillon [Lad00, LL83, LR97, LRBM99], and others [Kel84, DM99], to more relevant error measures and to problems without intrinsic minimization principles such as the advection-diffusion-reaction equation. Similarly, as the method solves equilibrated elemental residual subproblems, it can be conceptually viewed as an extension of the work of Bank and Weiser [BW85], Ainsworth and Oden [AO97, AO93b], and others [CKS99], which does not require exact minimums of infinite-dimensional subproblems to guarantee bounds. Like Becker and Rannacher [BR96a, BR96b, BKR00, RS98, RS97, RS99] and others [VD03, VD02], we are interested in the precision of integrated output quantities and focus the adaptive refinement process on improving the precision of the desired output quantity in particular and not the solution in isolation.

In contrast to the work of Ladevèze, we endeavor to compute uniformly guaranteed two-sided bounds on an output, not an estimate of the error in an abstract norm. While the work of Ainsworth and Oden as well as the related work of Cao, Kelly and Sloan [CKS99] require the exact solution of infinite-dimensional local problems in order to guarantee bounds, our method guarantees bounds uniformly with the solution of a finite-dimensional local problem. Our method differs from that of Destuynder in that it is not burdened with the explicit construction of globally conforming approximations to dual admissible vector fields and the local nature of our method readily provides an adaptive refinement indicator. Moreover, the method introduced in this thesis extends to problems without intrinsic minimization principles such as the advection-diffusion-reaction equation.

Bertsimas and Caramanis have recently proposed a novel global method for computing bounds on functionals of partial differential equations using semidefinite optimization [BC02, BC00]. Like the method presented in this thesis, their method reformulates the output problem as an optimization problem. Initial numerical trials which included the non-coercive Helmholtz equation were promising but unfortunately the cost of performing the semidefinite optimization makes the method impractical at present.

Tangibly, the work presented in this thesis extends earlier work done by Patera, Paraschivoiu, and Peraire [PPP97, PP98] on two-level residual based techniques for computing output bounds. The method presented in this thesis follows the overarching scheme of this and other implicit methods, but transforms the local uncomputable infinite-dimensional subproblem into a computable finite-dimensional one and thereby retains the strong bounding property other methods loose. While the method has the very strong properties mentioned above which are not provided by other methods, it cannot yet be applied to curved domains or mathematical models with non-polynomial forcing and the extension to non-coercive equations is non-trivial.

1.2 Overview

In Chapters 2 and 3, we focus on the overarching structure of the method and do not consider the details of its implementation, nor more general equations such as non-symmetric dissipative operators, which will be presented in Chapter 4. Chapter 2 presents the core concepts in the simpler setting of energy bounds for Poisson's equation, where the method has a clear variational meaning and a direct

relationship to hybrid methods. Chapter 3 recasts the energy bound method as a method for linear functional output bounds for Poisson's equation, simultaneously extending the energy bound to more relevant error measures and preparing the way for more general model problems. In Chapter 4 we generalize the method in a variety of ways while extending it to the advection-diffusion-reaction equation. Beginning with the description of the model problem and continued throughout the chapter, we give a more general presentation of the method which explicitly considers non-homogeneous boundary data. Numerical examples are given at the end of each chapter which demonstrate the potential for the method to deliver simulation results with certified precision.

Chapter 2

Energy Bounds for Poisson's Equation

In the first two chapters we will consider Poisson's equation posed on polygonal domains, Ω, in d spatial dimensions and, only for the sake of simplicity of presentation, homogeneous Dirichlet boundaries, $\Gamma = \partial\Omega$. The Poisson problem is formulated weakly as: find $u \in \mathcal{V}$ such that

$$\int_\Omega \nabla u \cdot \nabla v \, \mathrm{d}\Omega = \int_\Omega f v \, \mathrm{d}\Omega, \quad \forall v \in \mathcal{V}, \tag{2.0.1}$$

where $\mathcal{V}(\Omega) \equiv \{ u \in \mathcal{H}^1(\Omega) \mid u|_\Gamma = 0 \}$ and the domain Ω is assumed when otherwise unspecified, that is, $\mathcal{V} \equiv \mathcal{V}(\Omega)$. As a consequence of all the Dirichlet boundaries being homogeneous, $\mathcal{V}$ serves as both the function set and test space in our presentation. While we present the method for homogeneous Dirichlet data, it can be easily extended to non-homogeneous data and Neumann boundary conditions.

2.1 An Intrinsic Minimization Principle

We begin by developing a lower bound on the total energy of the system, $\frac{1}{2}\int_\Omega \nabla u \cdot \nabla u \, \mathrm{d}\Omega - \int_\Omega f u \, \mathrm{d}\Omega$, which in the context of heat conduction, combines the heat dissipation energy, $\frac{1}{2}\int_\Omega \nabla u \cdot \nabla u \, \mathrm{d}\Omega$, and the potential energy of the thermal loads, $-\int_\Omega f u \, \mathrm{d}\Omega$. There is a well known physical principle at work in this problem, related to the symmetric positive definite nature of the diffusion operator, which states that the solution, u, is the function that minimizes the total energy with respect to all other candidates in $\mathcal{V}$

$$u = \arg \inf_{w \in \mathcal{V}} \frac{1}{2}\int_\Omega \nabla w \cdot \nabla w \, \mathrm{d}\Omega - \int_\Omega f w \, \mathrm{d}\Omega, \tag{2.1.1}$$

as can easily be verified by comparing the Euler-Lagrange equation of this minimization statement to Poisson's equation (2.0.1). This minimization formulation makes it clear that if we look for a discrete approximation of (2.0.1) in a finite set of conforming functions, $\mathcal{V}_h$, for which $\mathcal{V}_h \subset \mathcal{V}$, then the resulting total energy predicted by the approximation will approach the exact value from above.

While insightful, this upper bound on the total energy has limited usefulness for two primary reasons. First, only rarely will the total energy be relevant to the purpose of solving the original problem. Second, even when it is relevant, the upper bound will most likely not be helpful for managing approximation uncertainty. In an engineering design task, the upper bound usually corresponds to the "best case scenario," as opposed to the "worst case scenario" which would be required to ensure feasibility of the design.

Our strategy for obtaining lower bounds on the energy in a cost efficient man-

ner is to first decompose the global problem into independent local elemental subproblems by relaxing the continuity of the set $\mathcal{V}$ along edges of a triangular partitioning of Ω, using approximate Lagrange multipliers, then accumulate the lower bound from the objective values of approximate local dual subproblems.

2.2 Weak Continuity Reformulation

We begin by partitioning the domain into a mesh, $\mathcal{T}_h$, of non-overlapping open sub domains, T, called elements. The partition has the property $\bigcup_{T\in\mathcal{T}_h} \overline{T} = \bar{\Omega}$, where the over-bar indicates the closure of the domain. We denote by ∂T the edges, γ, constituting the boundary of a single element T, and by $\partial\mathcal{T}_h$ the network of all edges in the mesh. We have not yet evoked a discretization of $\mathcal{V}$, but merely a domain decomposition represented by a mesh. With the broken space

$$\hat{\mathcal{V}} \equiv \left\{ v \in L^2(\Omega) \,\middle|\, v|_T \in \mathcal{H}^1(T),\ \forall T \in \mathcal{T}_h \right\}, \tag{2.2.1}$$

in which the continuity of $\mathcal{V}$ is broken across the mesh edges, $\partial\mathcal{T}_h$, we can reformulate the energy minimization statement (2.1.1) by explicitly enforcing continuity

$$\begin{aligned} u = \arg\inf_{\hat{w}\in\hat{\mathcal{V}}} \quad & \frac{1}{2}\int_\Omega \nabla\hat{w}\cdot\nabla\hat{w}\,\mathrm{d}\Omega - \int_\Omega f\hat{w}\,\mathrm{d}\Omega \\ \text{s.t.} \quad & \sum_{T\in\mathcal{T}_h}\int_{\partial T}\sigma_T\hat{w}\lambda\,\mathrm{d}\Gamma = 0, \quad \forall\lambda\in\Lambda, \end{aligned} \tag{2.2.2}$$

where, for $T_{\mathrm{N}} \in \mathcal{T}_h$ and an arbitrary ordering of the elements, $T < T_{\mathrm{N}}$,

$$\sigma_T(x) = \begin{cases} -1 & x \in \overline{T} \cap \overline{T}_{\mathrm{N}}, T < T_{\mathrm{N}} \\ +1 & \text{otherwise.} \end{cases} \tag{2.2.3}$$

Integrals over the broken domain, such as $\int_\Omega \nabla\hat{w} \cdot \nabla\hat{v}\,\mathrm{d}\Omega$, are understood as sums of integrals over the subdomains, such as $\sum_{T\in\mathcal{T}_h} \int_T \nabla\hat{w}|_T \cdot \nabla\hat{v}|_T\,\mathrm{d}\Omega$. As there is no ambiguity, we have suppressed the trace operators from our notation for the boundary integrals to simplify the appearance of the expressions.

To see how the constraint arises, consider a single edge, $\gamma \in \partial\mathcal{T}_h$, with neighboring elements T and T_{N}, for which a strong continuity constraint can be written roughly as $\hat{w}|_{T,\gamma} - \hat{w}|_{T_{\mathrm{N}},\gamma} = 0$ on γ. An integral weak representation is obtained by multiplying by an arbitrary test function, λ_γ, taken from an appropriate space, $\Lambda(\gamma)$, integrating along the edge, and ensuring the resulting integrated quantity is zero for all possible test functions: $\int_\gamma (\hat{w}|_{T,\gamma} - \hat{w}|_{T_{\mathrm{N}},\gamma})\,\lambda_\gamma\,\mathrm{d}\Gamma = 0, \quad \forall\lambda_\gamma \in \Lambda(\gamma)$. The constraint used above is obtained by re-writing the combination of all edge constraints as a combination of elemental contributions, using σ_T to track the sign of the contribution. Since $\hat{w}|_T$ is a member of $\mathcal{H}^1(T)$, the trace of $\hat{w}|_T$ on an edge γ is a member of $\mathcal{H}^{\frac{1}{2}}(\partial T)$. Therefore, λ on γ is a member of the dual of the trace space, $\mathcal{H}^{-\frac{1}{2}}(\gamma)$, and the continuity multiplier space Λ is the corresponding product space taken over all the edges of the mesh.

Notice that we have relaxed the Dirichlet boundary conditions as well as the interior continuity. The homogeneous Dirichlet conditions are weakly enforced implicitly by the continuity constraint. We shall not prove it here, but it is important to know that the minimizer of the constrained minimization problem (2.2.2)

is indeed u, the exact solution of Poisson's equation (2.0.1) [AO97, BF91].

2.3 Localization by Continuity Relaxation

Considering the Lagrangian of the constrained minimization (2.2.2),

$$\mathcal{L}(\hat{w};\lambda) \equiv \frac{1}{2}\int_\Omega \nabla\hat{w}\cdot\nabla\hat{w}\,\mathrm{d}\Omega - \int_\Omega f\hat{w}\,\mathrm{d}\Omega - \sum_{T\in\mathcal{T}_h}\int_{\partial T}\sigma_T\hat{w}\lambda\,\mathrm{d}\Gamma, \tag{2.3.1}$$

we recall from the saddle point property of Lagrange multipliers and the strong duality of convex minimizations that for all $\tilde{\lambda}\in\Lambda$

$$\varepsilon^- \le \inf_{\hat{w}\in\hat{\mathcal{V}}}\mathcal{L}(\hat{w};\tilde{\lambda}) \le \sup_{\lambda\in\Lambda}\inf_{\hat{w}\in\hat{\mathcal{V}}}\mathcal{L}(\hat{w};\lambda) = \inf_{\hat{w}\in\hat{\mathcal{V}}}\sup_{\lambda\in\Lambda}\mathcal{L}(\hat{w};\lambda) = \varepsilon,$$

where the value at optimality is the minimum total energy of the continuum system, $\varepsilon = \frac{1}{2}\int_\Omega \nabla u\cdot\nabla u\,\mathrm{d}\Omega - \int_\Omega fu\,\mathrm{d}\Omega$. The lower bounding minimization for a given $\tilde{\lambda}$ is separable, an important property allowing us to treat each element independently as will be discussed further in Section 2.4. In order to obtain a non-trivial (i.e. finite) lower bound, $\tilde{\lambda}$ cannot be chosen arbitrarily. We obtain $\tilde{\lambda}$ by approximating the problem using finite elements in a manner that guarantees the relaxed minimization is bounded from below.

2.3.1 Continuity Multiplier Approximation

We now introduce the finite element approximation of Poisson's equation (2.0.1) as means of obtaining an approximate Lagrange multiplier. We first solve the

finite-dimensional Poisson problem: find $u_h \in \mathcal{V}_h$ such that

$$\int_\Omega \nabla u_h \cdot \nabla v \, \mathrm{d}\Omega = \int_\Omega f v \, \mathrm{d}\Omega, \quad \forall v \in \mathcal{V}_h, \tag{2.3.2}$$

where $\mathcal{V}_h \equiv \{ v \in \mathcal{V} \mid v|_T \in \mathbb{P}^p(T), \forall T \in \mathcal{T}_h \}$ for $\mathbb{P}^p(T)$ the space of polynomials on element T (in d spatial dimensions) with degree less than or equal to p. Once we have obtained u_h, we solve the gradient condition of (2.3.1) to obtain λ_h: find a $\lambda_h \in \Lambda_h$ such that

$$\sum_{T \in \mathcal{T}_h} \int_{\partial T} \sigma_T \hat{v} \lambda_h \, \mathrm{d}\Gamma = \int_\Omega \nabla u_h \cdot \nabla \hat{v} \, \mathrm{d}\Omega - \int_\Omega f \hat{v} \, \mathrm{d}\Omega, \quad \forall \hat{v} \in \hat{\mathcal{V}}_h, \tag{2.3.3}$$

where $\Lambda_h \equiv \{ \lambda \in \Lambda \mid \lambda|_\gamma \in \mathbb{P}^p(\gamma), \forall \gamma \in \partial\mathcal{T}_h \}$ for $\mathbb{P}^p(\gamma)$ the space of polynomials on element edge γ (in $d-1$ spatial dimensions) with degree less than or equal to p. We call this the equilibration problem, and we call any compatible Lagrange multiplier "equilibrating," since the problem has a non-unique solution. In the context of hybrid methods [BF91], this continuity multiplier is often referred to as a hybrid flux. As mentioned previously, this particular choice for the Lagrange multiplier ensures a finite lower bound.

Lemma 2.3.1. *If a Lagrange multiplier $\lambda_h \in \Lambda_h$ satisfies the equilibration condition (2.3.3), then $\inf_{\hat{w} \in \hat{\mathcal{V}}} \mathcal{L}(\hat{w}; \lambda_h)$ is bounded from below.*

Proof. Recall that the null space for the Laplace operator is the one dimensional space of constants, $\mathbb{P}^0$, and let $\hat{\mathbb{P}}^0 = \prod_{T \in \mathcal{T}_h} \mathbb{P}^0(T)$ denote the null space of the broken operator. Considering $\hat{c} \in \hat{\mathbb{P}}^0 \subset \hat{\mathcal{V}}_h$ in the equilibration problem (2.3.3) and that any $\hat{w} \in \hat{\mathcal{V}}$ can be represented as $\hat{w}' + \hat{c}$ for $\hat{w}' \in \hat{\mathcal{V}} \setminus \hat{\mathbb{P}}^0$, it is easily shown that $\mathcal{L}(\hat{w}' + \hat{c}; \lambda_h) = \mathcal{L}(\hat{w}'; \lambda_h)$. For the Poisson equation, equilibration ensures

that null space of the operator does not cause the minimization to be become unbounded below. The existence of a minimum now follows from the coercivity of the Poisson operator in $\hat{\mathcal{V}} \setminus \hat{\mathbb{P}}^0$. □

While not part of the classical finite element problem set, the equilibration problem has been addressed a number of times and in a number of contexts in the finite element community, not the least of which is in the context of error estimation [AO93a, LM96, MP00]. The equilibration problem can solved with asymptotically linear computational cost in the number of mesh vertices and in some cases is already solved as a component of domain decomposition techniques for parallel computations [Par01]. For our implementation, we use a method due to Ladevèze [LL83, AO97].

2.4 Local Dual Subproblem

Now that we have successfully decomposed the global problem into local elemental subproblems, we can write the lower bounding minimization induced by the Lagrange saddle point property as

$$\inf_{\hat{w}\in\hat{\mathcal{V}}} \mathcal{L}(\hat{w};\tilde{\lambda}) = \sum_{T\in\mathcal{T}_h} \inf_{w\in\mathcal{V}(T)} J_T(w)$$

for

$$J_T(w) \equiv \frac{1}{2}\int_T \nabla w\cdot\nabla w\,\mathrm{d}\Omega - \int_T fw\,\mathrm{d}\Omega - \int_{\partial T}\sigma_T w\tilde{\lambda}\,\mathrm{d}\Gamma, \qquad (2.4.1)$$

and consider a representative minimization subproblem. The minimization subproblem simply corresponds to a Poisson problem of the type represented in equa-

tion (2.0.1) with Neumann boundary conditions posed on a single subdomain. We have done nothing to change the nature of original problem, but have only acted to decompose the global problem into a sequence of independent local problems.

We do not require, and in general cannot compute, the exact minimum of the infinite-dimensional local subproblem, but we do require a lower bound for it and we proceed now to introduce the primary ingredient for obtaining this local lower bound.

Proposition 2.4.1. *If we define the positive functional*

$$J_T^c(\boldsymbol{q}) \equiv \frac{1}{2}\int_T \boldsymbol{q}\cdot\boldsymbol{q}\,\mathrm{d}\Omega \tag{2.4.2}$$

where $\boldsymbol{q} \in \mathcal{H}(\mathrm{div};T)$ *and* $\mathcal{H}(\mathrm{div};T) \equiv \left\{\boldsymbol{q}\,|\,\boldsymbol{q}\in(L^2(T))^d,\ \nabla\cdot\boldsymbol{q}\in L^2(T)\right\}$ *for a problem posed in d spatial dimensions, then we have*

$$J_T(w) \geq -J_T^c(\boldsymbol{q}), \quad \forall w\in\mathcal{H}^1(T),\ \forall \boldsymbol{q}\in\mathcal{Q}(T), \tag{2.4.3}$$

for the set of functions

$$\begin{aligned}\mathcal{Q}(T) \equiv \Big\{\boldsymbol{q}\in\mathcal{H}(\mathrm{div};T)\ \Big|\ &\int_T \nabla\cdot\boldsymbol{q}\,v\,\mathrm{d}\Omega - \int_{\partial T}\boldsymbol{q}\cdot\boldsymbol{n}\,v\,\mathrm{d}\Gamma \\ &= -\int_T f\,v\,\mathrm{d}\Omega - \int_{\partial T}\tilde{\lambda}\,v\,\mathrm{d}\Gamma, \quad \forall v\in\mathcal{H}^1(T)\Big\}.\end{aligned} \tag{2.4.4}$$

Proof. We begin by appealing to the following positive expression

$$\frac{1}{2}\int_T (\boldsymbol{q}-\nabla w)^2\,\mathrm{d}\Omega \geq 0,$$

for any $w \in \mathcal{H}^1(T)$ and any $\boldsymbol{q} \in \mathcal{Q}(T)$. This expression expands to

$$\frac{1}{2}\int_T \boldsymbol{q}\cdot\boldsymbol{q}\,\mathrm{d}\Omega + \frac{1}{2}\int_T \nabla w\cdot\nabla w\,\mathrm{d}\Omega - \int_T \boldsymbol{q}\cdot\nabla w\,\mathrm{d}\Omega \geq 0,$$

in which we apply the Green's identity

$$-\int_T \boldsymbol{q}\cdot\nabla w\,\mathrm{d}\Omega = \int_T \nabla\cdot\boldsymbol{q}\,w\,\mathrm{d}\Omega - \int_{\partial T}\boldsymbol{q}\cdot\boldsymbol{n}\,w\,\mathrm{d}\Gamma$$

to obtain

$$\frac{1}{2}\int_T \boldsymbol{q}\cdot\boldsymbol{q}\,\mathrm{d}\Omega + \frac{1}{2}\int_T \nabla w\cdot\nabla w\,\mathrm{d}\Omega + \int_T \nabla\cdot\boldsymbol{q}\,w\,\mathrm{d}\Omega - \int_{\partial T}\boldsymbol{q}\cdot\boldsymbol{n}\,w\,\mathrm{d}\Gamma \geq 0. \quad (2.4.5)$$

The constraint included in the definition of $\mathcal{Q}(T)$ makes this expression equivalent to

$$\frac{1}{2}\int_T \boldsymbol{q}\cdot\boldsymbol{q}\,\mathrm{d}\Omega + \frac{1}{2}\int_T \nabla w\cdot\nabla w\,\mathrm{d}\Omega - \int_T f w\,\mathrm{d}\Omega - \int_{\partial T}\sigma_T w\tilde{\lambda}\,\mathrm{d}\Gamma \geq 0. \quad (2.4.6)$$

Identifying $J_T(w)$ and $J_T^c(\boldsymbol{q})$ we arrive at the desired expression for the local lower bound. □

To obtain the best possible local lower bound, we might consider the following maximization problem

$$\sup_{\boldsymbol{q}\in\mathcal{Q}(T)} -J_T^c(\boldsymbol{q}) \leq \inf_{w\in\mathcal{V}(T)} J_T(w),$$

with equality being obtained as a result of the convexity of J_T and J_T^c. It is

clear that we have derived a classic dual formulation[1] for our local elemental minimization problem and essentially transformed a primal minimization problem into a dual feasibility problem. As we have alluded to earlier, the functional $J_T^c(\boldsymbol{q})$ is often called the *complementary energy* functional [QV97], when taken over the whole domain, Ω, with a globally admissible complementary field.

2.4.1 Subproblem Computation

Significantly, we can make these subproblems computable by choosing an appropriate finite-dimensional set in which to search for $\boldsymbol{q}$. At the very least the set must be chosen so that the divergence of its functions contain the forcing function, f, in T and the normal traces of its functions contain the approximate continuity multiplier, λ_h, on ∂T. In multiple dimensions, however, the polynomial approximation for the continuity multiplier will nullify any components of the set with non-polynomial normal trace. Therefore, we choose the polynomial approximation subset

$$\mathcal{Q}_h(T) \equiv \Big\{ \boldsymbol{q} \in (\mathbb{P}^q(T))^d \;\Big|\; \int_T \nabla \cdot \boldsymbol{q}\, v \,\mathrm{d}\Omega - \int_{\partial T} \boldsymbol{q} \cdot \boldsymbol{n}\, v \,\mathrm{d}\Gamma = -\int_T f\, v \,\mathrm{d}\Omega - \int_{\partial T} \sigma_T \lambda_h\, v \,\mathrm{d}\Gamma,\ \forall v \in \mathcal{H}^1(T) \Big\}, \tag{2.4.7}$$

with $q \geq p$. As a consequence, the method as we have presented it is limited to forcing functions, $f|_T$, that are perforce members of the polynomial space $\mathbb{P}^r(T)$ for $q > r$ on each elemental domain. While in one dimension we gain no advantage

[1]The classic derivation for the dual of the Poisson problem would begin by letting $\boldsymbol{q} = \nabla w$ (a statement of Fourier's law in the context of heat conduction) and proceed by eliminating w from the problem.

in taking q greater than $r+1$, in multiple dimensions we can do so in an attempt to sharpen the bounds. The interior constraint data, f, and the boundary constraint data, $\sigma_T \lambda_h$, cannot be chosen independently of each other, but must satisfy a compatibility condition in order to ensure solvability as manifest by the following lemma.

Lemma 2.4.2. *Suppose the forcing function $f|_T$ is a member of $\mathbb{P}^r(T)$ and that λ_h satisfies (2.3.3), then there exists at least one dual feasible function, $\boldsymbol{q}$, that is a member of $\mathcal{Q}_h(T)$ for $q \geq p$ and $q > r$.*

Proof. We begin by expressing $\boldsymbol{q}$, a member of $(\mathbb{P}^q(T))^d$, as the combination $\boldsymbol{q} = \boldsymbol{q}_D + \boldsymbol{q}_0$, with $\boldsymbol{q}_D$ a normal boundary condition satisfying component, $\boldsymbol{q}_D \cdot \boldsymbol{n} = \sigma_T \lambda_h$ on ∂T, and $\boldsymbol{q}_0$ a homogeneous normal boundary condition satisfying component, $\boldsymbol{q}_0 \cdot \boldsymbol{n} = 0$ on ∂T. With this lifting, we can write the feasibility constraint as

$$-\int_T \nabla \cdot \boldsymbol{q}_0 \, v \, \mathrm{d}\Omega = \int_T f \, v \, \mathrm{d}\Omega + \int_T \nabla \cdot \boldsymbol{q}_D \, v \, \mathrm{d}\Omega.$$

Recognizing the divergence operator on the left hand side, which maps $(\mathbb{P}^q(T))^d$ into $\mathbb{P}^{q-1}(T)$, we note that we need only test against $v \in \mathbb{P}^{q-1}(T)$. Furthermore, finite-dimensional linear equations are solvable if and only if the right hand side data lies in the range of the operator, which is orthogonal to the null space of the adjoint operator. The adjoint operator is easily found to be $\int_T \boldsymbol{q}_0 \cdot \nabla v \, \mathrm{d}\Omega$ which has the null space $v \in \mathbb{P}^0(T)$, and thus the right hand side data must be in $\mathbb{P}^{q-1}(T) \setminus \mathbb{P}^0(T)$.

To prove solvability, we need only to verify that the right hand side data is orthogonal to the constants, since the requirements that $q \geq p$ and $q > r$ ensure that the right hand side data is in $\mathbb{P}^{q-1}$. Choosing $v = \text{const}$ in the right hand

side of the constraint, rewritten as

$$\int_T f\, v \,\mathrm{d}\Omega + \int_T \nabla \cdot \boldsymbol{q}_D \, v \,\mathrm{d}\Omega = \int_T f\, v \,\mathrm{d}\Omega - \int_T \boldsymbol{q}_D \cdot \nabla v \,\mathrm{d}\Omega + \int_{\partial T} \sigma_T \lambda_h \, v \,\mathrm{d}\Gamma,$$

reveals the compatibility condition

$$\int_{\partial T} \sigma_T \lambda_h \,\mathrm{d}\Gamma = -\int_T f \,\mathrm{d}\Omega, \tag{2.4.8}$$

which is satisfied by our choice for λ_h, as can be seen by choosing $\hat{v} = \text{const}$ on T in the equilibration condition (2.3.3). The equilibration condition thus ensures that the constraint data is compatible and that there exists at least one $\boldsymbol{q}$ satisfying the constraint. □

2.5 Energy Bound Procedure

In discussing the global procedure and its properties, we denote the global aggregate of independent elemental quantities by accenting them with a diacritical hat as we did for the global broken quantities, and we denote the aggregate of local functional forms by dropping the subscript T. In particular, $\hat{\mathcal{Q}}_h$ denotes the aggregate approximate dual function space, $\prod_{T\in\mathcal{T}_h} \mathcal{Q}_h(T)$, and $J^c(\hat{\mathbf{q}})$ the aggregate dual energy functional, $\sum_{T\in\mathcal{T}_h} J^c_T(\boldsymbol{q}|_T)$. The complete method for the energy bounds consists of three steps:

1. *Global Approximation:* Find $u_h \in \mathcal{V}_h$ such that

$$\int_\Omega \nabla u_h \cdot \nabla v \,\mathrm{d}\Omega = \int_\Omega f v \,\mathrm{d}\Omega, \quad \forall v \in \mathcal{V}_h, \tag{2.5.1}$$

and calculate the upper bound $\varepsilon_h^+ = -\frac{1}{2}\int_\Omega \nabla u_h \cdot \nabla u_h \, \mathrm{d}\Omega$.

2. *Global Equilibration:* Find $\lambda_h \in \Lambda_h$ such that

$$\sum_{T\in\mathcal{T}_h} \int_{\partial T} \sigma_T \hat{v} \lambda_h \, \mathrm{d}\Gamma = \int_\Omega \nabla u_h \cdot \nabla \hat{v} \, \mathrm{d}\Omega - \int_\Omega f\hat{v} \, \mathrm{d}\Omega, \quad \forall \hat{v} \in \hat{\mathcal{V}}_h. \tag{2.5.2}$$

3. *Local Dual Approximations:* Find ε_h^- such that

$$\varepsilon_h^- = \sup_{\hat{\mathbf{q}}_h \in \hat{\mathcal{Q}}_h} -J^c(\hat{\mathbf{q}}_h). \tag{2.5.3}$$

The last step requires the solution of a series of finite-dimensional quadratic programming problems with convex objective functions and linear equality constraints. The per-element cost remains low due to the small size of the elemental subproblems, while the total cost of computing the lower bound is asymptotically linear in the number elements.

2.5.1 Properties of the Energy Bound

As previously discussed, the upper bound follows directly from the conforming nature of the finite element approximation and the lower bound follows directly from Proposition 2.4.1. We close our presentation of the energy bound method by showing that the lower bound converges at the same rate as the upper bound, and thus inherits the well known *a priori* finite element convergence property for the energy norm of the error. We begin by proving an orthogonality result.

Lemma 2.5.1. *Let* $\hat{\mathbf{p}}_h$ *be any dual feasibility correction to* ∇u_h *such that* $\hat{\mathbf{q}}_h =$

$\nabla u_h + \hat{\mathbf{p}}_h$ is a member of $\hat{\mathcal{Q}}_h$, then $\hat{\mathbf{p}}_h$ satisfies the orthogonality property

$$\sum_{T\in\mathcal{T}_h}\int_T \hat{\mathbf{p}}_h\cdot\nabla\hat{v}\,\mathrm{d}\Omega = 0, \quad \forall\hat{v}\in\hat{\mathcal{V}}_h. \tag{2.5.4}$$

Proof. We begin by examining the condition that the feasibility correction $\hat{\mathbf{p}}_h$ must satisfy by substituting $\nabla u_h + \hat{\mathbf{p}}_h$ into the constraint contained in the definition of $\hat{\mathcal{Q}}_h$, summed over the elements, to obtain

$$\begin{aligned}\int_\Omega \nabla\cdot\hat{\mathbf{p}}_h\,\hat{v}\,\mathrm{d}\Omega - \sum_{T\in\mathcal{T}_h}\int_{\partial T}\hat{\mathbf{p}}_h\cdot\boldsymbol{n}\,\hat{v}\,\mathrm{d}\Gamma &= -\int_\Omega f\,\hat{v}\,\mathrm{d}\Omega - \int_\Omega \nabla\cdot\nabla u_h\,\hat{v}\,\mathrm{d}\Omega \\ &\quad - \sum_{T\in\mathcal{T}_h}\int_{\partial T}\sigma_T\lambda_h\,\hat{v}\,\mathrm{d}\Gamma + \sum_{T\in\mathcal{T}_h}\int_{\partial T}\nabla u_h\cdot\boldsymbol{n}\,\hat{v}\,\mathrm{d}\Gamma, \quad \forall\hat{v}\in\hat{\mathcal{V}}.\end{aligned} \tag{2.5.5}$$

Applying Green's formula to both the $\hat{\mathbf{p}}_h$ and u_h terms yields the equivalent constraint

$$\int_\Omega \hat{\mathbf{p}}_h\cdot\nabla\hat{v}\,\mathrm{d}\Omega = \int_\Omega f\,\hat{v}\,\mathrm{d}\Omega - \int_\Omega \nabla u_h\cdot\nabla\hat{v}\,\mathrm{d}\Omega + \sum_{T\in\mathcal{T}_h}\int_{\partial T}\sigma_T\lambda_h\,\hat{v}\,\mathrm{d}\Gamma, \quad \forall\hat{v}\in\hat{\mathcal{V}}. \tag{2.5.6}$$

Restricting $\hat{v}$ to $\hat{\mathcal{V}}_h$ produces the sought orthogonality property as a consequence of equilibration (2.5.2). □

Lemma 2.5.2. *Let $\hat{\mathbf{p}}_h^*$ be the dual feasibility correction to ∇u_h that maximizes $-J^c(\hat{\mathbf{p}}_h)$ such that $\nabla u_h + \hat{\mathbf{p}}_h^*$ is a member of $\hat{\mathcal{Q}}_h$, then $\hat{\mathbf{p}}_h^*$ is bounded from above by*

$$J^c(\hat{\mathbf{p}}_h^*) \le C|u-u_h|_1^2, \tag{2.5.7}$$

for the semi-norm $|v|_1^2 \equiv \int_\Omega \nabla v\cdot\nabla v\,\mathrm{d}\Omega$, if the approximate continuity multiplier

λ_h computed in (2.5.2) has the bound

$$\sum_{T\in\mathcal{T}_h} h^{\frac{1}{2}}\|\lambda-\lambda_h\|_{\partial T} \le C|u-u_h|_1, \tag{2.5.8}$$

where $\lambda|_{\partial T} \equiv \sigma_T \frac{\partial u}{\partial \boldsymbol{n}}$ is the exact continuity multiplier and $\|v\|^2_{\partial T} \equiv \int_{\partial T} v^2 \,\mathrm{d}\Gamma$. Everywhere, C is a generic constant independent of $h = \mathrm{diam}(T)$.

Proof. Using the constraint (2.5.6) and the definition $\hat{\mathcal{P}}_h = \prod_{T\in\mathcal{T}_h}(\mathbb{P}^q(T))^d$, the constrained maximization for $\hat{\mathbf{p}}_h^*$ can be written as $\sup_{\hat{\mathbf{p}}\in\hat{\mathcal{P}}_h} -\frac{1}{2}\int_\Omega \hat{\mathbf{p}}_h\cdot\hat{\mathbf{p}}_h \,\mathrm{d}\Omega$ such that

$$-\int_\Omega \hat{\mathbf{p}}_h\cdot\nabla\hat{\phi}\,\mathrm{d}\Omega = \int_\Omega \nabla u_h\cdot\nabla\hat{\phi}\,\mathrm{d}\Omega - \int_\Omega f\,\hat{\phi}\,\mathrm{d}\Omega - \sum_{T\in\mathcal{T}_h}\int_{\partial T}\sigma_T\lambda_h\,\hat{\phi}\,\mathrm{d}\Gamma, \tag{2.5.9}$$

for all $\hat{\phi}\in\hat{\mathbb{P}}^{q+1}$. The gradient condition, $\int_\Omega \hat{\mathbf{r}}_h\cdot\hat{\mathbf{p}}_h^*\,\mathrm{d}\Omega = \int_\Omega \hat{\mathbf{r}}_h\cdot\nabla\hat{\phi}^*\,\mathrm{d}\Omega, \forall\hat{\mathbf{r}}_h|_T\in\hat{\mathcal{P}}_h$, informs us that $\hat{\mathbf{p}}_h^* = \nabla\hat{\phi}^*$. Since $\hat{\phi}^*$ is defined uniquely only up to a constant on each element because of compatibility, we can choose $\hat{\phi}^*$ to be of zero mean over each element, $\int_T \hat{\phi}^*|_T\,\mathrm{d}\Omega = 0$.

The approximate solution u_h has an associated approximate continuity multiplier λ_h satisfying (2.5.2), while the exact solution u also has an associated exact continuity multiplier λ satisfying

$$\sum_{T\in\mathcal{T}_h}\int_{\partial T}\sigma_T\hat{v}\lambda\,\mathrm{d}\Gamma = \int_\Omega \nabla u\cdot\nabla\hat{v}\,\mathrm{d}\Omega - \int_\Omega f\hat{v}\,\mathrm{d}\Omega, \quad \forall\hat{v}\in\hat{\mathcal{V}}, \tag{2.5.10}$$

as can be verified by integration by parts. Adding (2.5.10) to the constraint

of (2.5.9) with $\hat{\mathbf{p}}_h = \hat{\mathbf{p}}_h^*$ and $\hat{v} = \hat{\phi}^*$ we find for $\|\hat{v}\|^2 = \sum_{T\in\mathcal{T}_h} \int_T v^2 \,\mathrm{d}\Omega$ that

$$\begin{aligned}\int_\Omega \hat{\mathbf{p}}_h^* \cdot \nabla\hat{\phi}^* \,\mathrm{d}\Omega = \int_\Omega \nabla(u-u_h)\cdot\nabla\hat{\phi}^* \,\mathrm{d}\Omega - \sum_{T\in\mathcal{T}_h}\int_{\partial T} \sigma_T(\lambda-\lambda_h)\hat{\phi}^* \,\mathrm{d}\Gamma \\ \leq C|u-u_h|_1\|\nabla\hat{\phi}^*\| + \sum_{T\in\mathcal{T}_h} C\|\lambda-\lambda_h\|_{\partial T}\|\hat{\phi}^*\|_{\partial T} \\ \leq C|u-u_h|_1\|\nabla\hat{\phi}^*\| + \sum_{T\in\mathcal{T}_h} Ch^{\frac{1}{2}}\|\lambda-\lambda_h\|_{\partial T}\|\nabla\hat{\phi}^*\|,\end{aligned}$$

in which we applied the inequality $\|w\|_{\partial T} \leq Ch^{\frac{1}{2}}|w|_{1,T}$, valid for any $w \in \mathcal{H}^1(T)$ that has zero mean [MP00]. Finally, after invoking the bound (2.5.8) we complete the proof by substituting $\nabla\hat{\phi}^* = \hat{\mathbf{p}}_h^*$, dividing both sides by $\|\hat{\mathbf{p}}_h\|$, and recognizing that $\|\hat{\mathbf{p}}_h^*\|^2 = 2J^c(\hat{\mathbf{p}}_h^*)$. □

Ainsworth and Oden prove in [AO93b] that under certain assumptions the flux average of the finite element solution across the edges is bounded by (2.5.8) so that, by way of the triangle inequality, the burden rests in showing that the non-unique equilibrating corrections required to satisfy (2.5.2) decrease at the requisite rate. Maday and Patera give in [MP00] a basic method for computing approximate continuity multipliers that has been proven *a priori* to satisfy (2.5.8).

Lemma 2.5.3. *Suppose that λ_h is the solution of the equilibration problem (2.5.2) for u_h the solution of the finite element approximation problem (2.5.1) then*

$$\varepsilon - \varepsilon^- \leq C|u-u_h|_1^2. \tag{2.5.11}$$

Proof. Let $\hat{\mathbf{p}}_h^*$ be chosen according to Lemma 2.5.2, then

$$-J^c(\nabla u_h + \hat{\mathbf{p}}_h^*) \leq \sup_{\hat{\mathbf{q}}_h \in \hat{\mathcal{Q}}_h} -J^c(\hat{\mathbf{q}}_h) = -J^c(\hat{\mathbf{q}}_h^*),$$

for $\hat{\mathbf{q}}_h^* = \arg\sup_{\hat{\mathbf{q}}_h \in \hat{\mathcal{Q}}_h} -J^c(\hat{\mathbf{q}}_h)$. From this relationship and from the definition of $\hat{\mathbf{p}}_h^*$ we know that $J^c(\hat{\mathbf{q}}_h^*) \leq J^c(\nabla u_h) + J^c(\hat{\mathbf{p}}_h^*)$, because $\sum_{T \in \mathcal{T}_h} \int_T \hat{\mathbf{p}}_h^* \cdot \nabla u_h \, \mathrm{d}\Omega = 0$ from Lemma 2.5.1 and the fact that u_h is a member of $\hat{\mathcal{V}}_h$. Adding the exact energy $\varepsilon = -J^c(\nabla u)$ to each side and recalling that $\varepsilon_h^+ = -J^c(\nabla u_h)$ and $\varepsilon_h^- = -J^c(\hat{\mathbf{q}}_h^*)$ we have our desired result

$$\varepsilon - \varepsilon_h^- \leq \varepsilon - \varepsilon_h^+ + J^c(\hat{\mathbf{p}}_h^*) \leq C|u - u_h|_1^2,$$

where we have again evoked Lemma 2.5.2 in addition to the well known finite element energy error bound. □

2.6 Numerical Results

We close this chapter by considering the unit square, $\Omega = [0,1]^2$, with all homogeneous Dirichlet boundary conditions and uniform forcing $f = 10$. The problem has the analytical solution

$$u(x,y) = \frac{160}{\pi^4} \sum_{\text{odd } i=1}^{\infty} \frac{(-1)^{(i+j)/2-1}}{ij(i^2+j^2)} \cos(i\frac{\pi}{2}x)\cos(j\frac{\pi}{2}y),$$

which yields the analytically exact energy $\varepsilon = -1.757$. We give in Table 2.1 and in Figure 2.6.1 the results of a uniform refinement trial with method parameters $p = 1$ and $q = 2$. The numerical results exhibit the bounding property and

asymptotically approach the optimal convergence rate of 2, corroborating the theoretical results developed in this chapter.

h	$(\varepsilon - \varepsilon_h^-)/\varepsilon$	$(\varepsilon_h^+ - \varepsilon)/\varepsilon$	$\frac{\varepsilon_h^+ - \varepsilon_h^-}{\varepsilon - \varepsilon_h^-}$
$\frac{1}{2}$	0.7982	0.5554	1.70
$\frac{1}{4}$	0.2678	0.1802	1.67
$\frac{1}{8}$	0.0738	0.0489	1.66
$\frac{1}{16}$	0.0190	0.0125	1.66

Table 2.1: Uniformly forced square domain.

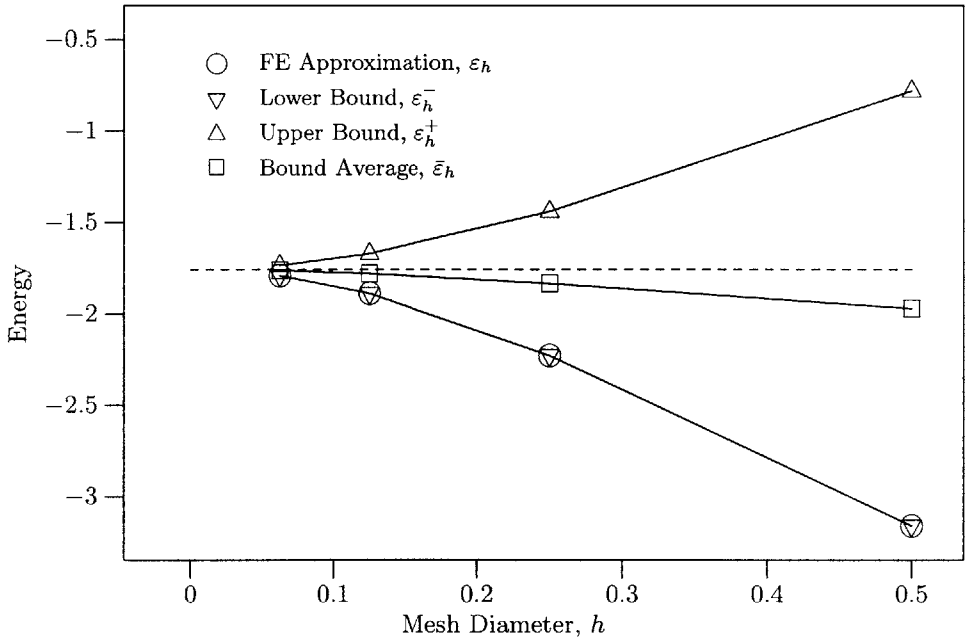

Figure 2.6.1: Uniformly forced square domain convergence history.

Chapter 3

Output Bounds For Poisson's Equation

In this chapter, we will continue to keep the presentation simple by considering only simple linear functional interior outputs of Poisson's equation. In particular, we will develop upper and lower bounds, $s^{\pm}$, on the output quantity

$$s \equiv \int_{\Omega} f^{\mathcal{O}} u \, \mathrm{d}\Omega, \tag{3.0.1}$$

where u is the exact solution of Poisson's equation (2.0.1) and $f^{\mathcal{O}}|_T$ is a member of $\mathbb{P}^r(T)$ for all elements T in $\mathcal{T}_h$. We stress, however, that more interesting outputs, such as boundary fluxes, can also be treated using techniques previously employed in the context of two-level methods (see, for example, the treatment of the normal force output for linear elasticity in [PPP97] or the normal derivative output used in the numerical examples of the next chapter).

3.1 Weak Continuity Reformulation

To begin, we must formulate a generalized analogue to the minimization statement (2.2.2). There are two parts to this task. First, we must replace the intrinsic energy of the variational problem with an energy reformulation of the linear output functional. Second, now that the minimization of the objective functional no longer corresponds to the solution of our original equation, we must explicitly ensure that the minimizer is the solution to our problem by including it as a constraint. Furthermore, to obtain both upper and lower bounds, we consider two cases which vary by the sign of the original output. The resulting pair of constrained minimization statements for the homogeneous[1] Dirichlet boundary problem under consideration are

$$\begin{aligned} \mp s = \inf_{\hat{w}^{\pm}\in\hat{\mathcal{V}}} \; & \mp \int_{\Omega} f^{\mathcal{O}}\hat{w}^{\pm}\,\mathrm{d}\Omega + \frac{\kappa}{2}\left\{\int_{\Omega}\nabla\hat{w}^{\pm}\cdot\nabla(\hat{w}^{\pm}-\bar{u})\,\mathrm{d}\Omega - \int_{\Omega} f(\hat{w}^{\pm}-\bar{u})\,\mathrm{d}\Omega\right\} \\ \text{s.t.} \quad & \int_{\Omega}\nabla\hat{w}^{\pm}\cdot\nabla\psi\,\mathrm{d}\Omega = \int_{\Omega} f\psi\,\mathrm{d}\Omega, \qquad \forall\psi\in\mathcal{V}, \\ & \sum_{T\in\mathcal{T}_h}\int_{\partial T}\sigma_T\hat{w}^{\pm}\lambda\,\mathrm{d}\Gamma = 0, \qquad \forall\lambda\in\Lambda, \end{aligned} \tag{3.1.1}$$

where $\bar{u}$ is any element of space $\mathcal{V}$, and κ is a positive real scaling parameter which serves both as a coefficient providing dimensional consistency in the engineering context and as an additional degree of freedom which we will use to tighten the bounds. The quadratic objective functional has been constructed so that all terms but the desired output functional vanish when $\hat{w}^{\pm}$ is the exact solution, u, while

[1]The extension to non-homogeneous Dirichlet boundaries requires choosing $\bar{u}$ from the set of admissible functions and weakly enforcing the Dirichlet boundary data, u_D, by replacing the continuity constraint with $\sum_{T\in\mathcal{T}_h}\int_{\partial T}\sigma_T\hat{w}^{\pm}\lambda\,\mathrm{d}\Gamma = \sum_{\gamma\in\partial\mathcal{T}_h}\int_{\gamma}\sigma_{T(\gamma)}\lambda\,u_D\,\mathrm{d}\Gamma$, $\forall\lambda\in\Lambda$.

the constraints enforce equilibrium and interelement continuity.

Paraschivoiu, Peraire and Patera [PPP97, PP98] originally proposed this reformulation in the context of two-level output bounding methods which appeal to a second refined but localized finite element approximation and therefore provided bounds only against a refined finite element approximation instead of the exact infinite-dimensional solution. With this constrained minimization reformulation, we can proceed more or less mechanically to apply the ideas from the energy bound to this more general context. The development of the output bound is very close to that for the energy bound, but with the extra burden of carrying an additional Lagrange multiplier for the equilibrium constraint and of managing the concurrent development of both upper and lower bounds on the output, as neither arise implicitly from the finite element discretization.

3.2 Localization by Continuity Relaxation

Considering the Lagrangian of problem (3.1.1),

$$\begin{aligned}
&\mathcal{L}^{\pm}(\hat{w}^{\pm};\psi^{\pm},\lambda^{\pm}) \\
&\equiv \mp\int_{\Omega} f^{\mathcal{O}}\hat{w}^{\pm}\,\mathrm{d}\Omega + \frac{\kappa}{2}\left\{\int_{\Omega}\nabla\hat{w}^{\pm}\cdot\nabla(\hat{w}^{\pm}-\bar{u})\,\mathrm{d}\Omega - \int_{\Omega} f(\hat{w}^{\pm}-\bar{u})\,\mathrm{d}\Omega\right\} \qquad (3.2.1)\\
&\quad + \int_{\Omega} f\psi^{\pm}\,\mathrm{d}\Omega - \int_{\Omega}\nabla\hat{w}^{\pm}\cdot\nabla\psi^{\pm}\,\mathrm{d}\Omega - \sum_{T\in\mathcal{T}_h}\int_{\partial T}\sigma_T\hat{w}^{\pm}\lambda^{\pm}\,\mathrm{d}\Gamma,
\end{aligned}$$

we know, as we did for the energy bound, from the saddle point property of Lagrange multipliers and from the strong duality of convex minimizations that

$$\inf_{\hat{w}^{\pm}\in\hat{\mathcal{V}}} \mathcal{L}^{\pm}(\hat{w}^{\pm};\tilde{\psi}^{\pm},\tilde{\lambda}^{\pm}) \leq \sup_{\substack{\psi^{\pm}\in\mathcal{V}\\ \lambda\in\Lambda}} \inf_{\hat{w}^{\pm}\in\hat{\mathcal{V}}} \mathcal{L}^{\pm}(\hat{w}^{\pm};\psi^{\pm},\lambda^{\pm}) = \mp s.$$

for all $(\tilde{\psi}^{\pm},\tilde{\lambda}^{\pm}) \in \mathcal{V}\times\Lambda$. The lower bounding minimization for a given $\tilde{\lambda}^{\pm}$ and $\tilde{\psi}^{\pm}$ is separable and, for an appropriate choice for $\tilde{\lambda}^{\pm}$, provides non-trivial upper and lower bounds on the exact output s.

3.2.1 Lagrange Multiplier Approximation

We proceed, as we did for the energy bound, to obtain approximate Lagrange multipliers with a finite element discretization of the gradient condition of Equation (3.2.1). Let $\psi_h^{\pm} = \pm\psi_h$, $\lambda_h^{\pm} = \frac{\kappa}{2}\lambda_h^u \pm \lambda_h^{\psi}$, and $\bar{u} = u_h$, all of which we find by solving the following discrete problems

1. Find $u_h \in \mathcal{V}_h$ such that

$$\int_\Omega \nabla u_h \cdot \nabla v \,\mathrm{d}\Omega = \int_\Omega f v \,\mathrm{d}\Omega, \quad \forall v \in \mathcal{V}_h, \tag{3.2.2}$$

2. Find $\psi_h \in \mathcal{V}_h$ such that

$$\int_\Omega \nabla v \cdot \nabla \psi_h \,\mathrm{d}\Omega = -\int_\Omega f^{\mathcal{O}} v \,\mathrm{d}\Omega, \quad \forall v \in \mathcal{V}_h, \tag{3.2.3}$$

3. Find $\lambda_h^u \in \Lambda_h$ such that

$$\sum_{T\in\mathcal{T}_h}\int_{\partial T}\sigma_T\hat{v}\lambda_h^u\,\mathrm{d}\Gamma = \int_\Omega \nabla u_h\cdot\nabla\hat{v}\,\mathrm{d}\Omega - \int_\Omega f\hat{v}\,\mathrm{d}\Omega,\quad \forall\hat{v}\in\hat{\mathcal{V}}_h, \tag{3.2.4}$$

4. Find $\lambda_h^\psi \in \Lambda_h$ such that

$$\sum_{T\in\mathcal{T}_h}\int_{\partial T}\sigma_T\hat{v}\lambda_h^\psi\,\mathrm{d}\Gamma = -\int_\Omega f^{\mathcal{O}}\hat{v}\,\mathrm{d}\Omega - \int_\Omega \nabla\hat{v}\cdot\nabla\psi_h\,\mathrm{d}\Omega,\quad \forall\hat{v}\in\hat{\mathcal{V}}_h. \tag{3.2.5}$$

The first two problems comprise the well known primal-adjoint pair which occur often in output oriented *a posteriori* error estimation techniques as well as in computational approaches to design optimization, while the last two problems are their independent equilibrations. The first and third problems are identical to the global approximation problems required for the energy bound. These particular choices for the Lagrange multipliers ensure a finite lower bound in the saddle point property.

Lemma 3.2.1. *If the Lagrange multipliers* $\psi_h^\pm = \pm\psi_h$ *and* $\lambda_h^\pm = \frac{\kappa}{2}\lambda_h^u \pm \lambda_h^\psi$ *satisfy the equilibration conditions (3.2.4) and (3.2.5), then the minimums*

$$\inf_{\hat{w}^\pm\in\hat{\mathcal{V}}}\mathcal{L}(\hat{w}^\pm;\psi_h^\pm,\lambda_h^\pm)$$

are bounded from below.

Proof. This is true for essentially the same reason that it is true for Lemma 2.3.1. The only algebraic difference being that in the present output bounding case the property $\mathcal{L}^\pm(\hat{w}^{\pm'}+\hat{c};\psi_h^\pm,\lambda_h^\pm) = \mathcal{L}(\hat{w}^{\pm'};\psi_h^\pm,\lambda_h)$ results from the combined action

of both equilibration conditions. □

3.3 Local Dual Subproblem

Restricting our attention to a single elemental subproblem, $T \in \mathcal{T}_h$, we first re-write our local Lagrangian functional in a form suitable for applying the ideas developed for the energy bound. Every term other than the dissipative energy term, $\frac{\kappa}{2}\int_T \nabla w \cdot \nabla w \, \mathrm{d}\Omega$, must not involve derivatives of $\hat{w}^{\pm}$, which we can do in the present case by application of the Green's identity $-\int_T \nabla u \cdot \nabla w \, \mathrm{d}\Omega = \int_T \Delta u \, w \, \mathrm{d}\Omega - \int_{\partial T} \nabla u \cdot \boldsymbol{n} \, w \, \mathrm{d}\Gamma$ to obtain the equivalent local Lagrangian functional

$$\begin{aligned}\mathcal{L}_T^{\pm}(w^{\pm}; \pm\tilde{\psi}, \frac{\kappa}{2}\tilde{\lambda}^u \pm \tilde{\lambda}^{\psi}) &\equiv \frac{\kappa}{2}\int_T \nabla w^{\pm} \cdot \nabla w^{\pm} \, \mathrm{d}\Omega \\ &\quad - \frac{\kappa}{2}\left\{ \int_T (f - \Delta\bar{u}) \, w^{\pm} \, \mathrm{d}\Omega + \int_{\partial T} \left(\sigma_T \tilde{\lambda}^u + \nabla\bar{u} \cdot \boldsymbol{n}\right) w^{\pm} \, \mathrm{d}\Gamma + \int_T f\bar{u} \, \mathrm{d}\Omega \right\} \\ \mp \left\{ \int_T \left(f^{\mathcal{O}} - \Delta\tilde{\psi}\right) w^{\pm} \, \mathrm{d}\Omega + \int_{\partial T} \left(\sigma_T \tilde{\lambda}^{\psi} + \nabla\tilde{\psi} \cdot \boldsymbol{n}\right) w^{\pm} \, \mathrm{d}\Gamma + \int_T f\tilde{\psi} \, \mathrm{d}\Omega \right\}. \quad (3.3.1)\end{aligned}$$

The functional we wish to minimize over $w^{\pm}$ can now be defined as

$$J_T^{\pm}(w^{\pm}) \equiv \frac{\kappa}{2}\int_T \nabla w^{\pm} \cdot \nabla w^{\pm} \, \mathrm{d}\Omega - \int_T f^{\pm} w^{\pm} \, \mathrm{d}\Omega - \int_{\partial T} g^{\pm} w^{\pm} \, \mathrm{d}\Gamma, \quad (3.3.2)$$

for $f^{\pm} \equiv \frac{\kappa}{2}\{f - \Delta\bar{u}\} \pm \{f^{\mathcal{O}} - \Delta\tilde{\psi}\}$ and $g^{\pm} \equiv \frac{\kappa}{2}\{\sigma_T\tilde{\lambda}^u + \nabla\bar{u} \cdot \boldsymbol{n}\} \pm \{\sigma_T\tilde{\lambda}^{\psi} + \nabla\tilde{\psi} \cdot \boldsymbol{n}\}$. Thus, the local relaxed primal minimization once again corresponds to a Poisson problem of the type represented in equation (2.0.1) with Neumann boundary conditions posed on a single element.

As was the case for the energy bound, we do not require, and in general cannot

compute, the exact minimum of this local infinite-dimensional primal subproblem, but we can apply the same technique of dualizing this minimization problem in order to procure a computable lower bounding approximate to it.

Proposition 3.3.1. *If we define the positive functional*

$$J_T^c(\boldsymbol{q}) \equiv \frac{1}{2}\int_T \boldsymbol{q}\cdot\boldsymbol{q}\,\mathrm{d}\Omega, \tag{3.3.3}$$

where $\boldsymbol{q} \in \mathcal{H}(\mathrm{div};T)$*, then we have*

$$J_T^{\pm}(w^{\pm}) \geq -\frac{1}{\kappa}J_T^c(\boldsymbol{q}^{\pm}), \quad \forall w^{\pm} \in \mathcal{H}^1(T),\ \forall \boldsymbol{q}^{\pm} \in \mathcal{Q}^{\pm}(T), \tag{3.3.4}$$

for the set of functions

$$\mathcal{Q}^{\pm}(T) \equiv \Big\{\boldsymbol{q} \in \mathcal{H}(\mathrm{div};T) \;\Big|\; \int_T \nabla\cdot\boldsymbol{q}\,v\,\mathrm{d}\Omega - \int_{\partial T}\boldsymbol{q}\cdot\boldsymbol{n}\,v\,\mathrm{d}\Gamma = -\int_T f^{\pm}\,v\,\mathrm{d}\Omega - \int_{\partial T} g^{\pm}\,v\,\mathrm{d}\Gamma,\ \forall v \in \mathcal{H}^1(T)\Big\}. \tag{3.3.5}$$

Proof. The local dual problem is derived as it was for the energy bound, but with modified data and the addition of the scaling parameter, κ. After expanding the positive expression for $\boldsymbol{q} \in \mathcal{Q}^{\pm}(T)$

$$\frac{1}{2\kappa}\int_T (\boldsymbol{q}^{\pm} - \kappa\nabla w)^2\,\mathrm{d}\Omega \geq 0, \tag{3.3.6}$$

applying a Green's formula, and substituting the constraint from $\mathcal{Q}^{\pm}(T)$, we ob-

tain the expression

$$\frac{1}{2\kappa}\int_T \boldsymbol{q}^{\pm}\cdot\boldsymbol{q}^{\pm}\,\mathrm{d}\Omega+\frac{\kappa}{2}\int_T \nabla w^{\pm}\cdot\nabla w^{\pm}\,\mathrm{d}\Omega-\int_T f^{\pm}\,w^{\pm}\,\mathrm{d}\Omega-\int_{\partial T} g^{\pm}\,w^{\pm}\,\mathrm{d}\Gamma\geq 0. \quad (3.3.7)$$

Identifying $J_T^{\pm}(w^{\pm})$ and $J_T^c(\boldsymbol{q}^{\pm})$ we arrive at the desired expression for the local lower bound. □

As the functional $J_T^{\pm}(w^{\pm})$ only contains the terms from the Lagrangian that depended on $w^{\pm}$, we must reintroduce the constant terms to secure the complete contributions from the local dual subproblems

$$\mp s_T^{\pm}=\int_T f\left(\frac{\kappa}{2}u_h\pm\psi_h\right)\,\mathrm{d}\Omega+\sup_{\boldsymbol{q}^{\pm}\in\mathcal{Q}^{\pm}(T)}-\frac{1}{\kappa}J_T^c(\boldsymbol{q}^{\pm}). \quad (3.3.8)$$

3.3.1 Subproblem Computation

Consider the splitting implied by the definition $\boldsymbol{q}_h=\kappa\nabla\bar{u}+\frac{\kappa}{2}\boldsymbol{q}_h^u\pm\boldsymbol{q}_h^{\psi}$. Propagation of this definition into the elemental subproblem reveals through the linearity of the gradient condition that indeed $\boldsymbol{q}_h^u$ and $\boldsymbol{q}_h^{\psi}$ can be computed independently. The resulting subproblems are

$$\begin{aligned}\boldsymbol{q}_h^u&=\arg\inf_{\boldsymbol{q}_h\in\mathcal{Q}_h^u(T)}J^c(\boldsymbol{q}_h),\\ \boldsymbol{q}_h^{\psi}&=\arg\inf_{\boldsymbol{q}_h\in\mathcal{Q}_h^{\psi}(T)}J^c(\boldsymbol{q}_h),\end{aligned} \quad (3.3.9)$$

for the dual feasible approximation sets

$$\mathcal{Q}_h^u(T) \equiv \left\{ \boldsymbol{q} \in (\mathbb{P}^q(T))^d \;\middle|\; \int_T \nabla \cdot \boldsymbol{q}\, v \,\mathrm{d}\Omega - \int_{\partial T} \boldsymbol{q} \cdot \boldsymbol{n}\, v \,\mathrm{d}\Gamma = -\int_T (f + \Delta u_h)\, v \,\mathrm{d}\Omega \right.$$
$$\left. - \int_{\partial T} (\sigma_T \lambda_h^u - \nabla u_h \cdot \boldsymbol{n})\, v \,\mathrm{d}\Gamma,\ \forall v \in \mathcal{H}^1(T) \right\},$$
$$\mathcal{Q}_h^\psi(T) \equiv \left\{ \boldsymbol{q} \in (\mathbb{P}^q(T))^d \;\middle|\; \int_T \nabla \cdot \boldsymbol{q}\, v \,\mathrm{d}\Omega - \int_{\partial T} \boldsymbol{q} \cdot \boldsymbol{n}\, v \,\mathrm{d}\Gamma = -\int_T (f^{\mathcal{O}} - \Delta \psi_h)\, v \,\mathrm{d}\Omega \right.$$
$$\left. - \int_{\partial T} (\sigma_T \lambda_h^\psi + \nabla \psi_h \cdot \boldsymbol{n})\, v \,\mathrm{d}\Gamma,\ \forall v \in \mathcal{H}^1(T) \right\}, \tag{3.3.10}$$

in which we have again chosen $\bar{u} = u_h$ commensurate with our choice for the approximate multipliers. As the additional terms in the data of the dual feasibility constraint are just polynomial functions in the local finite element basis, there are no difficulties in choosing our dual approximation sets in this manner. The solvability of these subproblems is addressed by the following result.

Lemma 3.3.2. *Suppose the forcing function $f|_T$ and output function $f^{\mathcal{O}}|_T$ are members of $\mathbb{P}^r(T)$, that λ_h^u satisfies (3.2.4), and that λ_h^ψ satisfies (3.2.5), then there exists at least one dual feasible function $\boldsymbol{q}_h^u$ that is a member of $\mathcal{Q}_h^u(T)$ and one dual feasible function $\boldsymbol{q}_h^\psi$ that is a member of $\mathcal{Q}_h^\psi(T)$, for $q \geq p$ and $q > r$.*

Proof. Applying Green's formula to the u_h Laplacian term in the constraint data for $\mathcal{Q}_h^u(T)$ of (3.3.10) and duplicating the proof of Lemma 2.4.2 with the resulting constraint data reveals the compatibility condition

$$\int_{\partial T} \sigma_T \lambda_h^u \,\mathrm{d}\Gamma = -\int_T f \,\mathrm{d}\Omega, \tag{3.3.11}$$

which is satisfied by our choice for λ_h^u as can be seen by choosing $\hat{v} = \text{const}$ on T in the equilibration condition (3.2.4). The same argument holds for the adjoint

dual subproblem, yielding the analogous compatibility condition

$$\int_{\partial T} \sigma_T \lambda_h^{\psi} \, \mathrm{d}\Gamma = -\int_T f^{\mathcal{O}} \, \mathrm{d}\Omega, \tag{3.3.12}$$

for $f^{\mathcal{O}}$ and λ_h^{ψ}. □

With the subproblem splitting just defined, the aggregated contributions to the upper and lower bounds become

$$\begin{aligned} s_h^{\pm} &= \mp \int_\Omega f \left(\frac{\kappa}{2} u_h \pm \psi_h \right) \mathrm{d}\Omega \pm \frac{1}{\kappa} J^c(\kappa \nabla u_h + \frac{\kappa}{2} \hat{\mathbf{q}}_h^u \pm \hat{\mathbf{q}}_h^{\psi}) \\ &= \mp \int_\Omega f \left(\frac{\kappa}{2} u_h \pm \psi_h \right) \mathrm{d}\Omega \pm \frac{\kappa}{2} \int_\Omega \nabla u_h \cdot \nabla u_h \, \mathrm{d}\Omega + \int_\Omega (\frac{\kappa}{2} \hat{\mathbf{q}}_h^u \pm \hat{\mathbf{q}}_h^{\psi}) \cdot \nabla u_h \, \mathrm{d}\Omega \\ &\quad + \frac{1}{2} \int_\Omega \hat{\mathbf{q}}_h^u \cdot \hat{\mathbf{q}}_h^{\psi} \, \mathrm{d}\Omega \pm \frac{\kappa}{4} J^c(\hat{\mathbf{q}}_h^u) \pm \frac{1}{\kappa} J^c(\hat{\mathbf{q}}_h^{\psi}) \\ &= -\int_\Omega f \psi_h \, \mathrm{d}\Omega + \frac{1}{2} \int_\Omega \hat{\mathbf{q}}_h^u \cdot \hat{\mathbf{q}}_h^{\psi} \, \mathrm{d}\Omega \pm \frac{\kappa}{4} J^c(\hat{\mathbf{q}}_h^u) \pm \frac{1}{\kappa} J^c(\hat{\mathbf{q}}_h^{\psi}), \end{aligned}$$

in which we have invoked (3.2.2) with $v = u_h$ as well as used orthogonality relationships analogous to that proved in Lemma 2.5.1.

3.4 Output Bound Procedure

The introduction of the scaling parameter κ allows us to optimize the sharpness of the computed bounds in addition to providing dimensional consistency. From the previous section we have the expression for the upper and lower output bounds

$$s_h^{\pm} = \bar{s}_h \pm \kappa z_h^u \pm \frac{1}{\kappa} z_h^{\psi},$$

where

$$\bar{s}_h = \frac{1}{2}\int_\Omega \hat{\mathbf{q}}_h^u \cdot \hat{\mathbf{q}}_h^\psi \,\mathrm{d}\Omega - \int_\Omega f\psi_h \,\mathrm{d}\Omega, \qquad z_h^u = \frac{1}{4}J^c(\hat{\mathbf{q}}_h^u), \qquad z_h^\psi = J^c(\hat{\mathbf{q}}_h^\psi), \tag{3.4.1}$$

Maximizing the lower bound and minimizing the upper bound with respect to κ yields the optimal value $\kappa^2 = z_h^\psi / z_h^u$.

The complete method with optimal scaling for upper and lower bounds on linear functional outputs can now be written as three steps:

1. *Global Approximation:*

   Find $u_h \in \mathcal{V}_h$ such that

$$\int_\Omega \nabla u_h \cdot \nabla v \,\mathrm{d}\Omega = \int_\Omega f v \,\mathrm{d}\Omega, \quad \forall v \in \mathcal{V}_h, \tag{3.4.2}$$

   and find $\psi_h \in \mathcal{V}_h$ such that

$$\int_\Omega \nabla v \cdot \nabla \psi_h \,\mathrm{d}\Omega = -\int_\Omega f^{\mathcal{O}} v \,\mathrm{d}\Omega, \quad \forall v \in \mathcal{V}_h. \tag{3.4.3}$$

2. *Global Equilibration:*

   Find $\lambda_h^u \in \Lambda_h$ such that

$$\sum_{T\in\mathcal{T}_h} \int_{\partial T} \sigma_T \hat{v} \lambda_h^u \,\mathrm{d}\Gamma = \int_\Omega \nabla u_h \cdot \nabla \hat{v} \,\mathrm{d}\Omega - \int_\Omega f\hat{v} \,\mathrm{d}\Omega, \quad \forall \hat{v} \in \hat{\mathcal{V}}_h, \tag{3.4.4}$$

   and find $\lambda_h^\psi \in \Lambda_h$ such that

$$\sum_{T\in\mathcal{T}_h} \int_{\partial T} \sigma_T \hat{v} \lambda_h^\psi \,\mathrm{d}\Gamma = -\int_\Omega f\hat{v} \,\mathrm{d}\Omega - \int_\Omega \nabla\hat{v} \cdot \nabla\psi_h \,\mathrm{d}\Omega, \quad \forall \hat{v} \in \hat{\mathcal{V}}_h. \tag{3.4.5}$$

3. *Local Dual Subproblems:*

   Find $\hat{\mathbf{q}}_h^u$ such that

$$\hat{\mathbf{q}}_h^u = \arg \inf_{\hat{\mathbf{q}}_h \in \hat{\mathcal{Q}}_h^u} J^c(\hat{\mathbf{q}}_h), \tag{3.4.6}$$

   find $\hat{\mathbf{q}}_h^\psi$ such that

$$\hat{\mathbf{q}}_h^\psi = \arg \inf_{\hat{\mathbf{q}}_h \in \hat{\mathcal{Q}}_h^\psi} J^c(\hat{\mathbf{q}}_h), \tag{3.4.7}$$

   and, from equation (3.4.1) and the optimal κ, calculate

$$s_h^\pm = \bar{s}_h \pm 2\sqrt{z_h^u z_h^\psi}. \tag{3.4.8}$$

The local dual subproblems for the output bounds can be solved in the same manner as the local energy dual subproblems. The important point being that once the finite element approximations u_h and ψ_h have been computed, the solutions can be equilibrated and quantitative bounds computed on the exact output to the infinite-dimensional continuum equation with asymptotically linear cost in the size of the finite element discretization and in parallel.

3.4.1 Properties of the Output Bounds

The upper and lower bounding properties are direct consequences of the saddle point property of the relaxed constrained minimization reformulation (3.1.1) and the local dual property of Proposition 3.3.1. The following proposition addresses the accuracy of the computed bounds by showing that the bounds will converge at the optimal rate when both the primal and adjoint finite element approximations are in the asymptotic convergence regime.

Proposition 3.4.1. *Suppose that u_h, ψ_h, λ_h^u, and λ_h^ψ are solutions of the above finite element approximation problems and equilibration problems, then*

$$\begin{aligned} s - s_h^- &\leq C|u - u_h|_1|\psi - \psi_h|_1, \\ s_h^+ - s &\leq C|u - u_h|_1|\psi - \psi_h|_1. \end{aligned} \tag{3.4.9}$$

Proof. Applying the definitions from the procedure, we know that the lower *a posteriori* bound, for instance, itself has the bound

$$s - s_h^- \leq s_h^+ - s_h^- = 2\sqrt{z_h^u z_h^\psi}.$$

The arguments of Lemma 2.5.2 can be applied to the z_h^u and z_h^ψ factors to show that they are bounded by $C|u - u_h|_1^2$ and $C|\psi - \psi_h|_1^2$, respectively. □

3.4.2 Computational Complexity

The first step of the procedure solves two standard finite element problems. The finite element solver has an asymptotic complexity of $\mathcal{O}(N^k)$, where N is the number of unknowns in the discretization and $1 \leq k \leq 3$ is a property of the solver. A fully dense direct solver would provide the worst case complexity of $k = 3$. Any solution method must visit each unknown at least once, in order to assign the solution, thus the best case complexity is $k = 1$. Using Ladevèze's method and assuming that the number of elements sharing a vertex is bounded from above, the second step can be performed by solving V small local patch subproblems, where V is the number of vertices in the triangulation. This yields an asymptotic complexity of $\mathcal{O}(V)$ for the equilibration step. Finally, solving a

sequence of small local elemental subproblems results in an asymptotic complexity of $\mathcal{O}(K)$. As we have assumed that the number of elements sharing a vertex is bounded from above, the asymptotic complexity of the latter two steps of the procedure can be stated as $\mathcal{O}(V)$. We deduce that the leading order asymptotic complexity of the entire procedure is $\mathcal{O}(N^k)$ since $V \leq N$ and $k \geq 1$. The important point being that the output bound computation does not increase the asymptotic cost of the approximation. Moreover, the output bound computation delivers certainty, which cannot be obtained by merely increasing N.

More relevant than the number of unknowns an approximation requires, however, is the desired precision of the approximation. Assuming that the finite element approximation achieves $\mathcal{O}(h^p)$ convergence in the $\mathcal{H}^1$-norm measure of the error for both the solution and the adjoint, Proposition 3.4.1 informs us that the bound gap will have $\mathcal{O}(h^{2p})$ asymptotic convergence. For a desired precision, Δ_{tol}, we have $\Delta_{\text{tol}} \sim h^{2p}$. Therefore the required element diameter, h, for a given precision will be $\mathcal{O}(\Delta_{\text{tol}}^{\frac{1}{2p}})$. Finally, uniform refinement yields $N \sim \frac{1}{h^d}$ and thus the asymptotic computational complexity of the complete procedure to produce an output approximation of a prescribed accuracy is $\mathcal{O}\left(\Delta_{\text{tol}}^{-\frac{dk}{2p}}\right)$. The important conclusion from this analysis is that the method can compute approximate outputs of prescribed precision in polynomial time. For example, a problem posed on a two-dimensional domain and approximated with a linear finite element approximation has an asymptotic computational complexity of $\mathcal{O}(\Delta_{\text{tol}}^{-k})$.

3.5 Adaptive Refinement

The elemental subproblems provide local error information which can be used as an indicator for mesh adaptivity via the elemental contribution to the bound gap, $\Delta_T = \frac{\kappa}{4} J_T^c(\boldsymbol{q}_h^u) + \frac{1}{\kappa} J_T^c(\boldsymbol{q}_h^\psi)$. The elemental bound gaps can serve as informative mesh adaptivity indicators for controlling the error in the *output*, as was done in [PP97] for a two-level error bound method. Adaptive indicators have long been the principle business of error estimators. For example, see [Ver94, ODRW89] for energy-norm error measures, and more recently [BR96a, BKR00, RS97, SBD+00] for more general measures. The principle business of the method we have presented, however, is to certify the precision of an approximate output. Nevertheless, the local bound gap contribution can be used to improve both the precision of the output and the sharpness of the certificate using adaptive refinement.

It is well known that the error in a finite element solution contains a local contribution as well as a global contribution called the pollution error which both need to be taken into account for effective adaptive refinement [BSUG95b, Ain99]. In addition, sophisticated adaptive algorithms attempt to predict the optimal element diameter in order to both reduce the number of adaptive steps required and the number of elements contained in the final mesh. We do not attempt to do either of these things, but instead provide a simple demonstration of the potential for the local bound gap contributions to act as refinement indicators.

At each level of refinement, only elements for which $\Delta_T > \Delta_{\text{tol}}/K$ are refined, where Δ_{tol} is a user specified tolerance for the precision of the output from the global approximation and K is the number of elements in the triangulation at that level. The meshes are generated and adaptively refined using the freely available

Triangle mesh generator [She96]. By preferentially refining the mesh elements contributing more than a target average error contribution, we obtain a simple but effective adaptive strategy.

3.6 Numerical Results

We verify the method numerically for three cases: constant forcing on the unit square, linear forcing on the unit square, and zero forcing on an L-shaped domain with a corner singularity. Linear finite elements, $p = 1$, and quadratic subproblems, $q = 2$, are employed with the domain average output

$$s = \int_\Omega f^{\mathcal{O}} u \, \mathrm{d}\Omega,$$

where $f^{\mathcal{O}} = \text{const}$, for all cases.

All three cases have analytically exact solutions with which we are able to verify the method and calculate the effectivities of the bounds,

$$\theta^{\pm} = \frac{|s - s_h^{\pm}|}{|s - s_h|}, \tag{3.6.1}$$

which indicate the sharpness by comparing the error in the bounds to the error in the finite element approximation. The results are summarized in Table 3.1.

	Uniformly Forced Square				Linearly Forced Square				Corner Singularity			
h	s^-	s^+	θ^-	θ^+	s^-	s^+	θ^-	θ^+	s^-	s^+	θ^-	θ^+
$\frac{1}{2}$	0.156	0.632	1.0	1.4	0.860	1.276	5.1	2.9	0.702	0.897	5.1	6.0
$\frac{1}{4}$	0.288	0.446	1.0	1.5	1.050	1.171	5.7	3.5	0.761	0.829	4.3	5.1
$\frac{1}{8}$	0.334	0.377	1.0	1.5	1.106	1.137	5.9	3.8	0.781	0.805	3.6	4.4
$\frac{1}{16}$	0.347	0.358	1.0	1.5	1.120	1.128	6.0	3.8	0.788	0.797	3.1	3.9

Table 3.1: Output bounds and effectivities for three numerical test cases.

3.6.1 Uniformly Forced Square Domain

The first case is a uniformly forced unit square domain with $f = f^{\mathcal{O}} = \sqrt{10}$. The analytical solution is given by

$$u(x,y) = \frac{16\sqrt{10}}{\pi^4} \sum_{\text{odd } i=1}^{\infty} \frac{(-1)^{(i+j)/2-1}}{ij(i^2+j^2)} \cos(i\frac{\pi}{2}x)\cos(j\frac{\pi}{2}y),$$

This case is special in that the forcing and output are identical and the boundary data is homogeneous, leading to primal and adjoint problem data which differ by only a sign. It is well known that for this special case, called compliance, the finite element approximation for the output is a lower bound. The numerical results demonstrate that our method, while more expensive, does no worse than the inherent bound for this special case. The results for both the finite element approximation and the output bounds asymptotically approach the optimal finite element convergence rate of $O(h^2)$. This example also evinces that the bound average, $\bar{s}_h$, can sometimes be a more accurate output approximation than the that from the finite element approximation.

The uniformly forced Poisson equation posed on a two-dimensional domain models the cross-sectional velocity distribution for viscous duct flow. Figure 3.6.2 illustrates how the method might be used to study the dependency of an output

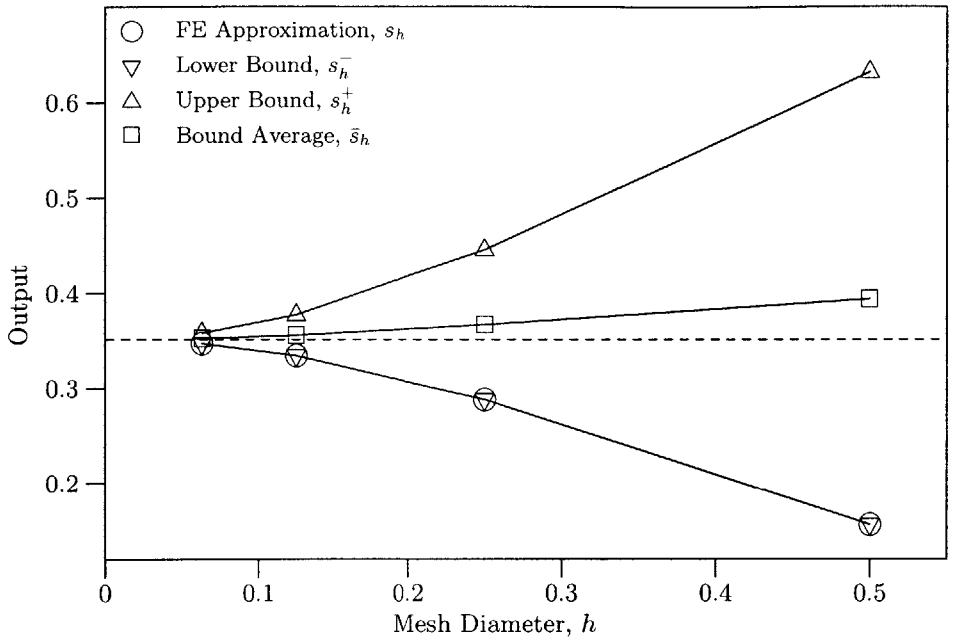

Figure 3.6.1: Uniformly forced square domain convergence history.

on a parameter. In the context of duct flow, the uniform output we have been considering calculates the flow rate. The upper and lower bounds our indicated by horizontal bars, the bound average by a black box, the finite element approximation by a hollow circle and the analytically exact solution by a grey line.

3.6.2 Linearly Forced Square Domain

The second case is a linearly forced square domain with $f^{\mathcal{O}} = 1$, and the forcing and non-homogeneous boundary conditions chosen to produce the exact solution

$$u(x, y) = \frac{3}{2}y^2(1 - y) + 4xy.$$

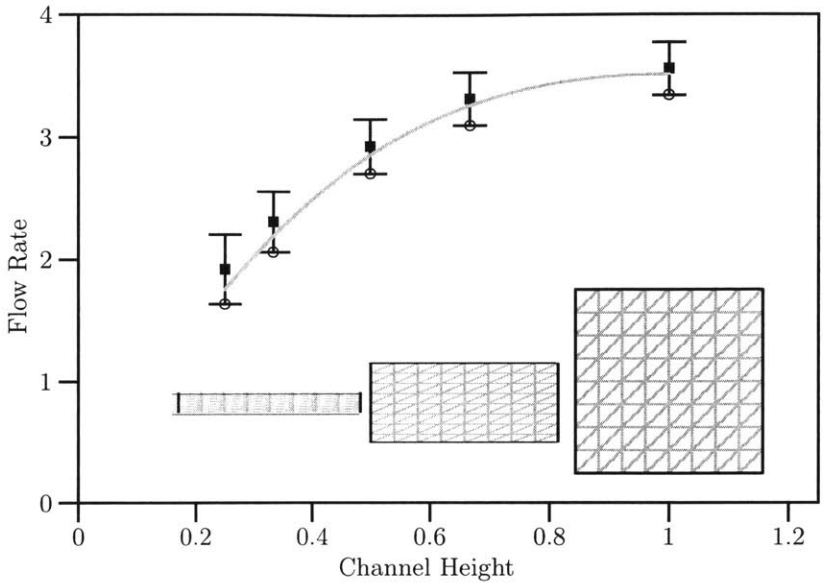

Figure 3.6.2: The dependency of flow rate through a viscous duct on channel height.

As this test case is not a special case, the convergence histories of Figure 3.6.3 depict the more general situation in which none of the computed quantities coincide. Whereas in the first example we saw that the bound average can possibly be a more accurate output approximation than the finite element approximation, in this example we see that this is definitely not always true since the finite element approximation for the output is 0.5% better. As for the first example, the results for both the finite element approximation and the output bounds asymptotically approach the optimal finite element convergence rate of $O(h^2)$.

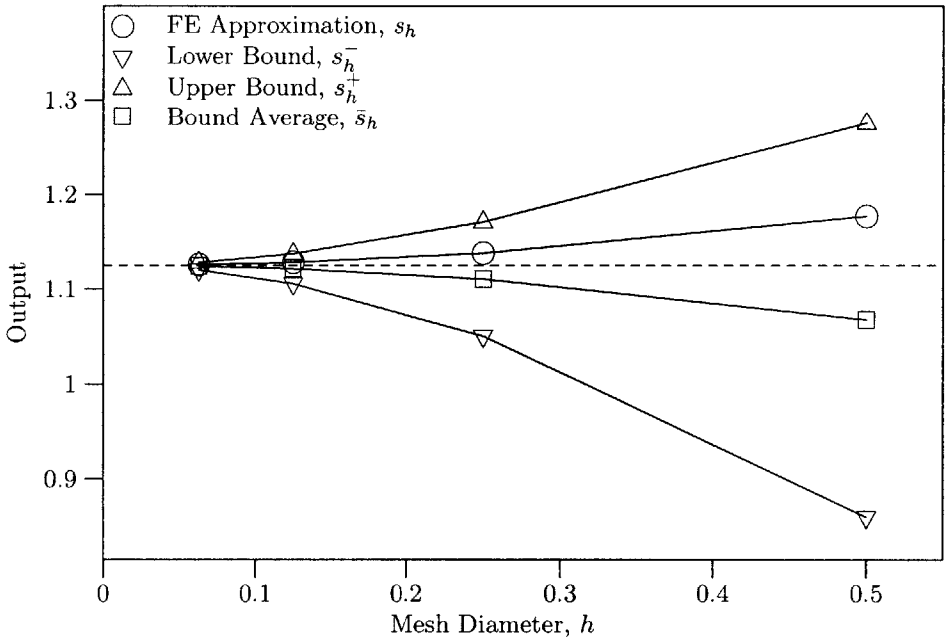

Figure 3.6.3: Linearly forced square domain convergence history.

3.6.3 Unforced Corner Domain

Last, we consider the Laplace equation on a non-convex domain with $f^{\mathcal{O}} = 1$. The domain is the standard L-shaped domain with a reentrant corner. The Dirichlet boundary conditions were chosen to produce the solution

$$u(r, \phi) = r^{\frac{2}{3}} \sin \frac{2}{3}\phi,$$

where r is the distance from the corner point and ϕ is the angle from the upper surface of the corner.

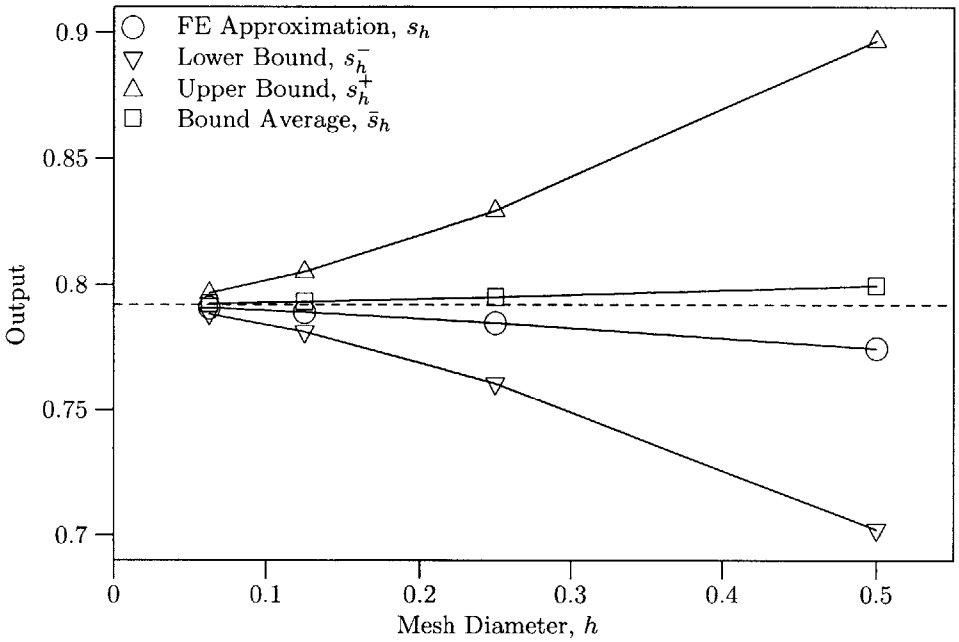

Figure 3.6.4: Unforced corner domain convergence history.

In this example we demonstrate that the bounds are valid even for problems with singularities. The results for both the finite element approximation and the

output bounds asymptotically approach the optimal finite element convergence rate of $O(h^{\frac{4}{3}})$ for elliptic problems posed on a domain with right-angled reentrant corner [SF73]. Once again we see that the bound average has the potential to be a better output approximation than the finite element method.

Finally, Figure 3.6.5 displays the end results of the simple adaptive strategy previously outlined applied to the unforced corner domain problem.

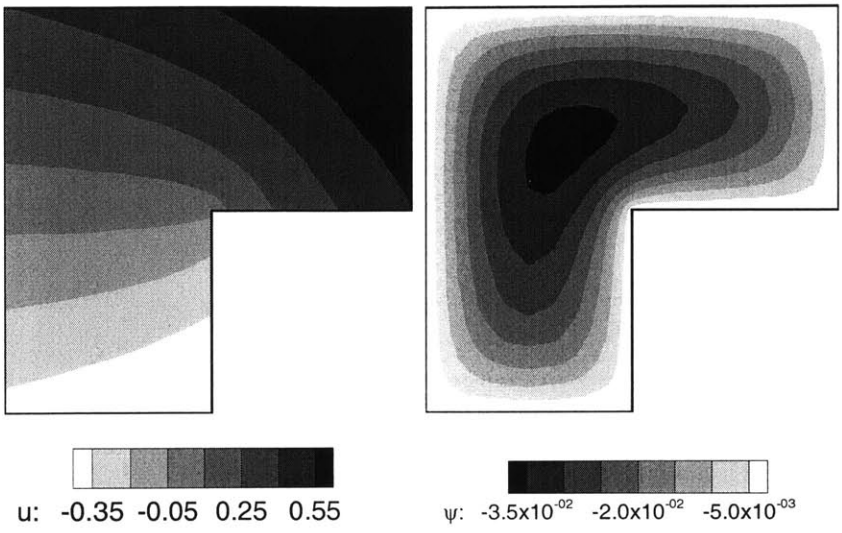

(a) Adaptive solution field.

(b) Adaptive adjoint field.

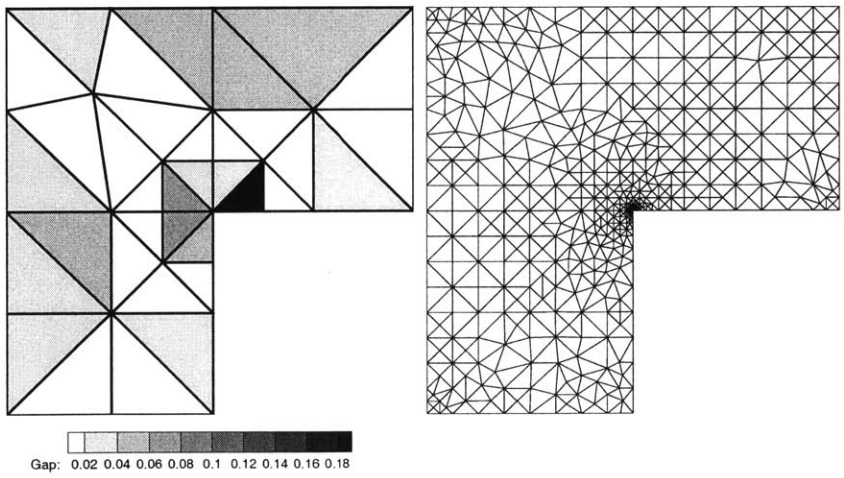

(c) Elemental bound gap contributions on intermediate mesh.

(d) Final adaptive mesh.

Figure 3.6.5: Unforced corner domain adaptive solutions, local indicators and meshes.

Chapter 4

Output Bounds for the Advection-Diffusion-Reaction Equation

We will consider the steady scalar diffusion-dominated advection-diffusion-reaction equation posed on a polygonal domain Ω in d spatial dimensions with boundary Γ composed of complementary regions Γ^{D} and Γ^{N}. The problem is written in weak form as: find $u \in \mathcal{U}$ such that

$$a(u, v) = \ell(v), \quad \forall v \in \mathcal{V}, \tag{4.0.1}$$

with the coercive non-symmetric bilinear form defined as

$$a(w, v) = \int_{\Omega} \nu \nabla w \cdot \nabla v + \mu w v + (\boldsymbol{\alpha} \cdot \nabla w)\, v \, \mathrm{d}\Omega, \tag{4.0.2}$$

for a strictly positive real coefficient $\nu \in \mathcal{L}^\infty(\Omega)$, a nonnegative real coefficient $\mu \in \mathcal{L}^\infty(\Omega)$, and a prescribed vector field $\boldsymbol{\alpha} \in \mathcal{H}(\mathrm{div};\Omega)$ which is assumed for simplicity to be incompressible, $\nabla\cdot\boldsymbol{\alpha} = 0$. The set of admissible functions is defined as $\mathcal{U}(\Omega) \equiv \{\, v \in \mathcal{H}^1(\Omega) \mid v|_{\Gamma^{\mathrm{D}}} = u_D \,\}$, with Dirichlet boundary data $u_D \in \mathcal{H}^{\frac{1}{2}}(\Gamma^{\mathrm{D}})$, and the space of test functions is defined as $\mathcal{V}(\Omega) \equiv \{\, v \in \mathcal{H}^1(\Omega) \mid v|_{\Gamma^{\mathrm{D}}} = 0 \,\}$. Additionally, we require the prescription of the solution field on inflow boundaries, that is $\Gamma^- \subset \Gamma^{\mathrm{D}} \subset \Gamma$ for $\Gamma^- = \{\mathbf{x} \in \Gamma \mid \boldsymbol{\alpha}\cdot\boldsymbol{n}(\mathbf{x}) \leq 0\}$. The linear forcing functional

$$\ell(v) = \int_\Omega fv \,\mathrm{d}\Omega + \int_{\Gamma^{\mathrm{N}}} gv \,\mathrm{d}\Gamma, \tag{4.0.3}$$

includes both interior $f \in \mathcal{H}^{-1}(\Omega)$ and Neumann boundary $g \in \mathcal{H}^{-\frac{1}{2}}(\Gamma^{\mathrm{N}})$ contributions.

We are not directly interested in the field solution u, however, but in bounded linear functional outputs from it, $s = \ell^{\mathcal{O}}(u)$. In particular, we will develop upper and lower bounds on the outputs produced by linear functionals such as

$$\ell^{\mathcal{O}}(w) = \int_{\Omega^{\mathcal{O}}} f^{\mathcal{O}} w \,\mathrm{d}\Omega + \int_{\Gamma^{\mathcal{O}}} g^{\mathcal{O}} w \,\mathrm{d}\Gamma, \tag{4.0.4}$$

for $f^{\mathcal{O}} \in \mathcal{H}^{-1}(\Omega^{\mathcal{O}})$ and $g^{\mathcal{O}} \in \mathcal{H}^{-\frac{1}{2}}(\Gamma^{\mathcal{O}})$.

In order to guarantee bounds for any level of refinement, the method presented in this chapter requires that the coefficients ν, μ, and $\boldsymbol{\alpha}$, and forcing data f, $f^{\mathcal{O}}$, g and $g^{\mathcal{O}}$ are all piecewise polynomial. In addition, we will consider only constant coefficients ν and μ for simplicity.

4.1 Constrained Minimization Reformulation

In the context of the Poisson problem, we reformulated the model problem as a constrained minimization with weakly enforced continuity in order to localize the bounds computations and to obtain bounds on more informative output quantities than the abstract energy. In the present context of a non-symmetric operator, the reformulation also provides the means by which we can treat problems without an intrinsic minimization principle.

4.1.1 Weak Continuity

As before, we begin by introducing a triangulation of the domain, $\mathcal{T}_h$, into non-overlapping open subdomains, T, called elements, for which $\bigcup_{T\in\mathcal{T}_h} \overline{T} = \bar{\Omega}$. We denote by ∂T the edges constituting the boundary of a single element T, and by $\partial\mathcal{T}_h$ the network of all edges in the mesh. On this triangulation, we introduce the broken space

$$\hat{\mathcal{V}} \equiv \left\{ v \in \mathcal{L}^2 \,|\, v|_T \in \mathcal{H}^1(T),\ \forall T \in \mathcal{T}_h \right\}. \tag{4.1.1}$$

in which the continuity of $\hat{\mathcal{V}}$ is broken across the mesh edges, $\partial\mathcal{T}_h$. Note that the broken space relaxes the Dirichlet boundaries in addition to the interelement continuity so that we have $\mathcal{V} \subset \hat{\mathcal{V}}$ and $\mathcal{U} \subset \hat{\mathcal{V}}$.

We enforce continuity between the elemental subdomains weakly through the bilinear form $b : \hat{\mathcal{V}} \times \Lambda \to \mathbb{R}$

$$b(\hat{w}, \lambda) = \sum_{T\in\mathcal{T}_h} \int_{\partial T} \sigma_T \hat{w} \lambda \, \mathrm{d}\Gamma,$$

where, for $T_{\mathrm{N}} \in \mathcal{T}_h$ and an arbitrary ordering of the elements, $T < T_{\mathrm{N}}$,

$$\sigma_T(x) = \begin{cases} -1 & x \in \overline{T} \cap \overline{T}_{\mathrm{N}}, T < T_{\mathrm{N}} \\ +1 & \text{otherwise} \end{cases} \tag{4.1.2}$$

is a constant on each edge, and the edge functions λ are members of the dual trace space $\Lambda = \prod_{T \in \mathcal{T}_h} \mathcal{H}^{-\frac{1}{2}}(\partial T)$.

In addition to weak enforcement of interelement continuity, the Dirichlet data will also be enforced weakly in our reformulation through the forcing provided by the linear functional $\ell^D : \Lambda \to \mathbb{R}$

$$\ell^D(\lambda) = \sum_{T \in \mathcal{T}_h} \int_{\Gamma_T^{\mathrm{D}}} \sigma_T u_D \lambda \, \mathrm{d}\Gamma, \tag{4.1.3}$$

so that $b(\hat{w}, \lambda) = \ell^D(\lambda)$ for all $\hat{w} \in \mathcal{U}$ and $\lambda \in \Lambda$.

4.1.2 Operator Decomposition

A non-symmetric operator can be split into symmetric, $a^{\mathrm{s}}(w, v) = a^{\mathrm{s}}(v, w)$, and antisymmetric, $a^{\mathrm{ss}}(w, v) = -a^{\mathrm{ss}}(v, w)$, contributions

$$a^{\mathrm{s}}(w, v) = \frac{1}{2}\left[a(w, v) + a^\star(v, w)\right], \quad a^{\mathrm{ss}}(w, v) = \frac{1}{2}\left[a(w, v) - a^\star(v, w)\right], \tag{4.1.4}$$

where $a^\star(v, w)$ is the formal adjoint of $a(w, v)$ for $w \in \mathcal{U}$ and $v \in \mathcal{V}$. Integration by parts yields $a(u, w) = a^\star(w, u) + C^\star$, from which we note that $a^{\mathrm{ss}}(w, w) = \frac{1}{2}C^\star$ and thus $a(w, w) = a^{\mathrm{s}}(w, w) + \frac{1}{2}C^\star$. Additionally, we note from the above that $a(v, w) = a^{\mathrm{s}}(v, w) + a^{\mathrm{ss}}(v, w) = a^{\mathrm{s}}(w, v) - a^{\mathrm{ss}}(w, v)$. It is easily shown for the

advection-diffusion-reaction equation that

$$\begin{aligned} a^\star(v,w) &= \int_\Omega \nu \nabla v \cdot \nabla w + \mu v w - (\boldsymbol{\alpha} \cdot \nabla v)\, w \,\mathrm{d}\Omega + \int_{\Gamma^{\mathrm{N}}} v\,(\boldsymbol{\alpha} \cdot \boldsymbol{n})\, w \,\mathrm{d}\Gamma, \\ C^\star &= \int_{\Gamma^{\mathrm{D}}} (\boldsymbol{\alpha} \cdot \boldsymbol{n})\, u_D^2 \,\mathrm{d}\Gamma, \end{aligned} \tag{4.1.5}$$

and therefore

$$\begin{aligned} a^{\mathrm{s}}(w,v) &= \int_\Omega \nu \nabla w \cdot \nabla v + \mu w v \,\mathrm{d}\Omega + \frac{1}{2}\int_{\Gamma^{\mathrm{N}}} w\,(\boldsymbol{\alpha} \cdot \boldsymbol{n})\, v \,\mathrm{d}\Gamma, \\ a^{\mathrm{ss}}(w,v) &= \int_\Omega (\boldsymbol{\alpha} \cdot \nabla w)\, v \,\mathrm{d}\Omega - \frac{1}{2}\int_{\Gamma^{\mathrm{N}}} w\,(\boldsymbol{\alpha} \cdot \boldsymbol{n})\, v \,\mathrm{d}\Gamma. \end{aligned} \tag{4.1.6}$$

4.1.3 Constrained Minimization Statement

Using the above definitions we can write the following energy-like functional $\varepsilon : \hat{\mathcal{V}} \to \mathbb{R}$

$$\varepsilon(\hat{w}) = a^{\mathrm{s}}(\hat{w},\hat{w}) + \frac{1}{2}C^\star - \ell(\hat{w}) + \ell(\bar{u}) - a(\hat{w},\bar{u}), \tag{4.1.7}$$

where $\bar{u}$ is a member of $\mathcal{U}$. This functional has two essential properties. First, it is coercive on the space $\hat{\mathcal{V}}$ for $\mu > 0$ and for $\mu = 0$ is coercive on the quotient space $\hat{\mathcal{V}} \setminus \hat{\mathbb{P}}^0$, where $\hat{\mathbb{P}}^0$ is the space of constants over each element. Second, it reduces to zero when $\hat{w} = u$.

The weakly continuous constrained minimization problem for the non-symmetric model problem can now be written as

$$\begin{aligned} \mp s = \inf_{\hat{w}^\pm \in \hat{\mathcal{V}}} \quad & \mp \ell^{\mathcal{O}}(\hat{w}^\pm) + \frac{\kappa}{2}\varepsilon(\hat{w}^\pm) \\ \text{s.t.} \quad & a(\hat{w}^\pm,\psi) = \ell(\psi), \qquad \forall \psi \in \mathcal{V}, \\ & b(\hat{w}^\pm,\lambda) = \ell^D(\lambda), \qquad \forall \lambda \in \Lambda, \end{aligned} \tag{4.1.8}$$

where κ is a strictly positive real scaling parameter which provides dimensional consistency as well as an additionally degree of freedom which we will later use to tighten the bounds. This apparently trivial constrained minimization reformulation, first introduced in [PP98, PPP97] and whose constraints also arise in the context hybrid finite element methods [BF91], serves as the launching point for developing our method.

4.1.4 Localization by Lagrangian Relaxation

The above constrained minimization (4.1.8) has the Lagrangian: $L^{\pm} : \hat{\mathcal{V}} \times \mathcal{V} \times \Lambda \rightarrow \mathbb{R}$

$$\begin{aligned} L^{\pm}(\hat{w}^{\pm}; \tilde{\psi}^{\pm}, \tilde{\lambda}^{\pm}) = & \mp \ell^{\mathcal{O}}(\hat{w}^{\pm}) \\ & + \frac{\kappa}{2}\left\{ a^{\mathrm{s}}(\hat{w}^{\pm}, \hat{w}^{\pm}) + \frac{1}{2}C^{\star} - \ell(\hat{w}^{\pm}) + \ell(\bar{u}) - a(\hat{w}^{\pm}, \bar{u}) \right\} \\ & + \ell(\tilde{\psi}^{\pm}) - a(\hat{w}^{\pm}, \tilde{\psi}^{\pm}) + \ell^{D}(\tilde{\lambda}^{\pm}) - b(\hat{w}^{\pm}, \tilde{\lambda}^{\pm}), \end{aligned} \tag{4.1.9}$$

for given candidate Lagrange multipliers $\tilde{\psi}^{\pm} \in \mathcal{V}$ and $\tilde{\lambda}^{\pm} \in \Lambda$. The Lagrangian saddle point property for the constrained minimization reformulation engenders the following relationships for all $(\tilde{\psi}^{\pm}, \tilde{\lambda}^{\pm}) \in \mathcal{V} \times \Lambda$

$$\inf_{\hat{w}^{\pm} \in \hat{\mathcal{V}}} L^{\pm}(\hat{w}^{\pm}; \tilde{\psi}^{\pm}, \tilde{\lambda}^{\pm}) \leq \sup_{\substack{\psi^{\pm} \in \mathcal{V} \\ \lambda^{\pm} \in \Lambda}} \inf_{\hat{w}^{\pm} \in \hat{\mathcal{V}}} L^{\pm}(\hat{w}^{\pm}; \psi^{\pm}, \lambda^{\pm}) = \mp s, \tag{4.1.10}$$

which we will exploit for developing inexpensive local subproblems for computing bounds. Equality on the right of (4.1.10) results from the strong duality of convex minimizations, but the bound property would still hold with weak duality.

4.1.4.1 Lagrange Multiplier Approximation

We compute approximate Lagrange multipliers using the finite element method by first choosing $\tilde{\psi}^{\pm} = \pm\psi_h$, $\tilde{\lambda}^{\pm} = -\frac{\kappa}{2}\lambda_h^u \pm \lambda_h^\psi$, and $\bar{u} = u_h$, where u_h and ψ_h are members of the usual piecewise polynomial finite element approximation set

$$\mathcal{U}_h \equiv \{\, w \in \mathcal{U} \mid w|_T \in \mathbb{P}^p(T),\ \forall T \in \mathcal{T}_h \,\},$$

and space

$$\mathcal{V}_h \equiv \{\, v \in \mathcal{V} \mid v|_T \in \mathbb{P}^p(T),\ \forall T \in \mathcal{T}_h \,\},$$

and both λ_h^u and λ_h^ψ are members of the piecewise polynomial space

$$\Lambda_h \equiv \{\, \lambda \in \Lambda \mid \lambda|_\gamma \in \mathbb{P}^p(\gamma),\ \forall \gamma \in \partial T \,\}$$

. We have used the notation $\mathbb{P}^p(T)$ for the space of polynomials on element T (in d spatial dimensions) with degree less than or equal to p, and $\mathbb{P}^p(\gamma)$ for the space of polynomials on edges γ (in $d-1$ spatial dimensions) with degree less than or equal to p.

By approximating u, the optimizer of the constrained minimization (4.1.8), with u_h and noting from (4.1.4) that $a(v,u_h) = a^{\mathrm{s}}(u_h,v) - a^{\mathrm{ss}}(u_h,v)$, we can write an approximate gradient condition

$$\frac{\kappa}{2}\{-\ell(\hat{v}) + a(\hat{v},u_h) + b(\hat{v},\lambda_h^u)\} \pm \{-\ell^{\mathcal{O}}(\hat{v}) - a(\hat{v},\psi_h) - b(\hat{v},\lambda_h^\psi)\} = 0, \quad \forall \hat{v} \in \hat{\mathcal{V}}_h, \quad (4.1.11)$$

with $\hat{\mathcal{V}}_h \equiv \{\, \hat{v} \in \mathcal{L}^2 \mid \hat{v}|_T \in \mathbb{P}^p(T),\ \forall T \in \mathcal{T}_h \,\}$. We can compute approximate Lagrange multipliers from (4.1.11) by solving the discrete problems:

Find $u_h \in \mathcal{U}_h$ such that

$$a(u_h, v) = \ell(v), \quad \forall v \in \mathcal{V}_h, \tag{4.1.12}$$

Find $\psi_h \in \mathcal{V}_h$ such that

$$a(v, \psi_h) = -\ell^{\mathcal{O}}(v), \quad \forall v \in \mathcal{V}_h, \tag{4.1.13}$$

Find $\lambda_h^u \in \Lambda_h$ such that

$$b(\hat{v}, \lambda_h^u) = \ell(\hat{v}) - a(u_h, \hat{v}), \quad \forall \hat{v} \in \hat{\mathcal{V}}_h, \tag{4.1.14}$$

Find $\lambda_h^\psi \in \Lambda_h$ such that

$$b(\hat{v}, \lambda_h^\psi) = -\ell^{\mathcal{O}}(\hat{v}) - a(\hat{v}, \psi_h), \quad \forall \hat{v} \in \hat{\mathcal{V}}_h. \tag{4.1.15}$$

The first two problems are standard finite element approximation problems and the second two problems are equilibration problems which can be solved with an asymptotic complexity that is linear in the number of vertices in the triangulation using Ladevèze's procedure [LL83].

Lemma 4.1.1. *If the Lagrange multipliers λ_h^u and λ_h^ψ satisfy the equilibration*

conditions (4.1.14) and (4.1.15), then the minimizations

$$\inf_{\hat{w}^{\pm}\in\hat{\mathcal{V}}} L^{\pm}(\hat{w}^{\pm}; \pm\psi_h, -\frac{\kappa}{2}\lambda_h^u \pm \lambda_h^{\psi}) \tag{4.1.16}$$

are bounded from below.

Proof. A strictly positive reaction term in $a^s(\hat{w}^{\pm}, \hat{w}^{\pm})$ ensures that the lower bounding minimization (4.1.10) is bounded below without the aid of equilibration. For $\mu = 0$, the constant function is not controlled by $a^s(\hat{w}^{\pm}, \hat{w}^{\pm})$ and without equilibration it would become possible for the subproblems, which only have Neumann boundary conditions, to be driven to arbitrarily large negative values of the Lagrangian functional. Equilibration ensures the nullification of the constant function, as can be checked by setting $\hat{v} = \text{const}$ in (4.1.14) and (4.1.15). □

4.2 Elemental Subproblems

The continuity relaxation of §4.1.4 decomposes the triangulation so that after computing the approximate Lagrange multipliers we may consider each element *independently* when computing the bounds. We perform the global lower bounding minimization (4.1.10) by minimizing the local contribution of the Lagrangian on each elemental subdomain and accumulating the results to produce upper and lower bounds on the exact output

$$\sum_{T\in\mathcal{T}_h} s_T^- \leq s \leq \sum_{T\in\mathcal{T}_h} s_T^+ \tag{4.2.1}$$

We can write the local contribution of the Lagrangian on an arbitrary element

T of the triangulation $\mathcal{T}_h$ as

$$\mp s_T^{\pm} = \inf_{w^{\pm} \in \mathcal{H}^1(T)} \frac{\kappa}{2} a_T^{\mathrm{s}}(w^{\pm}, w^{\pm}) + \ell_T^{\pm}(w^{\pm}) + C_T^{\pm}, \tag{4.2.2}$$

where we have collected the constant and linear contributions to the local Lagrangian with the definitions

$$\begin{aligned} \ell_T^{\pm}(v) = \frac{\kappa}{2} \Big\{ & - \ell_T(v) - a_T(v, u_h) + b_T(v, \lambda_h^u) \Big\} \\ & \pm \Big\{ - \ell_T^{\mathcal{O}}(v) - a_T(v, \psi_h) - b_T(v, \lambda_h^{\psi}) \Big\}, \end{aligned} \tag{4.2.3}$$

$$\begin{aligned} C_T^{\pm} = \frac{\kappa}{2} \Big\{ & \ell_T(u_h) - \ell_T^D(\lambda_h^u) + \frac{1}{2} C_T^{\star} \Big\} \\ & \pm \Big\{ \ell_T(\psi_h) + \ell_T^D(\lambda_h^{\psi}) \Big\}. \end{aligned} \tag{4.2.4}$$

The subscript T denotes restrictions to a single element of the triangulation. For example, we have

$$\begin{aligned} a_T(w, v) &= \int_T \nu \nabla w \cdot \nabla v + \mu w v + (\boldsymbol{\alpha} \cdot \nabla w)\, v \, \mathrm{d}\Omega, \\ \ell_T(v) &= \int_T f v \, \mathrm{d}\Omega + \int_{\Gamma_T^{\mathrm{N}}} g v \, \mathrm{d}\Gamma, \end{aligned}$$

in which Γ_T^{N} denotes the local Neumann edges, $\partial T \cap \Gamma^{\mathrm{N}}$, as well as

$$\begin{aligned} b_T(w, \lambda_h^u) &= \int_{\partial T} \sigma_T w \lambda_h^u \, \mathrm{d}\Gamma, \\ \ell_T^D(\lambda_h^u) &= \int_{\Gamma_T^{\mathrm{D}}} \sigma_T u_D \lambda_h^u \, \mathrm{d}\Gamma \end{aligned}$$

in which Γ_T^{D} denotes the local Dirichlet edges, $\partial T \cap \Gamma^{\mathrm{D}}$.

Recall from §4.1.2 that for the advection-diffusion-reaction equation we have

$$a_T^{\mathrm{s}}(w,w) = \int_T \nu|\nabla w|^2 + \mu w^2 \,\mathrm{d}\Omega + \frac{1}{2}\int_{\Gamma_T^{\mathrm{N}}} (\boldsymbol{\alpha}\cdot\boldsymbol{n})\, w^2 \,\mathrm{d}\Gamma, \tag{4.2.5}$$

which is coercive on $\mathcal{V}(T)$ for $\mu > 0$ (and on $\mathcal{V}(T) \setminus \mathbb{P}^0(T)$ for $\mu = 0$) for all T in $\mathcal{T}_h$ because $\boldsymbol{\alpha}\cdot\boldsymbol{n}$ is perforce positive on Γ_T^{N}.

4.2.1 Dualization of Local Minimization

The localized unconstrained minimization (4.2.2) remains uncomputable in general, since the minimization must be performed over an infinite-dimensional space in order to guarantee the bounding property. Nevertheless, by once again applying the powerful ideas of Lagrangian saddle point theory, we can compute a lower bound to this lower bound and thus procure guaranteed computable bounds on the exact output of interest.

Proposition 4.2.1. *The optimal value of the local unconstrained minimization problem (4.2.2) can be found by solving the local constrained maximization problem*

$$\begin{aligned} \mp s_T^{\pm} = \sup_{\substack{\boldsymbol{q}^{\pm}\in\left(\mathcal{L}^2(T)\right)^d \\ r^{\pm}\in\mathcal{L}^2(T)}} & -\frac{\kappa}{2} a_T^{\mathrm{du}}((\boldsymbol{q}^{\pm}, r^{\pm}), (\boldsymbol{q}^{\pm}, r^{\pm})) + C_T^{\pm} \\ \text{s.t.} \quad & \kappa c_T^{\mathrm{du}}((\boldsymbol{q}^{\pm}, r^{\pm}), v) = -\ell_T^{\pm}(v), \quad \forall v \in \mathcal{H}^1(T), \end{aligned} \tag{4.2.6}$$

where the form $a_T^{\mathrm{du}} : (\mathcal{L}^2(T))^d \times \mathcal{H}^1(T) \times (\mathcal{L}^2(T))^d \times \mathcal{H}^1(T) \to \mathbb{R}$ *is defined as*

$$a_T^{\mathrm{du}}((\boldsymbol{q}, r), (\mathbf{p}, v)) = \int_T \nu \boldsymbol{q}\cdot\mathbf{p} + \mu r v \,\mathrm{d}\Omega + \frac{1}{2}\int_{\Gamma_T^{\mathrm{N}}} (\boldsymbol{\alpha}\cdot\boldsymbol{n}) r v \,\mathrm{d}\Gamma. \tag{4.2.7}$$

and the form $c_T^{\mathrm{du}} : (\mathcal{L}^2(T))^d \times \mathcal{H}^1(T) \times \mathcal{H}^1(T) \to \mathbb{R}$ *is defined as*

$$c_T^{\mathrm{du}}((\boldsymbol{q}, r), v) = \int_T \nu \boldsymbol{q} \cdot \nabla v + \mu r v \, \mathrm{d}\Omega + \frac{1}{2} \int_{\Gamma_T^{\mathrm{N}}} (\boldsymbol{\alpha} \cdot \boldsymbol{n}) r v \, \mathrm{d}\Gamma. \tag{4.2.8}$$

Proof. We begin formulating the dual problem by introducing the auxiliary variable $\boldsymbol{\pi}^{\pm} \in (\mathcal{L}^2(T))^d$ which satisfies the constraint

$$\kappa \int_T \nu(\nabla w^{\pm} - \boldsymbol{\pi}^{\pm}) \cdot \mathbf{p} \, \mathrm{d}\Omega = 0, \quad \forall \mathbf{p} \in \left(\mathcal{L}^2(T)\right)^d, \tag{4.2.9}$$

and the auxiliary variable $\rho^{\pm} \in \mathcal{L}^2(T)$ which satisfies the constraint

$$\kappa \int_T \mu(w^{\pm} - \rho^{\pm}) v \, \mathrm{d}\Omega + \frac{\kappa}{2} \int_{\Gamma_T^{\mathrm{N}}} (\boldsymbol{\alpha} \cdot \boldsymbol{n})(w^{\pm} - \rho^{\pm}) v \, \mathrm{d}\Gamma = 0, \quad \forall v \in \mathcal{L}^2(T). \tag{4.2.10}$$

Defining Ξ to be the set of all triples $(w^{\pm}, \boldsymbol{\pi}^{\pm}, \rho^{\pm})$ in $\mathcal{H}^1(T) \times (\mathcal{L}^2(T))^d \times \mathcal{L}^2(T)$ which satisfy the constraints (4.2.9) and (4.2.10), we can write the local unconstrained minimization (4.2.2) as an equivalent constrained minimization

$$\begin{aligned} \mp s_T^{\pm} = \inf_{(w^{\pm}, \boldsymbol{\pi}^{\pm}, \rho^{\pm}) \in \Xi} \quad & \frac{\kappa}{2} \left\{ \int_T \nu(\boldsymbol{\pi}^{\pm})^2 + \mu(\rho^{\pm})^2 \, \mathrm{d}\Omega + \frac{1}{2} \int_{\Gamma_T^{\mathrm{N}}} (\boldsymbol{\alpha} \cdot \boldsymbol{n})(\rho^{\pm})^2 \, \mathrm{d}\Gamma \right\} \\ & + \ell_T^{\pm}(w^{\pm}) + C_T^{\pm} \end{aligned} \tag{4.2.11}$$

This equivalent constrained minimization can be formulated as the Lagrangian saddle point problem

$$\mp s_T^{\pm} = \sup_{\substack{\boldsymbol{q}^{\pm} \in \left(\mathcal{L}^2(T)\right)^d \\ r^{\pm} \in \mathcal{L}^2(T)}} \inf_{\substack{w^{\pm} \in \mathcal{H}^1(T) \\ \boldsymbol{\pi}^{\pm} \in \left(\mathcal{L}^2(T)\right)^d \\ \rho^{\pm} \in \mathcal{L}^2(T)}} J_T^{\pm}(w^{\pm}, \boldsymbol{\pi}^{\pm}, \rho^{\pm}; \boldsymbol{q}^{\pm}, r^{\pm}) + C_T^{\pm}, \tag{4.2.12}$$

where the Lagrangian functional is defined as

$$\begin{aligned} J_T^{\pm}(w^{\pm}, \boldsymbol{\pi}^{\pm}, \rho^{\pm}; \boldsymbol{q}^{\pm}, r^{\pm}) = \kappa \int_T \nu(\frac{1}{2}\boldsymbol{\pi}^{\pm} - \boldsymbol{q}^{\pm})\boldsymbol{\pi}^{\pm} + \mu(\frac{1}{2}\rho^{\pm} - r^{\pm})\rho^{\pm} \, \mathrm{d}\Omega \\ + \frac{\kappa}{2} \int_{\Gamma_T^{\mathrm{N}}} (\boldsymbol{\alpha} \cdot \boldsymbol{n})(\frac{1}{2}\rho^{\pm} - r^{\pm})\rho^{\pm} \, \mathrm{d}\Gamma \\ + \kappa \Big\{ \int_T \nu \nabla w^{\pm} \cdot \boldsymbol{q}^{\pm} + \mu w^{\pm} r^{\pm} \, \mathrm{d}\Omega \\ + \frac{1}{2} \int_{\Gamma_T^{\mathrm{N}}} (\boldsymbol{\alpha} \cdot \boldsymbol{n}) w^{\pm} r^{\pm} \, \mathrm{d}\Gamma \Big\} \\ + \ell_T^{\pm}(w^{\pm}). \end{aligned} \tag{4.2.13}$$

Equality on the left of (4.2.12) results from the quadratic Lagrangian functional, but the bound method can also be derived when only weak duality holds.

A necessary condition for optimality of the inner minimization of (4.2.12) with respect to the principle primal variable $w^{\pm}$ is

$$\kappa \Big\{ \int_T \nu \nabla v \cdot \boldsymbol{q}^{\pm,*} + \mu v r^{\pm,*} \, \mathrm{d}\Omega + \frac{1}{2} \int_{\Gamma_T^{\mathrm{N}}} (\boldsymbol{\alpha} \cdot \boldsymbol{n}) v r^{\pm,*} \, \mathrm{d}\Gamma \Big\} = -\ell_T^{\pm}(v), \ \forall v \in \mathcal{H}^1(T), \tag{4.2.14}$$

where the superscript $*$ indicates optimality of the variable. Necessary conditions for optimality with respect to the two auxiliary primal variables $\boldsymbol{\pi}^{\pm}$ and $\rho^{\pm}$ are

$$\kappa \int_T \nu(\boldsymbol{\pi}^{\pm,*} - \boldsymbol{q}^{\pm,*})\mathbf{p} \, \mathrm{d}\Omega = 0, \quad \forall \mathbf{p} \in \left(\mathcal{L}^2(T)\right)^d, \tag{4.2.15a}$$

$$\kappa \int_{\Omega} \mu(\rho^{\pm,*} - r^{\pm,*}) v \, \mathrm{d}\Omega + \frac{\kappa}{2} \int_{\Gamma_T^{\mathrm{N}}} (\boldsymbol{\alpha} \cdot \boldsymbol{n})(\rho^{\pm,*} - r^{\pm,*}) v \, \mathrm{d}\Gamma = 0, \quad \forall v \in \mathcal{L}^2(T). \tag{4.2.15b}$$

After substituting the auxiliary variable optimality conditions (4.2.15) into the

Lagrangian (4.2.13) and retaining the principle primal variable condition (4.2.14) as a constraint in the outer maximization of the saddle problem (4.2.12), we arrive at the local dual constrained maximization (4.2.6) formulation of the original unconstrained local minimization (4.2.2). □

Significantly, we may inexpensively compute a quantitative lower bound on $\mp s_T^{\pm}$, and thereby upper and lower bounds on the exact output s, by performing the local dual constrained maximization (4.2.6) over a *finite-dimensional* set so long as the set is rich enough to allow the dual constraint to be satisfied exactly. Indeed, while maximization will improve the sharpness of the bounds, we only require dual feasibility to obtain bounds.

4.2.2 Dual Subproblems

The local dual maximization problem (4.2.6) has the optimality conditions: find $(\boldsymbol{q}^{\pm}, r^{\pm}, \xi^{\pm}) \in (\mathcal{L}^2(T))^d \times \mathcal{H}^1(T) \times \mathcal{H}^1(T)$ such that

$$-\kappa a_T^{\mathrm{du}}((\boldsymbol{q}^{\pm}, r^{\pm}), (\mathbf{p}, v)) - \kappa c_T^{\mathrm{du}}((\mathbf{p}, v), \xi^{\pm}) = 0,\ \forall (\mathbf{p}, v) \in \left(\mathcal{L}^2(T)\right)^d \times \mathcal{H}^1(T), \tag{4.2.16a}$$

$$-\kappa c_T^{\mathrm{du}}((\boldsymbol{q}^{\pm}, r^{\pm}), v) = \ell_T^{\pm}(v),\ \forall v \in \mathcal{H}^1(T), \tag{4.2.16b}$$

which, as a result of the linear equality constraint and convex objective functional, are both necessary and sufficient. For the purpose of computing bounds, the Lagrange multiplier $\xi^{\pm}$ is an artifact of solving the constrained maximization problem and we will not make direct use of it.

As formulated, the optimality conditions depend explicitly upon the scaling

parameter κ, but the substitutions

$$(\boldsymbol{q}^{\pm}, r^{\pm}, \xi^{\pm}) = (\nabla u_h - \frac{1}{2}\boldsymbol{q}^u \pm \frac{1}{\kappa}\boldsymbol{q}^\psi, u_h - \frac{1}{2}r^u \pm \frac{1}{\kappa}r^\psi, -\frac{1}{2}\xi^u \pm \frac{1}{\kappa}\xi^\psi)$$

will transform the above κ-*dependent* problems into the following two κ-*independent* problems: find $(\boldsymbol{q}^u, r^u, \xi^u) \in (\mathcal{L}^2(T))^d \times \mathcal{H}^1(T) \times \mathcal{H}^1(T)$ such that

$$a_T^{\mathrm{du}}((\boldsymbol{q}^u, r^u), (\mathbf{p}, v)) + c_T^{\mathrm{du}}((\mathbf{p}, v), \xi^u) = 0, \quad \forall (\mathbf{p}, v) \in \left(\mathcal{L}^2(T)\right)^d \times \mathcal{H}^1(T), \tag{4.2.17a}$$

$$c_T^{\mathrm{du}}((\boldsymbol{q}^u, r^u), v) = \hat{R}_T^u(v), \quad \forall v \in \mathcal{H}^1(T), \tag{4.2.17b}$$

and find $(\boldsymbol{q}^\psi, r^\psi, \xi^\psi) \in (\mathcal{L}^2(T))^d \times \mathcal{H}^1(T) \times \mathcal{H}^1(T)$ such that

$$a_T^{\mathrm{du}}((\boldsymbol{q}^\psi, r^\psi), (\mathbf{p}, v)) + c_T^{\mathrm{du}}((\mathbf{p}, v), \xi^\psi) = 0, \quad \forall (\mathbf{p}, v) \in \left(\mathcal{L}^2(T)\right)^d \times \mathcal{H}^1(T), \tag{4.2.18a}$$

$$c_T^{\mathrm{du}}((\boldsymbol{q}^\psi, r^\psi), v) = \hat{R}_T^\psi(v), \quad \forall v \in \mathcal{H}^1(T), \tag{4.2.18b}$$

where we have defined the the localized residual forms

$$\hat{R}_T^u(v) = \ell_T(v) - a_T(u_h, v) - b_T(v, \lambda_h^u), \tag{4.2.19}$$

$$\hat{R}_T^\psi(v) = -\ell_T^{\mathcal{O}}(v) - a_T(v, \psi_h) - b_T(v, \lambda_h^\psi). \tag{4.2.20}$$

Equilibration ensures that all dual feasible functions $(\boldsymbol{q}^u, r^u)$ and $(\boldsymbol{q}^\psi, r^\psi)$ are orthogonal to the local finite element basis.

Lemma 4.2.2. *Any pair* $(\boldsymbol{q}^u, r^u)$ *in* $(\mathcal{L}^2(T))^d \times \mathcal{H}^1(T)$ *that satisfies the con-*

straint (4.2.17b) has the orthogonality property

$$a_T^{\mathrm{du}}((\boldsymbol{q}^u, r^u), (\nabla v, v)) = c_T^{\mathrm{du}}((\boldsymbol{q}^u, r^u), v) = 0, \quad \forall v \in \mathcal{V}_h(T), \tag{4.2.21}$$

and any pair $(\boldsymbol{q}^\psi, r^\psi)$ *in* $(\mathcal{L}^2(T))^d \times \mathcal{H}^1(T)$ *that satisfies the constraint (4.2.18b) has the orthogonality property*

$$a_T^{\mathrm{du}}((\boldsymbol{q}^\psi, r^\psi), (\nabla v, v)) = c_T^{\mathrm{du}}((\boldsymbol{q}^\psi, r^\psi), v) = 0, \quad \forall v \in \mathcal{V}_h(T). \tag{4.2.22}$$

Proof. This is a direct consequence of equilibration provided by (4.1.14) and (4.1.15), and the definitions (4.2.19) and (4.2.20). □

With the above orthogonality property we can calculate the objective from dual feasible functions $(\boldsymbol{q}^u, r^u)$ and $(\boldsymbol{q}^\psi, r^\psi)$ using

$$\begin{aligned} \mp s_T^{\pm} = -\frac{\kappa}{2} \Bigg\{ & \frac{1}{4} a_T^{\mathrm{du}}((\boldsymbol{q}^u, r^u), (\boldsymbol{q}^u, r^u)) - C_T^u \Bigg\} \\ & - \frac{1}{2\kappa} a_T^{\mathrm{du}}((\boldsymbol{q}^\psi, r^\psi), (\boldsymbol{q}^\psi, r^\psi)) \\ & \pm \left\{ \frac{1}{2} a_T^{\mathrm{du}}((\boldsymbol{q}^u, r^u), (\boldsymbol{q}^\psi, r^\psi)) + C_T^\psi \right\}, \end{aligned} \tag{4.2.23}$$

with the definitions

$$C_T^u = \ell_T(u_h) - a_T^{\mathrm{s}}(u_h, u_h) - \ell_T^D(\lambda_h^u) + \frac{1}{2} C_T^\star, \tag{4.2.24}$$

$$C_T^\psi = \ell_T(\psi_h) + \ell_T^D(\lambda_h^\psi). \tag{4.2.25}$$

4.2.3 Subproblem Computation

Recall from §4.2.1 that, by virtue of the dualization of the local minimization problem, we can choose a finite-dimensional set within which to search for the dual functions $(\boldsymbol{q}^u, r^u)$ and $(\boldsymbol{q}^\psi, r^\psi)$, so long as the set is rich enough to admit at least one pair $(\boldsymbol{q}^u, r^u)$ satisfying (4.2.17b) and at least one pair $(\boldsymbol{q}^\psi, r^\psi)$ satisfying (4.2.18b).

Lemma 4.2.3. *If the interior data $f|_T$, $(\boldsymbol{\alpha}\cdot\nabla u_h)|_T$, $f^{\mathcal{O}}|_T$, and $(\boldsymbol{\alpha}\cdot\nabla\psi_h)|_T$ are all members of $\mathbb{P}^m(T)$, the boundary data $g|_\gamma$, $g^{\mathcal{O}}|_\gamma$, and $((\boldsymbol{\alpha}\cdot\boldsymbol{n})\psi_h)|_\gamma$ are all members of $\mathbb{P}^m(\gamma)$ for all $\gamma\in\partial T$, and the continuity multipliers λ_h^u and λ_h^ψ are equilibrated according to (4.1.14) and (4.1.15), then there exists at least one pair $(\boldsymbol{q}_h^u, r_h^u)\in(\mathbb{P}^q(T))^d\times\mathbb{P}^q(T)$ satisfying (4.2.17b) and at least one pair $(\boldsymbol{q}_h^\psi, r_h^\psi)\in(\mathbb{P}^q(T))^d\times\mathbb{P}^q(T)$ satisfying (4.2.18b) for $q>p$ and $q>m$.*

Proof. Let $\boldsymbol{q}_h^u=\boldsymbol{q}_D^u+\boldsymbol{q}_0^u$, with $\boldsymbol{q}_D^u\cdot\boldsymbol{n}=-\sigma_T\lambda_h^u-\nu(\nabla u_h\cdot\boldsymbol{n})$ on $\partial T\setminus\Gamma_T^{\mathrm{N}}$, $\boldsymbol{q}_D^u\cdot\boldsymbol{n}=-\sigma_T\lambda_h^u$ on Γ_T^{N}, $\boldsymbol{q}_0^u\cdot\boldsymbol{n}=0$ on ∂T, and let $r_h^u=0$ on Γ_T^{N}. With this lifting and a Green's formula we can write the constraint (4.2.17b) as

$$\int_T(-\nu\nabla\cdot\boldsymbol{q}_0^u+\mu r^u)v\,\mathrm{d}\Omega=\int_T(f+\nu\Delta u_h-\mu u_h+\boldsymbol{\alpha}\cdot\nabla u_h+\nu\nabla\cdot\boldsymbol{q}_D^u)v\,\mathrm{d}\Omega,$$

for all v in $\mathbb{P}^q(T)$. The requirements of the lemma ensure that the data on the right is in the range of the operator on the left for the case $\mu>0$ and r^u, and therefore at least one solution exists. Existence for the case $\mu=0$ is guaranteed by equilibration, as we previously addressed in [SBBHP03]. Analogous reasoning applies for the pair $(\boldsymbol{q}_h^\psi, r_h^\psi)$ with the exception that a Green's formula must also be applied to the advection term, which results in the additional requirement of

$(\boldsymbol{\alpha} \cdot \boldsymbol{n})\psi_h)|_\gamma$ being in $\mathbb{P}^m(\gamma)$. □

Note that the requirement $q \geq p$ suffices in the above lemma when $\boldsymbol{\alpha} \cdot \boldsymbol{n} = 0$ on Γ_T^{N} or $\Gamma_T^{\mathrm{N}} = \emptyset$, as well as when $\mu = 0$ and both r_h^u and r_h^ψ have been set to zero. Further note that the Dirichlet data does not need to be piecewise polynomial in order to guarantee bounds since it does not appear as data for the local dual problem.

The above proof suggests one way to solve the subproblem, but other approaches are possible. For instance, we could set r_h^u and r_h^ψ to zero from the outset in order to produce a method which treats Poisson's equation, the advection-diffusion equation and the advection-diffusion-reaction equation uniformly. Existence would be ensured by equilibration, but doing so reduces the number of available degrees of freedom in the maximization and thus would most likely reduce the sharpness of the resulting bounds.

A particularly favorable circumstance for solving the subproblem arises for both Poisson's equation and the advection-diffusion equation ($\mu = 0$) when the problem data consists only of constants ($m = 0$) and linear finite elements ($p = 1$) are employed with $q = 1$, and both $r_h^u = 0$ and $r_h^\psi = 0$. Under these circumstances, the dual functions $\boldsymbol{q}_h^u$ and $\boldsymbol{q}_h^\psi$ can be explicitly constructed from the subproblem boundary data.

More generally, we can formulate the pair of computable subproblems as: find $(\boldsymbol{q}_h^u, r_h^u, \xi_h^u) \in \mathcal{Q}_h^u(T) \times \mathbb{P}^q(T) \times \mathbb{P}^q(T)$ such that

$$a_T^{\mathrm{du}}((\boldsymbol{q}_h^u, r_h^u), (\mathbf{p}, v)) + c_T^{\mathrm{du}}((\mathbf{p}, v), \xi^u) = 0, \quad \forall (\mathbf{p}, v) \in (\mathbb{P}^q(T))^d \times \mathbb{P}^q(T), \tag{4.2.26a}$$

$$c_T^{\mathrm{du}}((\boldsymbol{q}_h^u, r_h^u), v) = \hat{R}_T^u(v), \quad \forall v \in \mathbb{P}^q(T), \tag{4.2.26b}$$

and find $(\boldsymbol{q}_h^\psi, r_h^\psi, \xi_h^\psi) \in \mathcal{Q}_h^\psi(T) \times \mathbb{P}^q(T) \times \mathbb{P}^q(T)$ such that

$$a_T^{\mathrm{du}}((\boldsymbol{q}_h^\psi, r_h^\psi), (\mathbf{p}, v)) + c_T^{\mathrm{du}}((\mathbf{p}, v), \xi^\psi) = 0, \quad \forall (\mathbf{p}, v) \in (\mathbb{P}^q(T))^d \times \mathbb{P}^q(T), \tag{4.2.27a}$$

$$c_T^{\mathrm{du}}((\boldsymbol{q}_h^\psi, r_h^\psi), v) = \hat{R}_T^\psi(v), \quad \forall v \in \mathbb{P}^q(T), \tag{4.2.27b}$$

where we have defined the sets

$$\mathcal{Q}_h^u(T) = \left\{ \boldsymbol{q} \in (\mathbb{P}^q(T))^d \;\middle|\; \boldsymbol{q} \cdot \boldsymbol{n} = \begin{cases} -\sigma_T \lambda_h^u \text{ on } \partial T \setminus \Gamma_T^{\mathrm{N}} \\ -\sigma_T \lambda_h^u + g \text{ on } \Gamma_T^{\mathrm{N}} \end{cases} \right\}, \tag{4.2.28}$$

$$\mathcal{Q}_h^\psi(T) = \left\{ \boldsymbol{q} \in (\mathbb{P}^q(T))^d \;\middle|\; \boldsymbol{q} \cdot \boldsymbol{n} = \begin{cases} -\sigma_T \lambda_h^\psi \text{ on } \partial T \setminus \Gamma_T^{\mathrm{N}} \\ -\sigma_T \lambda_h^\psi - g^{\mathcal{O}} \text{ on } \Gamma_T^{\mathrm{N}} \end{cases} \right\}. \tag{4.2.29}$$

4.3 Output Bound Procedure

The elemental subproblems explicated in the previous section can be computed independently and in parallel, accumulating the local contributions (4.2.23) to the output bounds in the process. If we define the aggregated values

$$\begin{gathered} z_h^u = \frac{1}{8} \sum_{T \in \mathcal{T}_h} a_T^{\mathrm{du}}((\boldsymbol{q}_h^u, r_h^u), (\boldsymbol{q}_h^u, r_h^u)), \qquad z_h^\psi = \frac{1}{2} \sum_{T \in \mathcal{T}_h} a_T^{\mathrm{du}}((\boldsymbol{q}_h^\psi, r_h^\psi), (\boldsymbol{q}_h^\psi, r_h^\psi)), \\ \bar{z}_h = \frac{1}{2} \sum_{T \in \mathcal{T}_h} a_T^{\mathrm{du}}((\boldsymbol{q}_h^u, r_h^u), (\boldsymbol{q}_h^\psi, r_h^\psi)), \end{gathered} \tag{4.3.1}$$

then we can write the total output bound expression as

$$s_h^\pm = -\bar{z}_h - C^\psi \pm \left\{ \kappa z_h^u + \frac{1}{\kappa} z_h^\psi \right\}, \tag{4.3.2}$$

in which the constant C^u defined in (4.2.24) is eliminated by the fact that $\ell(u_h) - a^s(u_h, u_h) - \ell^D(\lambda_h^u) + \frac{1}{2}C^\star = 0$ which results from equilibration.

We introduced the scaling parameter κ at the outset to allow us to optimize the sharpness of the computed bounds as well as provide dimensional consistency. Maximizing the lower bound and minimizing the upper bound with respect to κ yields the optimal value $\kappa^2 = z_h^\psi / z_h^u$ with which we can write the upper and lower bounds succinctly as

$$s_h^\pm = \bar{s}_h \pm 2\sqrt{z_h^u z_h^\psi}, \tag{4.3.3}$$

where we have defined the bound average $\bar{s}_h = -\bar{z}_h - C^\psi$.

The complete method for computing output bounds can now be written as a four steps procedure.

Step 1: Finite Element Approximation Find $u_h \in \mathcal{U}_h$ such that

$$a(u_h, v) = \ell(v), \quad \forall v \in \mathcal{V}_h, \tag{4.3.4}$$

Find $\psi_h \in \mathcal{V}_h$ such that

$$a(v, \psi_h) = -\ell^{\mathcal{O}}(v), \quad \forall v \in \mathcal{V}_h, \tag{4.3.5}$$

Step 2: Finite Element Equilibration Find $\lambda_h^u \in \Lambda_h$ such that

$$b(\hat{v}, \lambda_h^u) = \ell(\hat{v}) - a(u_h, \hat{v}), \quad \forall \hat{v} \in \hat{\mathcal{V}}_h, \tag{4.3.6}$$

Find $\lambda_h^\psi \in \Lambda_h$ such that

$$b(\hat{v}, \lambda_h^\psi) = -\ell^{\mathcal{O}}(\hat{v}) - a(\hat{v}, \psi_h), \quad \forall \hat{v} \in \hat{\mathcal{V}}_h. \tag{4.3.7}$$

Step 3: Elemental Subproblems Find $(\boldsymbol{q}_h^u, r_h^u, \xi_h^u) \in \mathcal{Q}_h^u(T) \times \mathbb{P}^q(T) \times \mathbb{P}^q(T)$ such that

$$\begin{aligned} a_T^{\mathrm{du}}((\boldsymbol{q}_h^u, r_h^u), (\mathbf{p}, v)) + c_T^{\mathrm{du}}((\mathbf{p}, v), \xi_h^u) &= 0, \ \forall (\mathbf{p}, v) \in (\mathbb{P}^q(T))^d \times \mathbb{P}^q(T), \\ c_T^{\mathrm{du}}((\boldsymbol{q}_h^u, r_h^u), v) &= \hat{R}_T^u(v), \ \forall v \in \mathbb{P}^q(T). \end{aligned} \tag{4.3.8}$$

Find $(\boldsymbol{q}_h^\psi, r_h^\psi, \xi_h^\psi) \in \mathcal{Q}_h^\psi(T) \times \mathbb{P}^q(T) \times \mathbb{P}^q(T)$ such that

$$\begin{aligned} a_T^{\mathrm{du}}((\boldsymbol{q}_h^\psi, r_h^\psi), (\mathbf{p}, v)) + c_T^{\mathrm{du}}((\mathbf{p}, v), \xi_h^\psi) &= 0, \ \forall (\mathbf{p}, v) \in (\mathbb{P}^q(T))^d \times \mathbb{P}^q(T), \\ c_T^{\mathrm{du}}((\boldsymbol{q}_h^\psi, r_h^\psi), v) &= \hat{R}_T^\psi(v), \ \forall v \in \mathbb{P}^q(T). \end{aligned} \tag{4.3.9}$$

Calculate $\bar{z}_T$, z_T^u, and z_T^ψ

$$\begin{gathered} z_{T,h}^u = \frac{1}{8} a_T^{\mathrm{du}}((\boldsymbol{q}_h^u, r_h^u), (\boldsymbol{q}_h^u, r_h^u)), \qquad z_{T,h}^\psi = \frac{1}{2} a_T^{\mathrm{du}}((\boldsymbol{q}_h^\psi, r_h^\psi), (\boldsymbol{q}_h^\psi, r_h^\psi)), \\ \bar{z}_{T,h} = \frac{1}{2} a_T^{\mathrm{du}}((\boldsymbol{q}_h^u, r_h^u), (\boldsymbol{q}_h^\psi, r_h^\psi)). \end{gathered} \tag{4.3.10}$$

Step 4: Bounds

$$z_h^u = \sum_{T \in \mathcal{T}_h} z_{T,h}^u, \qquad z_h^\psi = \sum_{T \in \mathcal{T}_h} z_{T,h}^\psi, \qquad \bar{s}_h = -\sum_{T \in \mathcal{T}_h} \bar{z}_{T,h} - C_T^\psi. \tag{4.3.11}$$

$$s_h^\pm = \bar{s}_h \pm 2\sqrt{z_h^u z_h^\psi} \tag{4.3.12}$$

The upper and lower bounding property of s_h^+ and s_h^- follows directly from

the Lagrangian saddle point property of the constrained minimization reformulation of the model problem. Either a strictly positive reaction coefficient, μ, or equilibration ensure that the independent local subproblems resulting from the Lagrangian relaxation can provide non-trivial bounds. Forming the dual of the unconstrained local minimization enables the computation of a lower bound on the infinite-dimensional minimization problem with a finite-dimensional feasibility problem. That the resulting dual subproblems are indeed computable is a consequence of the subproblem constraint data being being polynomial and choosing a polynomial subset for the local dual problem. The resulting bounds converge to the exact linear functional output at twice the rate of the $\mathcal{H}^1$-norm measure of the error in the finite element solution, as proven in Chapter 2 and verified by the numerical examples.

To a large extent the subproblems are independent of the finite element approximation. We need only check that the localized data $u_h|_T$, $\psi_h|_T$, $\lambda_h^u|_{\partial T}$ and $\lambda_h^\psi|_{\partial T}$ passed to the subproblem equilibrates the element according to (4.3.6) and (4.3.7). As alluded to in the introduction, this precondition is entirely local and can easily be checked. Moreover, it has very practical implications for building correct simulation software as it acts as a verifiable contract between the relatively simple bounds subproblem and the much more complicated global approximation.

4.4 Numerical Examples

In this last section, we demonstrate the method with two numerical examples. In both examples we employ a very simple adaptive strategy of Chapter 3 that uses the local information produced during the calculation of the bounds to drive the

output to a prescribed precision. At each level of refinement, only elements for which $\Delta_T = \kappa z^u_{T,h} + \frac{1}{\kappa} z^\psi_{T,h} > \Delta_{\text{tol}}/K$ are refined, where Δ_{tol} is a user specified tolerance for the bound gap and K is the number of elements in the triangulation at that level.

4.4.1 Quasi-2D Transport

In our first example we consider the unit square $(x, y) \in [0, 1]^2$ with the parameters $\nu = 1$, $\boldsymbol{\alpha} = (\alpha, 0)$, the Dirichlet boundary conditions $u(0, y) = 1$ on the left side and $u(1, y) = 0$ on the right side, and homogeneous Neumann boundary conditions on the top and bottom sides. These conditions result in the well known one-dimensional solution

$$u(x, y) = \frac{e^{\beta} e^{\frac{1}{2}(\alpha-\beta)x} - e^{\frac{1}{2}(\alpha+\beta)x}}{e^{\beta} - 1}, \tag{4.4.1}$$

where $\beta = \sqrt{4\mu + \alpha^2}$.

For the output, we examine the average normal gradient on the right side of the square, $\int_0^1 \nabla u(1, y) \cdot \boldsymbol{n} \, \mathrm{d}\Gamma$, which we write with the interior test function, $\chi = x$, as

$$\ell^{\mathcal{O}}(v) = \int_\Omega \nu \nabla v \cdot \nabla \chi + \mu v \chi + (\boldsymbol{\alpha} \cdot \nabla v) \, \chi \, \mathrm{d}\Omega \tag{4.4.2}$$

using the technique discussed in [PPP97].

Since we know the exact output for this example, we can calculate the effectiveness of the bounds as an indicator of the error in the finite element solution using

$$\eta = \frac{s_h^+ - s_h^-}{2|s_h - s|}. \tag{4.4.3}$$

Our primary goal, however, is not estimating the error in the finite element solution but providing an upper and lower bound on the exact output. The finite element solution is mostly just a means to this end.

Table 4.1 and Figure 4.4.1 summarizes the results of uniformly refining an initial mesh of 16 elements with method parameters $p = 1$ and $q = 1$. Both the output and the bound gap asymptotically converge at the optimal rate of 2. The last level of uniform refinement contains 16284 elements and produces a bound gap of 0.000747, while the simple adaptive method described above can be used to produce a bound gap of 0.000646 with a mesh containing only 4114 elements.

K	$(s_h - s)/s$	$(s - s_h^-)/s$	$(s_h^+ - s)/s$	$(s_h^+ - s_h^-)/s$	η
16	0.029963	0.296452	0.160602	0.457054	7.63
256	0.001178	0.023548	0.021966	0.045514	19.32
1024	0.000295	0.006097	0.005713	0.011810	20.01
16384	0.000018	0.000385	0.000362	0.000747	20.25

Table 4.1: Quasi-2D uniform refinement results with $q = 1$, $\alpha = 10$ and $\mu = 10$.

In the presentation of the method we left the door open for the parameter q to be chosen larger than required for guaranteeing bounds in order to take advantage of the possibility that doing so would improve the sharpness of the resulting bounds. On the one hand one might expect a few extra degrees of freedom to go to some utility, while on the other hand one will expect that eventually the low dimensional finite element data driving the subproblem would cause the problem to saturate. The evidence of Table 4.2 comparing the effect of using $q = 2$ and $q = 3$ reveals that there is no tangible benefit in solving higher order subproblems than required.

Table 4.3 summarizes the influence of the Peclet number, α, on the effectivity

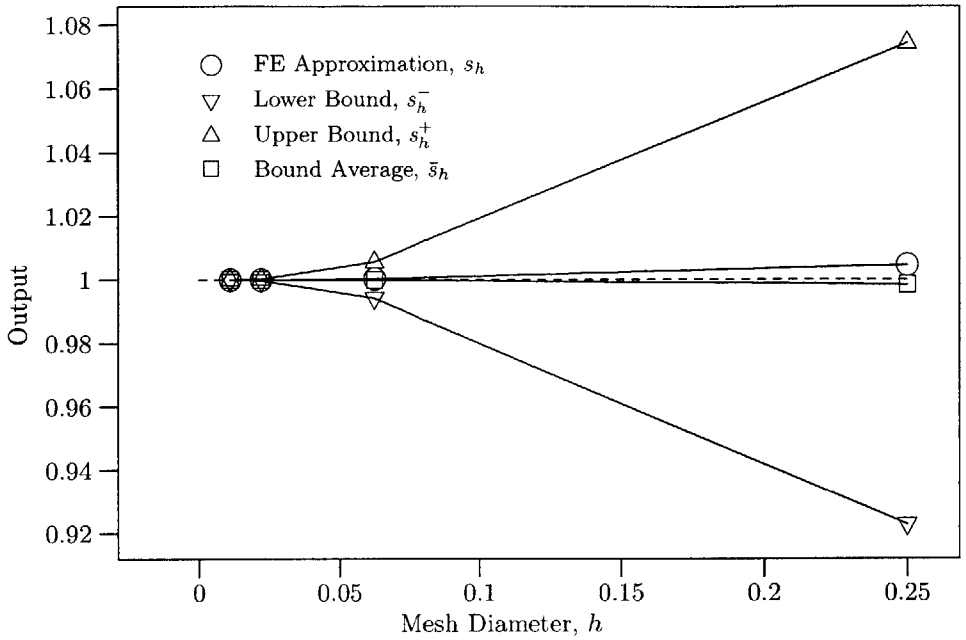

Figure 4.4.1: Quasi-2D uniform refinement results with $q = 1$, $\alpha = 10$ and $\mu = 10$.

	$q = 2$			$q = 3$		
K	$(s - s_h^-)/s$	$(s_h^+ - s)/s$	η	$(s - s_h^-)/s$	$(s_h^+ - s)/s$	η
16	0.2701	0.1496	7.00	0.2637	0.1471	6.85
256	0.0223	0.0217	18.66	0.0223	0.0216	18.64
1024	0.0058	0.0056	19.39	0.0058	0.0056	19.38
16384	0.0004	0.0004	19.63	0.0004	0.0004	19.63

Table 4.2: Quasi-2D uniform refinement results with $q = 2$ or 3, $\alpha = 10$ and $\mu = 10$.

of the bounds in the context of the simple adaptive method with a tolerance of $\Delta_{\text{tol}} = 0.001s$. Although the method is valid for nonnegative α, the sharpness of the bound degrades significantly with increasing Peclet number, but the bounding property is retained.

We strive to produce guaranteed, if conservative, bounds on quantities typi-

α	K	$(s_h - s)/s$	$(s - s_h^-)/s$	$(s_h^+ - s)/s$	$(s_h^+ - s_h^-)/s$	η
0	384	-0.000045	0.000342	0.000068	0.000410	4.52
1	256	-0.000051	0.000535	0.000186	0.000721	7.12
5	2883	-0.000056	0.000412	0.000404	0.000816	7.23
10	6108	-0.000005	0.000458	0.000456	0.000913	98.21

Table 4.3: Quasi-2D transport adaptive refinement results with $\mu = 1$ and various values of α.

cally queried from simulations and not estimates of the error. Consequentially, we trade better estimates of the error for the confidence provided by one-sidedness. Nevertheless, various enhancements to the basic method presented here, such as the incorporation of gradient recovery heuristics, could be considered in order to improve the effectiveness of the error estimate.

4.4.2 Rotating Transport

Our second example provides a qualitative demonstration of the method on a more complicated example problem. We consider the unit square $(x, y) \in [0, 1]^2$ with the equation parameters $\nu = 1$, $\boldsymbol{\alpha} = 500(y - \frac{1}{2}, \frac{1}{2} - x)$, $\mu = 10$, and all homogeneous Dirichlet boundary conditions. The problem is forced in the square region $[0.7, 0.8]^2$ with $f = 1000$ and the output is the average, $f^{\mathcal{O}} = 1$, over the square region $\Omega^{\mathcal{O}} = [0.2, 0.3]^2$ as indicated in Figure 4.4.3. The initial mesh contains 100 elements and the method parameters are $p = 1$ and $q = 2$.

We examine the result of adaptively solving the output problem with $\Delta_{\text{tol}} = 0.0005$. Figure 4.4.5 displays u and ψ for the final solution, which has a guaranteed precision of 0.000488 and contains 2917 elements. The figure also shows the distribution of elemental bound gap contributions, Δ_T, for the initial solution,

and it shows the final mesh obtained at the end of the adaptive process.

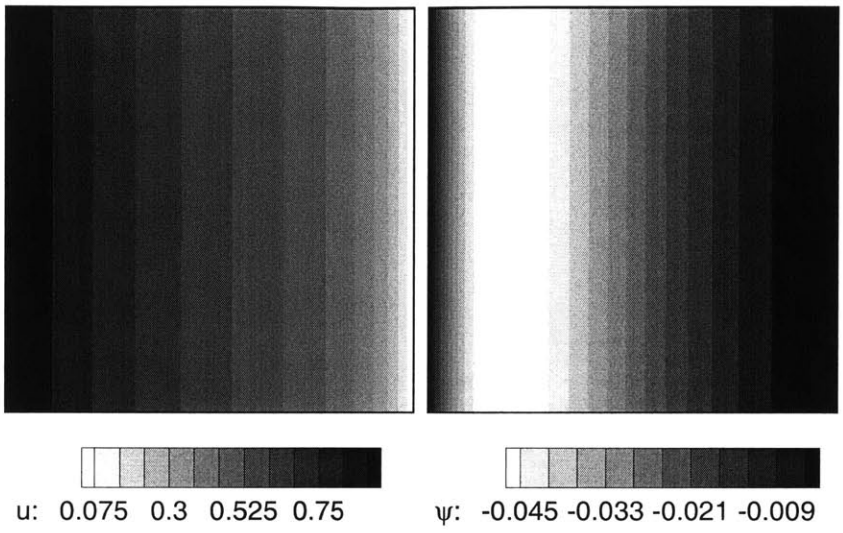

(a) Adaptive solution field.

(b) Adaptive adjoint field.

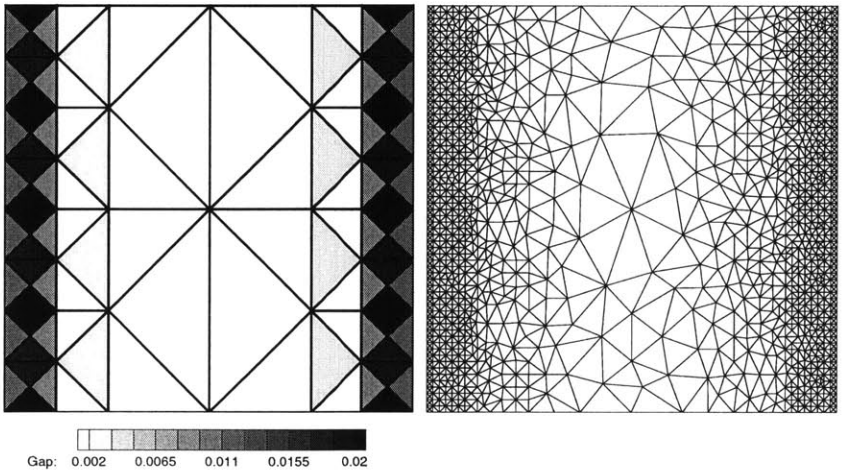

(c) Elemental bound gap contributions on intermediate mesh.

(d) Final adaptive mesh.

Figure 4.4.2: Quasi-2D transport adaptive solutions, local indicators and meshes.

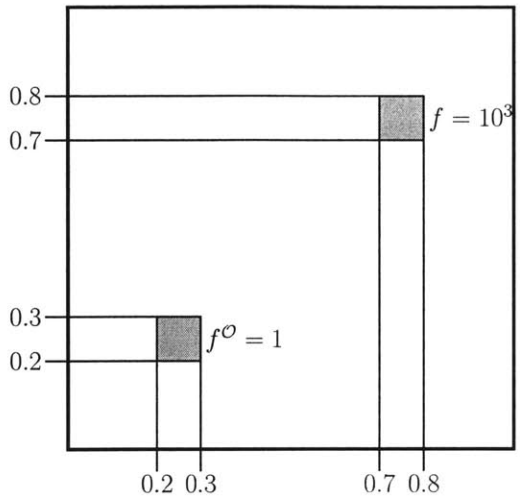

Figure 4.4.3: Rotational transport forcing and output regions.

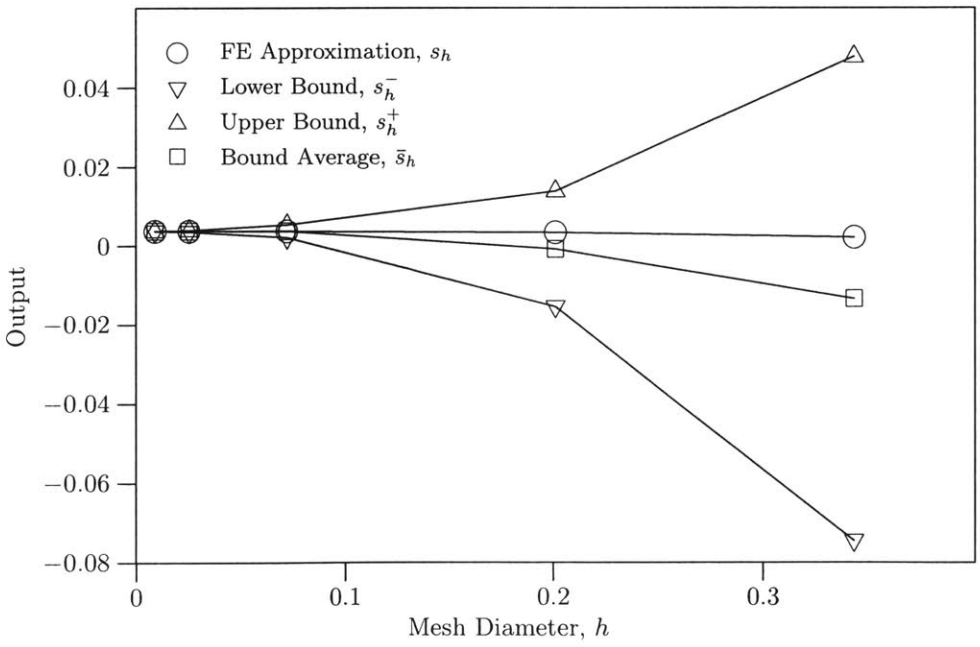

Figure 4.4.4: Rotating transport uniform refinement results.

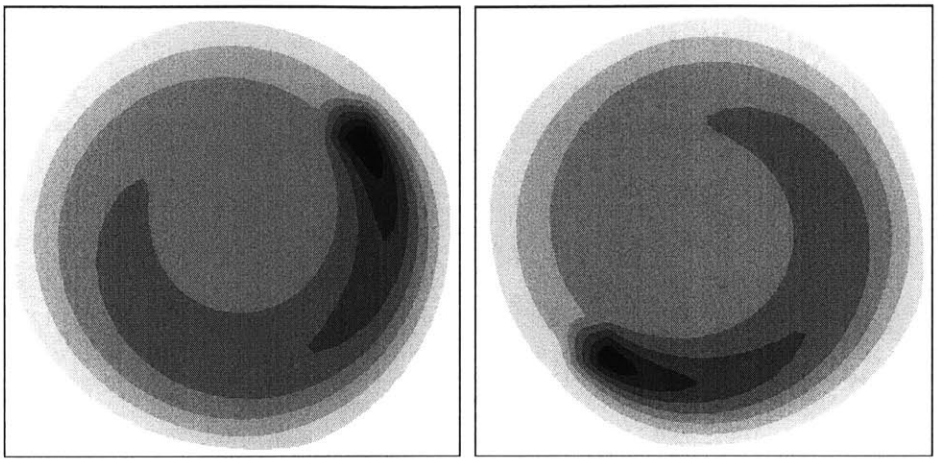

(a) Adaptive solution field.

(b) Adaptive adjoint field.

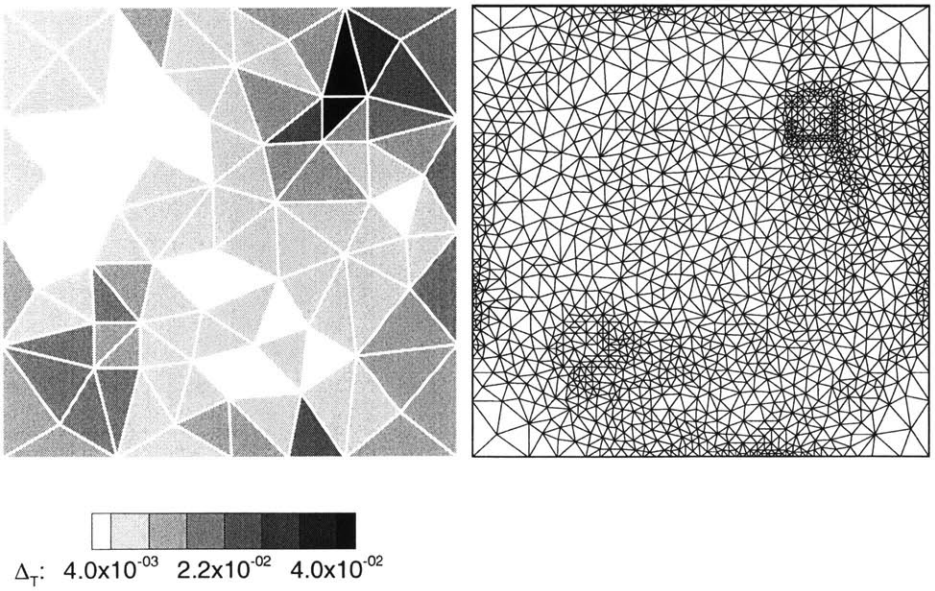

(c) Elemental bound gap contributions on initial mesh.

(d) Final adaptive mesh.

Figure 4.4.5: Rotating transport adaptive solutions, local indicators and meshes.

Chapter 5

Conclusion

Numerous barriers exist to safely and effectively exploiting partial differential equation based computational models in the decision making process. The barriers range from the expense required to develop the software and compute each individual result to uncertainty over the reliability of the computed results. Uncertainty about the reliability of the results undermines their utility by causing them to not be trusted in the decision making process. Assessing the reliability of computational results poses a key challenge to their safe and effective exploitation.

5.1 Contribution

This thesis contributes a cost-effective method for rigorously assessing the reliability of results from partial differential equation based computational models. The proposed method computes upper and lower bounds on linear functional outputs from exact weak solutions to linear coercive partial differential equations. There are five practical consequences of this statement.

First, the method assesses the reliability of a simulation with respect to the *quantity of interest.* Typically queried quantities of interest, such as average regional concentrations, forces acting on bodies, and mass flow rates, can be represented as linear functionals of the field solution. Although attention has started to turn to estimating errors in outputs, the vast majority of proposed estimators measure the numerical error in an abstract norm, such as the energy norm. While abstract measures can readily be integrated into the simulation process as adaptive indicators, they are usually uninformative for the practitioner. Assessing the reliability of a simulation with respect to the quantity of interest makes the assessment immediately and unambiguously accessible to the human decision makers.

Second, the method assesses the reliability of a simulation by producing *upper and lower bounds* on the quantity of interest. Error estimates which do not have the guarantee of one-sidedness forfeit the ability to quantitatively assess the error because there remains uncertainty about the accuracy of the estimate. Upper and lower bounds inform the practitioner of the range of possible values for the exact answer. The important and practical corollary being that the method guarantees the exact answer to not have a value outside this interval.

Third, the method bounds linear functionals of *exact weak solutions* to the continuum mathematical model. Other proposed methods either evoke an approximate computation where an exact one would be required to guarantee the error bound, or resort to solving an expensive global problem. Whether a method solves a high order local problem as a surrogate for an infinite-dimension one or appeals to quadrature in lieu of exact integration, the reference solution is tac-

itly exchanged for the solution of a modified equation. The method proposed in this thesis transforms an infinite-dimensional minimization problem into a finite-dimensional feasibility problem without breaking guaranteed bounds property. By maintaining the original mathematical model as the reference, the proposed method removes ambiguity over how well the modified equation represents the original.

Fourth, the method can be applied to mathematical models with *non-symmetric operators*, and thus no intrinsic minimization principle. Intrinsic minimization principles are powerful allies in constructing error bounds measured by the energy norm, but many interesting mathematical models contain advective contributions which preclude such natural minimization principles.

Fifth, the method guarantees the validity of the *bounds for all simulation fidelities*. Nearly all error estimation techniques only provide accurate estimates in the asymptotic limit as the simulation fidelity is increased. By providing uniform bounds, the proposed method removes ambiguity over whether the simulation fidelity is high enough for the error assessment to be reliable. Furthermore, since the validity of the bounds are mesh independent, the method can be applied to adaptive meshes without concern about the mesh being sufficiently refined everywhere to be considered asymptotic.

In addition to these five powerful properties, the method proposed by this thesis has three attributes which make it a cost-effective approach to reliability assessment. First, in the asymptotic regime the bound gap computed by the method *converges at the optimal rate* of twice the $\mathcal{H}^1$-norm of the error in the finite element solution. This rate is optimal in the sense that it is the same

rate with which the finite element output itself asymptotically converges. Thus, the reliability assessment experiences the same gains in precision with increasing fidelity as the simulation result itself.

Second, the method is *inexpensive*. Another benefit of not solving finite-dimensional problems as surrogates for infinite-dimensional ones is that the subproblems are low dimensional.

Finally, the method naturally generates *local refinement indicators* for mesh adaptivity as a byproduct of calculating the bounds with contributions from independent local subproblems. Even though the contribution from a single subproblem may contain pollution error from other regions of the domain, the quantitative character of the bounds ensures that the bound gap will be lowered by successive adaptive refinement steps.

5.2 Recommendations

The method proposed by this thesis offers a rich context for future research. In particular, we mention four broad directions of future pursuit. First, future research should investigate extending the method to non-polynomial forcing and non-polygonal domains. As formulated, the method is limited to polygonal domains and piecewise polynomial interior and boundary forcing data, while many applications contain non-polynomial forcing and curved boundaries. Extending to non-polynomial forcing will either require including non-polynomial functions in the local finite-dimensional dual basis, or deriving an inexpensively computable bound on the influence of the non-polynomial forcing contribution on the local minimization problem. Adding non-polynomial functions to the dual basis may

require the concomitant enrichment of the continuity multipliers. Alternatively, the "flux-free" partition of unity domain decomposition can be investigated as an approach to eliminating the continuity multipliers altogether. A flux-free method has the advantage of not requiring the Lagrange multipliers to be equilibrating. Extending to curved boundaries requires formulating the method for parametric elements in a manner which maintains solvability despite of the possibly non-polynomial character of the subproblem data.

Second, future research should investigate extending the method to different classes of problems. Constrained problems such as the Stokes equations require either the introduction of a consistent penalty term on the Lagrange multiplier for the constraint of the mathematical model (i.e. pressure) into the constrained minimization reformulation of the output bound method, or modifying the local subproblem in a manner which allows the Lagrange multipliers of the constrained minimization reformulation to be locally projected onto a constraint-satisfying subspace. Extension to non-coercive equations requires the formulation of an appropriate energy-like augmented Lagrangian functional for the constrained minimization reformulation in a manner which produces computable subproblems. Extending to nonlinear problems requires careful attention to ensuring that the global extremizations used in the derivation and implementation of the method can be found.

Third, future research should investigate improving the effectiveness of the method through more sophisticated adaptive strategies and enhanced Lagrange multipliers. The sharpness of the bounds depend upon the quality of the Lagrange multipliers. In general, solution error consists of both local and pollution error,

so that the local bound gap contribution may not be the best indicator of the relative benefit to refining a particular element. Adaptive refinement strategies can gain advantage by attempting to predict which elements will be most beneficially refined using additional information available in the Lagrange multipliers. The Lagrange multipliers can be enhanced as they need not be finite element approximations per se, but they do need to equilibrate. Significant potential exists for increasing the computational efficiency of computing certifiable high precision approximations by constructing equilibrating recovered solutions as is done for recovery based error estimators.

Finally, future research should investigate integration of the method with reduced basis approximations [MMP01]. Reduced basis approximations can greatly reduce the cost of repeatedly appealing to a mathematical model with different problem parameters, but such approximations add an additional layer of numerical uncertainty to computational models. By building equilibrating reduced basis models for the Lagrange multipliers, the output bound method proposed by this thesis can be used to compute low order approximations with certified precision.

Appendix A

Equilibration Procedure

This appendix gives a brief overview of the equilibration procedure we employ in our numerical examples. We will restrict the presentation to linear finite element approximations in two dimensions. The presentation draws on that of Ainsworth and Oden contained in[AO00, AO97], to which we refer the reader for a more detailed discussion of Ladevèze's method and related methods. Additionally, we refer the reader to the original presentation of the method in [LL83] and to the work of Bank and Weiser [BW85].

A.1 Problem Statement

Recall that we have a mesh, $\mathcal{T}_h$, of non-overlapping open subdomains, T, called elements. We denote by ∂T the set of edges, γ, constituting the boundary of a single element T, and by $\partial\mathcal{T}_h$ the network of all edges in the mesh. We denote by $\mathcal{I}_h$ the set of vertices in the mesh and by $\mathcal{I}_h^m$ the set of vertices in a patch of elements sharing vertex m. Further recall that the goal of equilibration is to find

a $\lambda_h^u \in \Lambda_h$, which are polynomial functions defined independently over each edge of the triangulation, such that

$$b(\hat{v}, \lambda_h^u) = \ell(\hat{v}) - a(u_h, \hat{v}), \quad \forall \hat{v} \in \hat{\mathcal{V}}_h. \tag{A.1.1}$$

Equivalently, this "p-th order equilibration" problem can be posed as: find for each element, T, a $\lambda_h^u|_T \in \prod_{\gamma \in \partial T} \mathbb{P}^p(\gamma)$ such that

$$\int_{\partial T} \sigma_T v \lambda_h^u \, \mathrm{d}\Gamma = \ell_T(v) - a_T(u_h, v), \quad \forall v \in \mathbb{P}^p(T). \tag{A.1.2}$$

Note that these problems are not independent, as adjacent elements are coupled by the unknown edge function supported by their common edge. The solvability of the bounds subproblems requires only zeroth-order equilibration, but optimal convergence of the bound gap requires the full p-th order equilibration. In general this problem has many solutions, but any zeroth-order equilibrating solution will ensure solvability and and p-th order equilibrating solution satisfying the conditions of Lemma 2.3.1 will yield optimal convergence of the bound gap.

A.2 Preliminaries

Ladevèze's method decomposes the continuity multiplier function on an edge, $\lambda_h^u|_\gamma$, often referred to as an "equilibrated flux," into a flux average, $\langle \nabla u_h \cdot \boldsymbol{n} \rangle |_\gamma$, and a correction, $\sigma_T g'_\gamma$. The flux average, taking into account the known Neumann

data, is defined as

$$\langle \nabla u_h \cdot \boldsymbol{n} \rangle |_\gamma = \begin{cases} \frac{1}{2} \left(\nabla u_h|_T + \nabla u_h|_{T'} \right) \cdot \boldsymbol{n}|_T, & \text{on } \partial T \setminus \Gamma_T^{\mathrm{N}}, \\ g, & \text{on } \Gamma_T^{\mathrm{N}}, \end{cases} \tag{A.2.1}$$

where T' is the neighboring element sharing edge γ with element T. Commensurately, the correction $\sigma_T g'_\gamma$ is set to zero on Γ_T^{N}.

The globally coupled problem we must solve for the first-order equilibrating correction can be decoupled into local *vertex patch* subproblems by choosing the two function basis for the edge correction, g'_γ, required for first-order equilibration so that the "left" correction basis function is orthogonal to the "right" finite element edge function and visa versa. More precisely, for an edge γ with endpoints $\mathbf{x}_m$ and $\mathbf{x}_n$, where $m \in \mathcal{I}_h$ and $n \in \mathcal{I}_h^m$, we require that

$$\int_\gamma \theta_{m,n} \beta_{m,n} \, \mathrm{d}\Gamma = \delta_{m,n} \tag{A.2.2}$$

where $\beta_{m,n}$ is the correction basis function associated with point $\mathbf{x}_m$ and edge γ, and $\theta_{m,n}$ is the linear Lagrange finite element edge function that is unity at $\mathbf{x}_m$ and zero at $\mathbf{x}_n$. The resulting basis functions are found to be

$$\beta_{m,n} = \frac{2}{|\gamma|} (2\theta_{n,m} - \theta_{m,n}), \tag{A.2.3}$$

where $|\gamma|$ is the length of edge γ. The representation for g'_γ can now be written in terms of basis functions $\beta_{m,n}$ and coefficients $\mu_{m,n}$ as

$$g'_\gamma = \mu_{m,n} \beta_{m,n} + \mu_{n,m} \beta_{n,m}, \tag{A.2.4}$$

with which we can construct local problems for the equilibrating fluxes.

A.3 Subproblems

A particular subproblem is identified by its *center* vertex, $m \in \mathcal{I}_h$. In addition to the center vertex, there are N *halo* vertices, $n \in \mathcal{I}_h^m$, participating in the local subproblem. The equilibration algorithm computes the coefficients $\mu_{m,n}$ by solving a local problem involving all of the edges containing the center vertex m as an endpoint. There are as many edges as there are halo vertices. We introduce a local index, $i = 1 \ldots N$, which orders the halo vertices clockwise with increasing index number. For boundary patches, the index is chosen to begin with the counter-clockwise-most halo vertex.

There is a one-to-one correspondence between the local index i and the global index pairs (m, n) formalized by the mapping $i = \iota(m, n)$. Each halo vertex is connected to the center vertex by an edge which contributes one unknown coefficient to the local problem. We label the local unknown coefficients with the corresponding local index associated to the halo vertex serving as the outer endpoint of the edge. That is, the edges are indexed from 1 to N in counter-clockwise order. Furthermore, each edge has an edge residual associated with it defined as

$$R_i = R_{\iota(m,n)} = \ell(\theta_{m,n}) - a(u_h, \theta_{m,n}), \tag{A.3.1}$$

where we have again used the linear Lagrange finite element edge basis functions $\theta_{m,n}$.

Figure A.3.1 depicts the typical case for an interior subproblem. An interior

subproblem consists of N linear equations in N unknowns. Although the equations are linearly dependent with a rank deficiency of one, the equilibrium of the patches produced by the finite element method ensures that the data is in the range of the operator. We solve the resulting subproblem using the singular value decomposition to compute a pseudo-inverse which provides us with a solution that minimizes the discrete $\mathcal{L}^2$-norm of the correction coefficients.

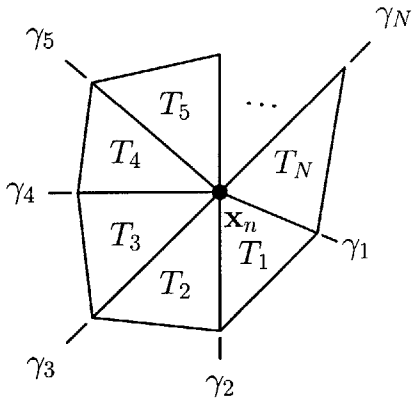

$$\begin{bmatrix} -1 & 1 & & \\ & \ddots & \ddots & \\ & & -1 & 1 \\ 1 & & & -1 \end{bmatrix} \begin{bmatrix} \mu_1 \\ \vdots \\ \mu_{N-1} \\ \mu_N \end{bmatrix} = \begin{bmatrix} R_1 \\ \vdots \\ R_{N-1} \\ R_N \end{bmatrix}$$

Figure A.3.1: Equilibration subproblem interior case.

Figure A.3.2 enumerates the boundary cases. From the planar geometry of the subproblem, there arises three distinct boundary cases possible for local boundary vertex patch subproblems. Case selection arises from the Neumann boundary conditions inherited by the patch. The form of the boundary problems comes about from our requirement that Neumann edges, for which we know the exact flux, do not require a correction. In the special case of both boundary edges being Neumann that Case 2 subsumes, it turns out that the Nth equation is satisfied automatically as a result of finite element equilibrium.

Finally, the flux averages of (A.2.1) are updated using the edge basis defini-

tion (A.2.3) as well as the flux correction definition (A.2.4).

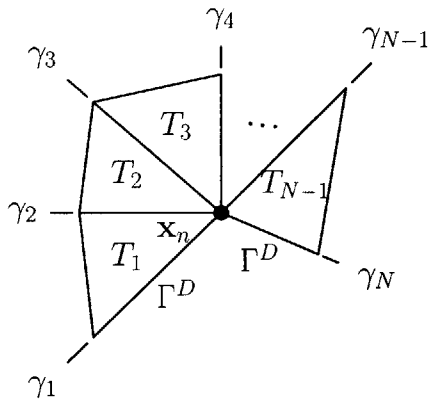

$$\begin{bmatrix} -1 & 1 & & \\ & \ddots & \ddots & \\ & & -1 & 1 \end{bmatrix} \begin{bmatrix} \mu_1 \\ \vdots \\ \mu_N \end{bmatrix} = \begin{bmatrix} R_1 \\ \vdots \\ R_N \end{bmatrix}$$

Case 1: No edges are Neumann.

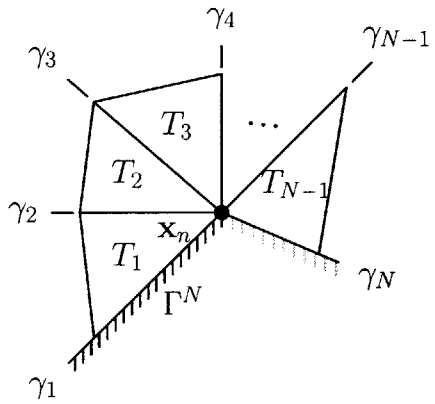

$$\begin{bmatrix} -1 & 1 & & \\ & \ddots & \ddots & \\ & & -1 & 1 \\ 1 & & & \end{bmatrix} \begin{bmatrix} \mu_1 \\ \vdots \\ \mu_{N-1} \\ \mu_N \end{bmatrix} = \begin{bmatrix} R_1 \\ \vdots \\ R_{N-1} \\ 0 \end{bmatrix}$$

Case 2: First edge is Neumann.

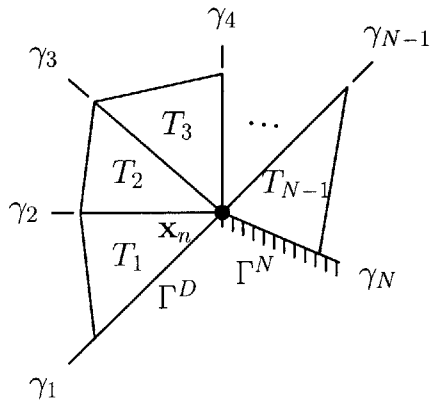

$$\begin{bmatrix} -1 & 1 & & \\ & \ddots & \ddots & \\ & & -1 & 1 \\ & & & 1 \end{bmatrix} \begin{bmatrix} \mu_1 \\ \vdots \\ \mu_{N-1} \\ \mu_N \end{bmatrix} = \begin{bmatrix} R_1 \\ \vdots \\ R_{N-1} \\ 0 \end{bmatrix}$$

Case 3: Last edge is Neumann.

Figure A.3.2: Equilibration subproblem boundary cases.

Bibliography

[ABF99] S. Adjerid, B. Belguendouz, and J. E. Flaherty. A posteriori finite element error estimation for diffusion problems. *SIAM Journal of Scientific Computing*, 21(2):728–746, 1999.

[AC92] M. Ainsworth and A. Craig. A posteriori error estimators in the finite element method. *Numerische Mathematik*, 60:429–463, 1992.

[AIA98] AIAA. Guide for the verification and validation of computational fluid dynamics simulations, 1998.

[Ain96] M. Ainsworth. The influence and selection of subspaces for a posteriori error estimators. *Numerische Mathematik*, 73(4):399–418, June 1996.

[Ain99] M. Ainsworth. Identification and a posteriori estimation of transported errors in finite element analysis. *Computer Methods in Applied Mechanics and Engineering*, 176:3–18, 1999.

[AK01] M. Ainsworth and D. W. Kelly. A posteriori error estimators and adaptivity for finite element approximation of the non-homogeneous dirichlet problem. *Advances in Computational Mathematics*, 15:3–23, 2001.

[AO93a] M. Ainsworth and J. T. Oden. A posteriori error estimators for 2nd-order elliptic-systems: 2. an optimal order process for calculating self-equilibrating fluxes. *Computers & Mathematics with Applications*, 26(9):75–87, November 1993.

[AO93b] M. Ainsworth and J. T. Oden. A unified apporach to a posteriori error estimation using element residual methods. *Numerische Mathematik*, 65:23–50, 1993.

[AO97] M. Ainsworth and J. T. Oden. A posteriori error estimation in finite element analysis. *Computer Methods in Applied Mechanics and Engineering*, 142:1–88, March 1997.

[AO00] M. Ainsworth and T. J. Oden. *A posteriori error estimation in finite element analysis.* Wiley-Interscience, New York, 2000.

[BBRW98] M. Braack, R. Becker, R. Rannacher, and J. Warnatz. An adaptive finite element method for combustion problems. Preprint 98-10 (SFB 359), 1998.

[BC00] D. Bertsimas and C. Caramanis. Solving linear partial differential equations via semidefinite optimization. In *International Symposium on Mathematical Programming*, 2000.

[BC02] D. Bertsimas and C. Caramanis. Bounds on linear pdes via semidefinite optimization. In *SMA-HPCES Symposium*, 2002.

[BF91] F. Brezzi and M. Fortin. *Mixed and Hybrid Finite Element Methods.* Springer Series in Computational Mathematics. Springer-Verlag, 1991.

[BKR00] R. Becker, H. Kapp, and R. Rannacher. Adaptive finite element methods for optimal control of partial differential equations: Basic concept. *SIAM Journal of Control and Optimization*, 39(1):113–132, 2000.

[BM87] I. Babuška and A. Miller. A feedback finite element method with a posteriori error estimations: Part i. the finite element method and some basic properties of the a posteriori error estimator. *Computer Methods in Applied Mechanics and Engineering*, 61:1–40, 1987.

[BM02] F. Brezzi and D. Marini. Augmented spaces, two-level methods, and stabilizing subgrids. *International Journal for Numerical Methods in Fluids*, 40(1-2):31–46, September 10 2002.

[BP02] A. M. Budge and J. Peraire. Finite element output bounds for a stabilized discretization incompressible stokes flow. SMA-HPCES Symposium, Singapore, January 2002.

[BPP01] A. M. Budge, A. T. Patera, and J. Peraire. Output bounds for isoparamteric finite element discretizations of the heat conduction and incompressible stokes flow problems. SMA-HPCES Symposium, Singapore, January 2001.

[BR78a] I. Babuška and W. C. Rheinboldt. Error estimates for adaptive finite element computations. *SIAM Journal of Numerical Analysis*, 15(4):736–754, August 1978.

[BR78b] I. Babuška and W. C. Rheinboldt. A posteriori error estimates for the finite element method. *International Journal for Numerical Methods in Engineering*, 123(10):1597–1615, 1978.

[BR79] I. Babuška and W. C. Rheinboldt. Analsysis of optimal finite-element meshes in R^1. *Mathematics of Computation*, 33(146):435–463, 1979.

[BR81] I. Babuška and W. C. Rheinboldt. A posteriori error analysis of finite-element solutions for one-dimensional problems. *SIAM Journal of Numerical Analysis*, 18(3):565–589, 1981.

[BR96a] R. Becker and R. Rannacher. A feed-back approach to error control in finite element methods: Basic analysis and examples. *East - West Journal of Numerical Mathematics*, 4:237–264, 1996.

[BR96b] R. Becker and R. Rannacher. Weighted a posteriori error control in fe methods. Preprint 96-1 (SFB 359), 1996.

[BSG99] I. Babuška, T. Strouboulis, and S. K. Gangaraj. Guaranteed computable bounds for the exact error in the finite element solution, part i: One-dimensional model problem. *Computer Methods in Applied Mechanics and Engineering*, 176:51–79, 1999.

[BSU+94] I. Babuška, T. Strouboulis, C. S. Upadhyay, S. K. Gangaraj, and K. Copps. Validation of a-posteriori error estimators by numerical approach. *International Journal for Numerical Methods in Engineering*, 37(7):1073–1123, April 1994.

[BSUG94] I. Babuška, T. Strouboulis, C. S. Upadhyay, and S. K. Gangaraj. A model study of the quality of a posteriori error estimators for linear elliptic problems– error estimation in the interior of patchwise uniform grids of triangles. *Computer Methods in Applied Mechanics and Engineering*, 1148(3-4):307–378, April 1994.

[BSUG95a] I. Babuška, T. Strouboulis, C. S. Upadhyay, and S. K. Gangaraj. A model study of element residual estimators for linear elliptic problems – the quality of the estimators in the interior of meshes of triangles and quadrilaterals. *Computers and Structures*, 57(6):1009–1028, December 1995.

[BSUG95b] I. Babuška, T. Strouboulis, C. S. Upadhyay, and S. K. Gangaraj. A posteriori estimation and adaptive control of the pollution error in the h-version of the finited element method. *International Journal for Numerical Methods in Engineering*, 38:4207–4235, 1995.

[BSUG97] I. Babuška, T. Strouboulis, C. S. Upadhyay, and S. K. Gangaraj. A model study of the quality of a posteriori error estimators for finite element solutions of linear elliptic problems, with particular reference to the behavior near the boundary. *International Journal for Numerical Methods in Engineering*, 40(142):2521–2577, July 1997.

[BV84] I. Babuška and M. Vogelius. Feedback and adaptive finite element solution of one-dimensional boundary value problems. *Numerische Mathematik*, 44:75–102, 1984.

[BW85] R. E. Bank and A. Weiser. Some a posteriori error estimators for elliptic partial differential equations. *Mathematics of Computation*, 44(170):283–301, 1985.

[CB02] C. Carsten and S. Bartels. Each averaging technique yields reliable a posteriori error control in fem on unstructured grids. part i: Low order conforming, nonconforming, and mixed fem. *Mathematics of Computation*, 71(239):945–969, 2002.

[Cia78] P. G. Ciarlet. *The finite element method for elliptic problems.* North-Holland, 1978.

[CKS99] T. Cao, D. W. Kelly, and I. H. Sloan. Local error bounds for post-processed finite element calculations. *International Journal for Numerical Methods in Engineering*, 45(8):1085–1098, jul 20 1999.

[CV99] C. Carsten and R. Verfürth. Edge residuals dominate a posteriori error estimates for low order finite element methods. *SIAM Journal on Numerical Analysis*, 36(5):1571–1587, September 1999.

[DM99] P. Destuynder and B. Métivet. Explicit error bounds in a conforming finite element method. *Mathematics of Computation*, 68(228):1379–1396, 1999.

[Dor96] W. Dorfler. A convergent adaptive algorithm for poisson's equation. *SIAM Journal of Numerical Analysis*, 330:1106–1124, 1996.

[FH72] B. M. Fraeijs de Veubeke and M. A. Hogge. Dual analysis for heat conduction problems by finite elements. *International Journal for Numerical Methods in Engineering*, 50:65–82, 1972.

[Fra64] B. M. Fraeijs de Veubeke. Upper and lower bounds in matrix structural analysis. Technical report, Advisory Group for Aerospace Research and Development, North Atlantic Treaty Organization, 1964.

[Fra65] B.M. Fraeijs de Veubeke. *Stress Analysis*, chapter Displacement and Equilibrium Models in the Finite Element Method, pages 145–197. John Wiley & Sons, 1965.

[HR99] F. K. Hebeker and R. Rannacher. An adaptive finite element method for unsteady convection-dominated flows with stiff source terms. *SIAM Journal on Scientific Computing*, 21(3):799–818, December 6 1999.

[Kel84] D. W. Kelly. The self-equilibration of residuals and complementary a posteriori error estimates in the finite element method. *International Journal for Numerical Methods in Engineering*, 20:1491–1506, 1984.

[KGZB83] D. W. Kelly, J. P. D. R. Gago, O. C. Zienkiewicz, and I. Babuška. A-posteriori error analysis and adaptive processes in the finite-element method: 1. error analysis. *International Journal for Numerical Methods in Engineering*, 19(11):1593–1619, 1983.

[KV00] G. Kunert and R. Verfürth. Edge residuals dominate a posteriori error estimates for linear finite element methods on anisotropic triangular and tetrahedral meshes. *Numerische Mathematik*, 86:283–303, 2000.

[Lad00] P. Ladevèze. Constitutive relation error estimators for time-dependent non-linear fe analysis. *Computer Methods in Applied Mechanics and Engineering*, 188(5):775–788, August 2000.

[LL83] P. Ladevèze and D. Leguillon. Error estimate procedure in the finite element method and applications. *SIAM Journal of Numerical Analysis*, 20(3):485–509, June 1983.

[LM96] P. Ladevèze and E. A. W. Maunder. A general method for recovering equilibrating element tractions. *Computer Methods in Applied Mechanics and Engineering*, 137(2):111–151, October 1996.

[LR97] P. Ladevèze and Ph. Rougeot. New advances on a posteriori error on constitutive relation in f.e. analysis. *Computer Methods in Applied Mechanics and Engineering*, 150(1-4):239–249, December 1997.

[LRBM99] P. Ladeveze, Ph. Rougeot, P. Blanchard, and J.P. Moreau. Local error estimators for finite element linear analysis. *Computer Methods in Applied Mechanics and Engineering*, 176:231–246, 1999.

[MMP00] L. Machiels, Y. Maday, and A. T. Patera. A "flux-free" nodal neumann subproblem approach to output bounds for partial differential equations. *Comptes Rendus de L'Academie des Sciences Serie I– Mathematique*, 330(3):249–254, Feburary 2000.

[MMP01] L. Machiels, Y. Maday, and A. T. Patera. Output bounds for reduced-order approximations of elliptic partial differential equations. *Computer Methods in Applied Mechanics and Engineering*, 190(26-27):3413–3426, 2001.

[MNS02] P. Morin, R. H. Nochetto, and K. G. Siebert. Convergence of adaptive finite element methods. *SIAM Review*, 44(4):631–658, 2002.

[MP00] Y. Maday and A. T. Patera. Numerical analysis of a posteriori finite element bounds for linear functional outputs. *Mathematical Models and Methods in Applied Sciences*, 10(5):785–799, 2000.

[MPP99] Y. Maday, A. T. Patera, and J. Peraire. A general formulation for a posteriori bounds for output functionals of partial differential equations; application to the eigenvalue problem. *Comptes Rendus de L'Academie des Sciences Serie I– Mathematique*, 328(9):823–828, May 1999.

[ODRW89] J. T. Oden, L. Demkowicz, W. Rachowicz, and T. A. Westermann. Toward a universal h-p adaptive finite element strategy, part 2. a posteriori error estimation. *Computer Methods in Applied Mechanics and Engineering*, 77(1-2):113–180, December 1989.

[OT02] W. L. Oberkampf and T. G. Trucano. Verification and validation in computational fluid dynamics. *Progress in Aerospace Sciences*, 38(3):209–272, April 2002.

[Par01] M. Paraschivoiu. A posteriori finite element output bounds in three space dimensions using the feti method. *Computer Methods in Applied Mechanics and Engineering*, 190:6629–6640, 2001.

[PP97] J. Peraire and A. T. Patera. Bounds for linear-functional outputs of coercive partial differential equations: Local indicators and adaptive refinement. In P. Ladevèze and J. T. Oden, editors, *Proceedings of the Workshop On New Advances in Adaptive Computational Methods in Mechanics*, Cachan, September 17-19 1997. Elsevier.

[PP98] M. Paraschivoiu and A. T. Patera. A hierarchical duality approach to bounds for the outputs of partial differential equations. *Computer Methods in Applied Mechanics and Engineering*, 158(3-4):389–407, June 1998.

[PP00] M. Paraschivoiu and A. T. Patera. A posteriori bounds for linear functional outputs of crouzeix-raviart finite element discretizations of the incompressible stokes. *International Journal for Numerical Methods in Fluids*, 32(7):823–849, April 15 2000.

[PPP97] M. Paraschivoiu, J. Peraire, and A. T. Patera. A posteriori finite element bounds for linear-functional outputs of elliptic partial differential equations. *Computer Methods in Applied Mechanics and Engineering*, 150(1-4):289–312, December 1997.

[QV97] A. Quarteroni and A. Valli. *Numerical Approximation of Partial Differential Equations*. Springer Series in Computational Mathematics. Springer, 1997.

[RS97] R. Rannacher and F.-T. Surrmeier. A feed-back approach to error control in finite element methods: application to linear elasticity. *Computational Mechanics*, 19:434–446, 1997.

[RS98] R. Rannacher and F.-T. Surrmeier. A posteriori error control in finite element methods via duality techniques: Application to perfect plasticity. *Computational Mechanics*, 21:123–133, 1998.

[RS99] R. Rannacher and F.-T. Suttmeier. A posteriori error estimation and mesh adaptation for finite element models in elasto-plasticity. *Computer Methods in Applied Mechanics and Engineering*, 176(1-4):333–361, July 6 1999.

[SBBHP03] A. M. Sauer-Budge, J. Bonet, A. Huerta, and J. Peraire. Computing bounds for linear functional outputs of exact weak solutions to poisson's equation. Submitted to SINUM, March 2003.

[SBD+00] T. Strouboulis, I. Babuška, D. K. Datta, K. Copps, and S. K. Gangaraj. A posteriori estimation and adaptive control of the error in the quantity of interest. part i: A posteriori estimation of the error in the von mises stres and the stress intensity factor. *Computer Methods in Applied Mechanics and Engineering*, 181:261–294, 2000.

[SBG+99] T. Strouboulis, I. Babuška, S. K. Gangaraj, K. Copps, and D. K. Datta. A posteriori estimation of the error in the error estimate. *Computer Methods in Applied Mechanics and Engineering*, 176:387–418, 1999.

[SBG00] T. Strouboulis, I. Babuška, and S. K. Gangaraj. Guaranteed computable bounds for the exact error in the finite element solution, part ii: bounds for the energy norm of the error in two dimensions. *International Journal for Numerical Methods in Engineering*, 47:427–475, 2000.

[SF73] G. Strang and G. J. Fix. *An Analysis of the Finite Element Method.* Prentice-Hall, 1973.

[SH98] J. R. Stewart and T. J. R. Hughes. A tutorial in elementary finite element error analysis: A systematic presentation of a priori and a posteriori error estimates. *Computer Methods in Applied Mechanics and Engineering*, 158:1–22, 1998.

[She96] J. R. Shewchuk. Triangle: Engineering a 2D quality mesh generator and delaunay triangulator. In Ming C. Lin and Dinesh Manocha, editors, *Applied Computational Geometry: Towards Geometric Engineering*, volume 1148 of *Lecture Notes in Computer Science*, pages 203–222. Springer-Verlag, 1996. From the First ACM Workshop on Applied Computational Geometry.

[SWCP01] F. Stern, R. V. Wilson, H. W. Coleman, and E. G. Paterson. Comprehensive approach to verfication and validation of cfd simulations–part1: Methodology and procedures. *ASME Journal of Fluids Engineering*, 123:793–802, 2001.

[VD02] D. A. Venditti and D. L. Darmofal. Grid adaptation for functional outputs: Application to two-dimensional inviscid flows. *Journal of Computational Physics*, 176(1):40–69, Feburary 2002.

[VD03] D. A. Venditti and D. L. Darmofal. Anisotropic grid adaptation for functional outputs: application to two-dimensional viscous flows. *Journal of Computational Physics*, 187(1):22–46, May 2003.

[Ver94] R. Verfürth. A posteriori error estimation and adaptive mesh refinement techniques. *Journal of Computational and Applied Mathematics*, 50(1-3):67–83, May 1994.

[ZBS99] O. C. Zienkiewicz, B. Boroomand, and J. Z. Shu. Recovery procedures in error estimation and adaptivity - part i: Adaptivity in linear problems. *Computer Methods in Applied Mechanics and Engineering*, 176(1-4):111–125, July 1999.

[Zhu97] J. Z. Zhu. A posteriori error estimation– the relationship between different procedures. *Computer Methods in Applied Mechanics and Engineering*, 150:411–422, 1997.

[ZSB01] L. Zhang, T. Strouboulis, and I. Babuška. A posteriori estimators for the fem: Analysis of the robustness of the estimators for the poisson equation. *Advances in Computational Mathematics*, 15(1-4):375–392, 2001.

[ZZ87] O. C. Zienkiewicz and J. Z. Zhu. A simple error estimator and adaptive procedure for practical engineering analysis. *International Journal for Numerical Methods in Engineering*, 24(2):337–357, Feburary 1987.

[ZZ92a] O. C. Zienkiewicz and J. Z. Zhu. The superconvergent patch recovery and a-posteriori error-estimates: 1. the recovery technique. *International Journal for Numerical Methods in Engineering*, 33(7):1331–1364, May 1992.

[ZZ92b] O. C. Zienkiewicz and J. Z. Zhu. The superconvergent patch recovery and a-posteriori error-estimates: 2. error-estimates and adaptivity. *International Journal for Numerical Methods in Engineering*, 33(7):1365–1382, May 1992.

[ZZ99] J. Z. Zhu and Z. Zhang. The relationship of some a posteriori estimators. *Computer Methods in Applied Mechanics and Engineering*, 176:463–475, 1999.